EVALUATION OF CRUSHED ORE AGGLOMERATION, LIQUID RETENTION CAPACITY, AND COLUMN LEACHING

by

Thien Vethosodsakda

A thesis submitted to the faculty of
The University of Utah
in partial fulfillment of the requirements for the degree of

Master of Science

Department of Metallurgical Engineering

The University of Utah

August 2012

The University of Utah Graduate School

STATEMENT OF THESIS APPROVAL

The thesis of **Thien Vethosodsakda**

has been approved by the following supervisory committee members:

Michael L Free	, Chair	**2/9/2012** Date Approved
Michael S Moats	, Member	**2/9/2012** Date Approved
Raj K Rajamani	, Member	**2/9/2012** Date Approved

and by **Jan D Miller** , Chair of the Department of **Metallurgical Engineering**

and by Charles A. Wight, Dean of The Graduate School.

ABSTRACT

In heap leaching operations, large fractions of fines and clays in ores may cause uneven solution distribution and plugging at the bottom of a heap. Agglomeration is a processing step that reduces the mobility of fine particles by agglomerating them with other particles. Agglomeration is used as a pretreatment step in many gold and copper heap leaching operations. Agglomeration is achieved by addition of moisture, and in many case binder in agglomeration equipment. Agglomeration often results in reduced fine particle migration and reduced leaching time. The objectives of this thesis research are to improve the fundamental understanding of agglomeration and to develop quality control methods for agglomeration.

Agglomerated ore size distribution, electro conductivity, permeability and soak tests have been developed to evaluate the quality of the agglomerates. Scanning electron microscope (SEM), Quantitative Evaluation of Minerals by Scanning electron microscopy (QEMSCAN), and X-ray computed tomography (CT) were used as agglomerates analysis techniques.

Initial binding mechanisms in the agglomeration process involve interfacial forces such as capillary forces. Capillary forces depend on three-phase contact, such as a solid-liquid-gas interface. Therefore, appropriate liquid or moisture content plays a very important role in agglomerate formation. This thesis research shows optimal moisture

needed for acidic or nonacidic solution based ore agglomeration can be estimated using liquid retention capacity measurements. Column leaching was also performed to evaluate the effect of agglomeration on fine particle migration and leaching recovery.

TABLE OF CONTENTS

LIST OF TABLES

LIST OF FIGURES

ACKNOWLEDGMENTS

This thesis would not have been possible without the great support and encouragement of many people. First, I would like to express my greatest gratitude to my research advisor, Dr. Michael L. Free, for his guidance, inspiration and support for my research project. I owe my deepest gratitude to Dr. Michael S. Moats and Dr. Raj Rajamani for giving me a golden opportunity to study in the Metallurgical Engineering Department, and for being on my supervisory committee and for contributing their valuable time and opinions.

My special thanks are extended to Dr. J. D. Miller and Dr. C. L. Lin for useful discussions and tremendous support, Nikhil Dhawan who completed size distribution analysis, Adirek Janwong for his helpful support and comments, Avi Jurovitzki for helping with column leaching experiments, Tim Phipps and Heather Wampler for unfailing support and sound advice.

I also thank the department administrative assistant, Evelyn Wells, and Executive Secretary, Kay Argyle, who carried out all manner of tasks with a friendly attitude.

Finally, sincere appreciation is expressed to my parents, Wantanee Wathiranwonge and Chukiat Vethosodsakda, for their outstanding support.

CHAPTER 1

INTRODUCTION

Gold is one of the most desired materials in every culture around the world. Its unique, attractively bright yellow color, which does not rust or tarnish, has been widely known to mankind. Gold has been used initially for decorative objects, jewelry, and a standard medium for exchange and trading (Buranelli, 1979). Recently, gold also has been used in a wide range of electronic devices and medical applications due to its unique properties such as great conductivity and nontoxicity (Dierks, 2005). There are several methods to extract and recover gold, but most gold is extracted and recovered by hydrometallurgical processes.

Gold ore from a mine is reduced in size to a 0.5 inch top size by crushing. Typically, gyratory crushers, jaw crushers, and cone crushers are used in the mining industry for size reduction. Crushed ore may be fed to a grinding circuit to further reduce the ore particle size to a desired size. Crushed ores are often introduced into rotating agglomeration drums with cement binder and cyanide solution. The cascading action inside the agglomeration drums combines binder, fine ore particles, coarser particles, and liquid to form bonds through liquid bridges. Agglomerated ores are typically placed on heap leaching pads. Agglomeration reduces fine particle migration and improves permeability in the heap. Leaching is performed using a cyanide solution that is

introduced on top of the heap by sprinkling or dripping. The cyanide solution dissolves gold from the agglomerated ore in the heap and the pregnant solution is collected in a pregnant solution pond. Gold is recovered from the pregnant solution by carbon adsorption and electrowinning. A schematic diagram of gold heap leaching and recovery is shown in Figure 1.1.

1.1 Ore Agglomeration Overview

Agglomeration is a processing step which binds fine ore particles to coarser ore particles. Typical objectives of agglomeration are to improve heap leaching recovery and reduce leaching time. These objectives are achieved by enhancing solution distribution and by reducing fine particle migration and associated plugging at the bottom of a heap. Fine particle migration occurs because of the leach solution flowing over the heap which carries with it fine particles. Additionally, percolation problems in heaps are caused by the segregation of coarse and fine particles during heap construction and operation. Fine particle migration and ore segregation results in reduced permeability and dead zones which make leaching solution flow non-uniform in the heap. Agglomeration work was performed more than 100 years ago. T.C. Scrutton used a 60° inclined chute to agglomerate ore in 1905 (Bouffard, 2005). In 1937, Shepard worked on agglomerating gold tailings with lime and calcium carbonate (Bouffard, 2005). Numerous publications have shown fundamentals and benefits of agglomeration to the mining industry. During the 1970s the U.S. Bureau of Mines in Reno (Heinen, McClelland, & Lindstrom, 1979), Nevada publicized advanced agglomeration technology for heap leaching. This agglomeration technology helps to improve recovery from low grade gold-silver ore tailings. Most of these tailings are low grade and contain more than 50% minus 200 mesh

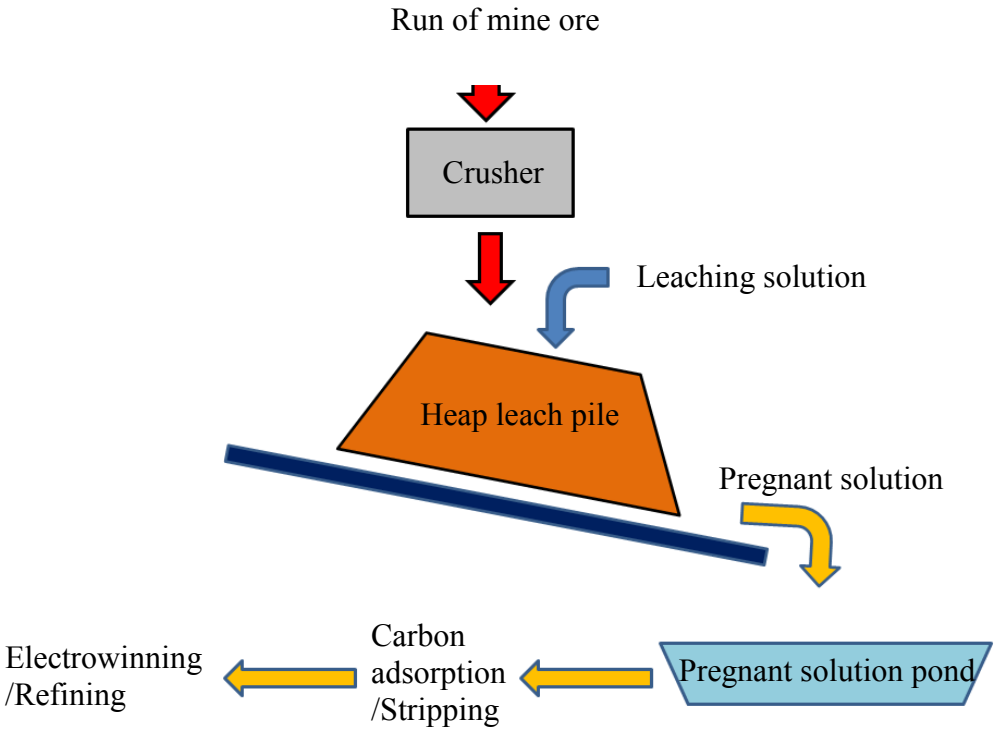

Figure 1.1 Schematic diagram of heap leaching procedures

particles. The fine particles and clay prevent uniform flow of leaching solution through the heap as shown in Figure 1.2. After agglomeration, reactive liquid and gas are more evenly distributed throughout the ore being processed as shown in Figure 1.3.

The U.S. Bureau of Mines determined practical parameters for low grade gold-silver ore tailings agglomeration and leaching. The important parameters include moisture level, binder type, binder dosage, curing time, agglomeration equipment type, and residence time. In 1979, Heinan show a comparative test of nonagglomerated ore and agglomerated ore in which the percolation rate can be improved by a factor of 10 to 100 times by agglomeration (Heinen, McClelland, & Lindstrom, 1979). This improvement in percolation by agglomeration can result in a 33% reduction in leach time compared to nonagglomerated ore. Reagent consumption is also reduced because of the shorter leach time. In 1981, McClelland and Eisele worked on improvements in heap leaching to recover silver and gold from low-grade resources (McClelland & Eisele, 1981). The experiments showed that percolation in cyanide leaching was enhanced by agglomeration. A 39-inch rotation disk agglomerator was used to investigate the effects of agglomeration moisture, binder dosage, and curing time on percolation rate. Fifty-pound low-grade gold-silver ore samples were dry mixed with portland cement (Type II). A controlled amount of liquid was added while agglomerating in a disk agglomerator. The agglomerated ore was cured then placed in a 5.5-inch diameter column (5 feet tall) for leaching experiments. After leaching was completed, the flow rate of the leaching solution was measured by flooding (agglomerates in the column were flooded with leaching solution and the flow rate of the drained solution was measured). The effect of moisture addition on flow rate is shown in Figure 1.4.

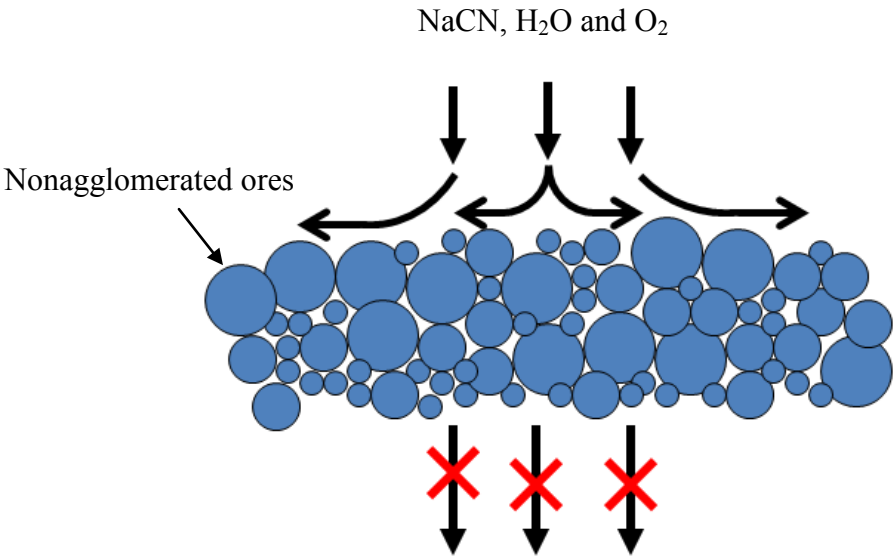

Figure 1.2 Schematic diagram showing that fine particles and clay inhibit uniform flow of leaching solution and gas through the heap.

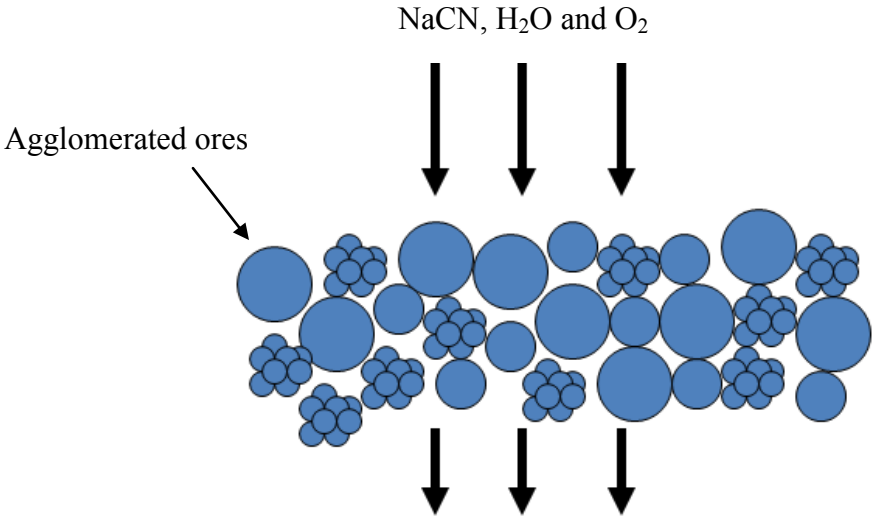

Figure 1.3 Schematic diagram showing that reactive liquid and gas can be more evenly distributed throughout agglomerated ore.

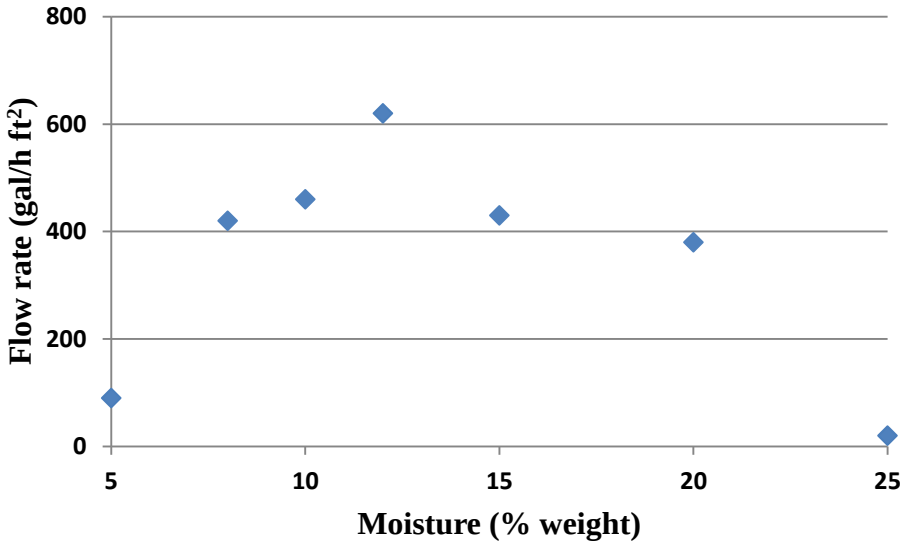

Figure 1.4 Effect of agglomerate moisture content on flow rate measuring by column flooding and draining [adapted from McClelland and Eisele (1981)]

These agglomeration experiments used 10 lb of cement binder and 24 hours of curing. These data show a significant effect of moisture addition during agglomeration. Solution flow rate increased with increasing moisture content until it reached a maximum of about 600 gal/hr ft^2 at 12 wt% moisture and then readily decreased if further moisture was added. Inadequate moisture results in insufficient liquid bridge formation (Kristensen & Schaefer, 1987). Excessive moisture leads to unstable agglomerates and mud formation. Adequate agglomeration moisture produces larger agglomerates, usually resulting in better permeability than small agglomerates.

The effect of binder addition on flow rate was studied (McClelland & Eisele, 1981). Agglomeration experiments were operated at 12 wt% moisture, 24 hours curing

time, and 5 to 15 pounds of portland cement (Type II) per ton of feed. The effect of binder addition on flow rate is shown in Figure 1.5. Results showed that increasing the amount of binder up to 10 lb/ton increased the flow rate approximately to 600 gal/hr ft^2 (measured from column flooding). Further binder addition beyond 10 lb/ton did not significantly affect the flow rate.

The effect of duration of curing on the flow rates was also studied (McClelland & Eisele, 1981). Cement does not cure by completely drying. Heinen (1979) observed cured and dried agglomerates easily broke down during leaching solution application. Proper curing requires water (at least 40 wt% of cement). The strength of cement increases if unhydrated cement is still present. An agglomerate moisture content of 12 wt% with 10 pounds of portland cement (Type II) per ton of feed were used in McClelland and Eisele's work. The agglomerates were cured for 0 to 36 hours at room temperature in capped leaching columns. The effect of duration of curing on the flow rates is shown in Figure 1.6.

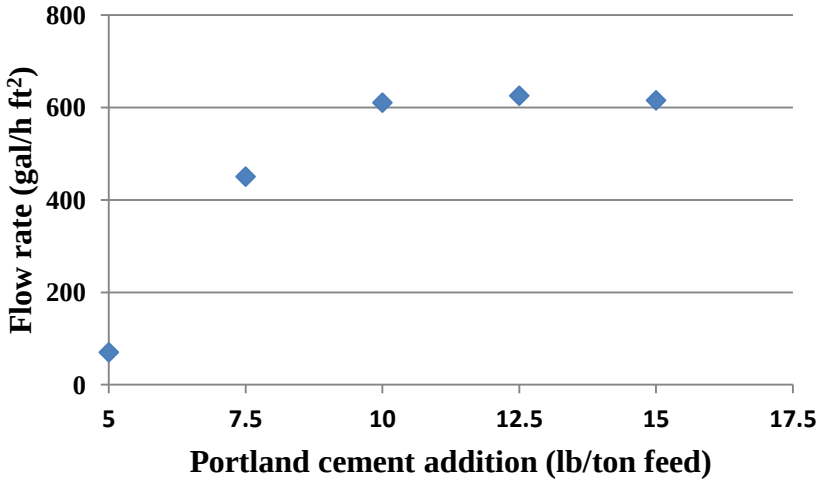

Figure 1.5 Effect of binder addition on flow rate measuring by column flooding and draining [adapted from McClelland and Eisele (1981)]

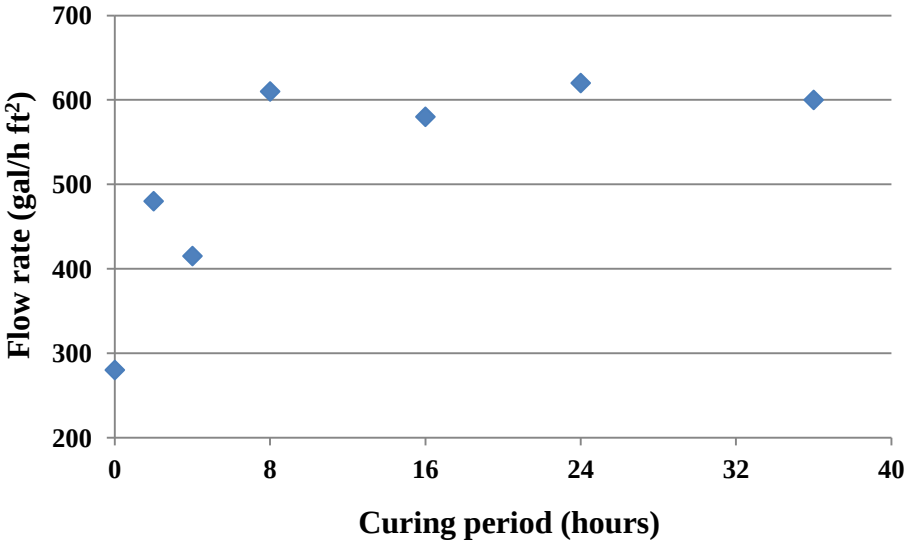

Figure 1.6 Effect of duration of curing on flow rate measuring by column flooding and draining [adapted from McClelland and Eisele (1981)]

Although standard requirements for the concrete curing period in the concrete industry are 28 days, agglomeration/leaching data show that 8 hours of curing is sufficient. The flood draining rate did not improve after curing more than 8 hours based on Figure 1.6. From the work of McClelland and Eisele (1981), proper agglomeration can increase the flow rate from 0.1 gal/hr ft^2 (post flooding draining rate measured from nonagglomerated ore) to 600 gal/hr ft^2 (post flooding draining rate measured from agglomerated ore at optimal conditions).

Ore size enlargement processes are generally known as pelletization and agglomeration. Lipiec and Bautista (1998) defined fine particle coated larger particles as rim agglomerates. Agglomerates which contain only fine particles are referred to pellets.

The benefits of agglomeration can be categorized into three major benefits: improvements of heap physical structure, improvements of leach chemistry and reduced environmental impact.

Improvements of heap structure are preventing ponding, slope failure or solution channeling due to uneven ore size and inadequate spread of size distribution, and reducing segregation when coarse particles rolled down to the toe of the heap during heap construction. Agglomeration may increase strength and stability of the heap. An example of extreme ore agglomeration is from Kinard and Schweizer (1987). An ore contained approximately 60 wt% of kaolinite, montmorillonite and clay. Agglomeration produced uniformly sized agglomerates of 0.3 to 1 cm in diameter. The agglomerates stacked up to a 9-meter tall heap. After leaching, the agglomerated ore distributed leaching solution through the heap evenly in spite of swelling clay expansion.

Agglomeration reduces fines migration. Low application flow rates applied to the heap carry enough momentum to transport fines up to 0.3 meters after agglomeration. The real problem of the fines migration often happens during improper sprinkler application or rainfall, particularly in tropical climates (Phifer, 1988).

The porosity of the heap can be increased via agglomeration, leading to better air and solution distribution. Heap porosity generally relatively determines the efficiency of oxygen-based heap leaching system. The bulk density of the heap has been used as a porosity indicator. Miller (2003) reported that bulk density of the nonagglomerated ore is often 1.15-1.30 t/m^3 at the surface to 2.0-2.1 t/m^3 at 4 meters below. After agglomeration, the bulk density can be 0.88 t/m^3 as measured at the Gooseberry mine in Nevada (Butwell, 1990).

From a leaching chemistry standpoint, agglomeration reduces leaching time, improves recovery and allows the heap leaching application of ore containing a lot of fines particles or tailings, which may not be economically processed by conventional leaching. Reduction of the leaching solution travel time and increased initial recovery rate are great benefits from agglomeration. DeMull and Womakc (1984) compared leaching efficiency of agglomerated and nonagglomerated gold ores. The agglomerated ore had a faster initial recovery and less overall cyanide consumption. Up to 80% recovery of the metal value of tailings required 20-70 days. Agglomerated ore can be extracted with as high as 90% recovery in 10 days. An example of incredible results at an Arizona silver heap leach operation showed that the recovery increased from 37% to 90%, while the leaching time was reduced from 90 days to 7 days. Another example of agglomerated ore benefits is the improvement observed at a gold heap leaching operation in Nevada, where the gold extraction increased by 60% while leaching time was reduced by half due to agglomeration.

From an environmental standpoint, good agglomerate quality reduces dust emissions. A faster leaching time may reduce the duration of the rinse cycle and reduce the amount of necessary wash water. Reduction of cyanide consumption also reduces environmental impact in the surrounding area.

1.2 Agglomeration Equipment

Agglomeration equipment mixes binder, ore particles, and moisture. Fine particles adhere to coarser particles during agglomeration. There are several types of

agglomeration equipment and techniques, which are useful to evaluate and determine the optimal procedures for agglomerating ores of different types and size distributions.

1.2.1 Belt Agglomeration

This equipment is suited for ore containing less than 15wt% of minus 150 mesh (104 micrometers) fines. In this technique, binder is added to the ore while transferring it on a series of inclined (about 15°) belt conveyors. At the transfer point, moisture, which is a cyanide solution for gold agglomeration, is added to the ores. The mixture tends to agglomerate during handling associated with transfers. The belt typically moves at a rate of 1.25-1.50 m/s (Chamberlin, 1986). The number of required transfer points depends on the amount of fines particles. A Schematic diagram of traditional belt agglomeration operation is shown in Figure 1.7.

Moisture can be added along the belts or at the drop points. Excessive moisture results in slurry formation, which leads to spillage, belt damage, and frequent shutdown. Inadequate moisture results in bad agglomeration and excessive dusting at drop points.

An alternative approach for belt agglomeration involves dropping the ore from a low-angle conveyor to a fast moving conveyor, which is steeply inclined (about 35-55°), in the opposite direction of the low-angle feed conveyor as shown in Figure 1.8. Agglomeration occurs when ore drops to the high velocity conveyor belt. The high-angle of the belt forces the agglomerates to roll down to the bottom transfer belt while the fines and bad agglomerates move up to the top due to the forward momentum of the belt. If the belt angle is too high, the agglomerates slide down, rather than roll.

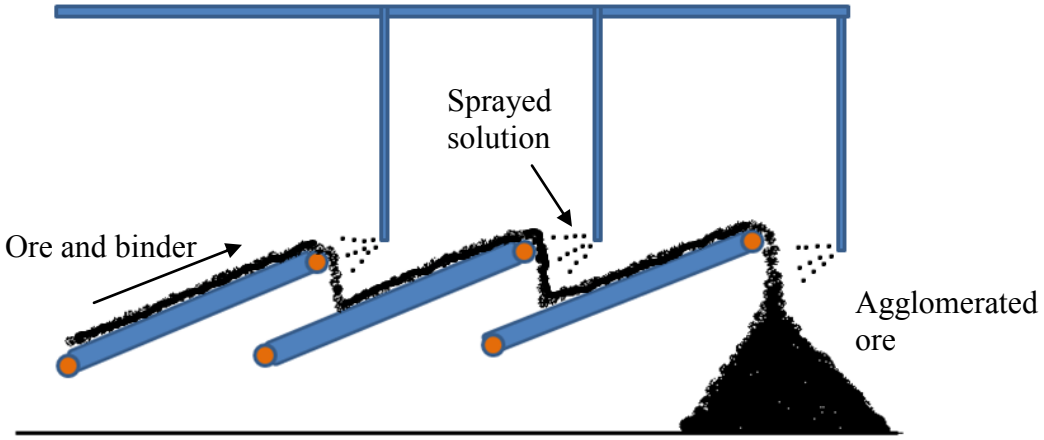

Figure 1.7 Schematic diagram of traditional belt agglomeration
adapted from Chamberlin (1986)

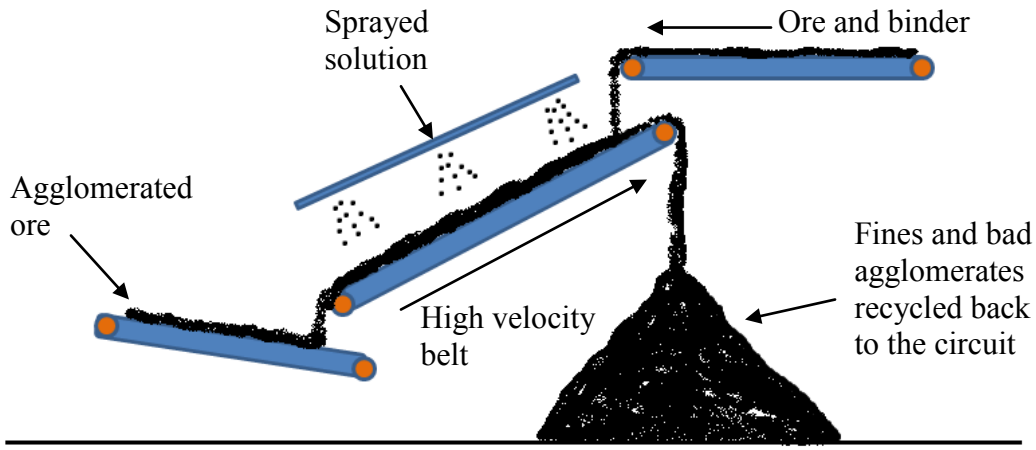

Figure 1.8 Schematic diagram of alternative belt agglomeration
[adapted from Chamberlin (1986)]

Belt agglomeration also can be done using a vibrating conveyor. When the ore with binder falls onto the vibrating conveyor, moisture is added and agglomeration occurs due to bouncing of ore particles on the belt.

1.2.2 Drum Agglomeration

Drum agglomeration is suitable for ore containing greater than 15wt% clay and/or fines. The ore and binder are fed through the inclined rolling drum. Moisture is added through the nozzles located along the first 2/3^{rds} of the drum length. A schematic diagram of drum agglomeration is shown in Figure 1.9. Rubber may be installed on the inside wall of the drum to minimize corrosion and prevent ore from sticking to the drum's wall. Agglomeration occurs due to the cascading action of particles inside the drum. There are three variables that typically affect the quality of the agglomerates produced in drum agglomerators.

The first variable is the agglomeration moisture addition. Excessive moisture results in the formation of slurry and mud inside the drum. Inadequate moisture results in poor agglomerate size and quality due to insufficient moisture for particle adhesion.

The second variable is drum rotation speed. The drum's rotation speed is determined by the fraction of the critical speed. The critical speed is the minimum speed to keep a single particle on the drum's wall during rotation. The critical speed is given by

$$C = \sqrt{\frac{g \sin\theta}{2\pi^2 D}} \approx \frac{42.3}{\sqrt{D}} \tag{1.1}$$

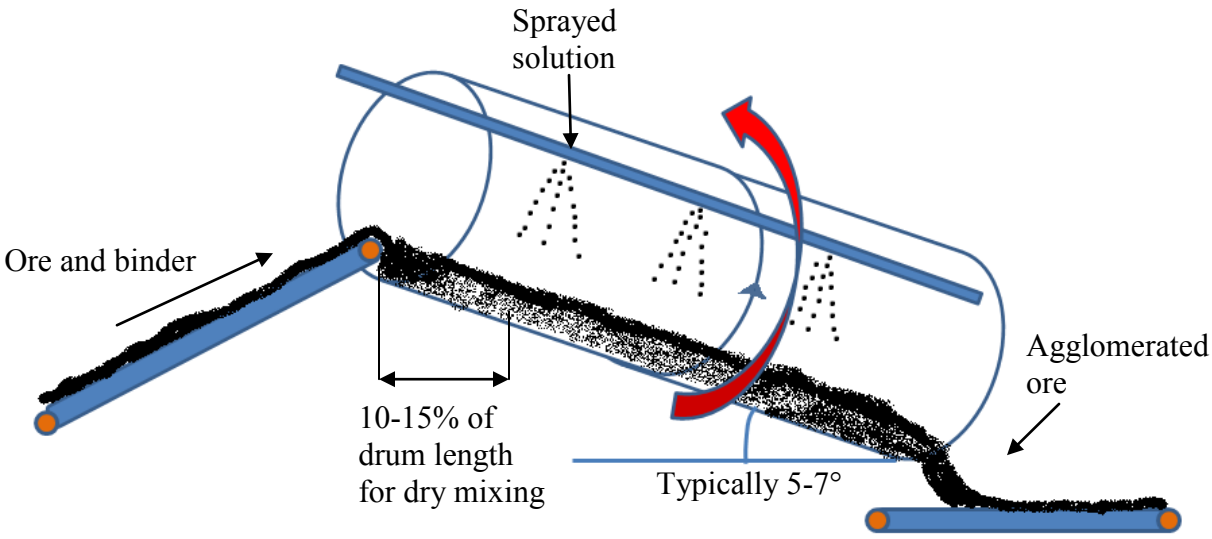

Figure 1.9 Schematic diagram of drum agglomeration [adapted from Chamberlin (1986)]

where

C: critical speed (rpm), D: drum diameter (m), g: gravitational acceleration (m/min^2), θ: angle of the drum from the vertical (usually 80 and 90°)

Typical drum rotation speed is about 30-50% of the critical speed. Slow rotation speed results in rolling rather than cascading of the agglomerates. Excessive rotation speed results in agglomerates sticking to the drum's wall due to centrifugal force.

The third variable is retention time. Longer length and larger diameter of the agglomeration drum as well as lower inclined angle and slower rotation speed increase the retention time. If the retention time is too short, added moisture will not have enough time to mix with the particles resulting in non-uniform agglomerates. Excessive retention time results in breakage of the agglomerates as well as wasted time and energy.

1.2.3 Disc Agglomeration

Most disc agglomerators are used in iron ore, agricultural, and chemical industries. Low throughputs of this technique make it unsuitable for heap leaching industries. Disc agglomerators use rotating, tilted discs or pans with rims. Solids and moisture are continuously fed to the disc. Solution is applied by a series of spray nozzles. Feed materials are mixed and roll along the rim until the agglomerates reach the desired size, which is controlled by a scraper or a plow. A schematic diagram of disc agglomeration is shown in Figure 1.10. The feed rate of disc agglomeration affects the rolling action. Nozzle locations have a significant effect on agglomerate quality (Holley, 1979). Nozzle spraying on large agglomerates tends to increase size or form mud depending upon the size distribution of the ore and the amount of moisture in the ore.

Nozzle spraying on feed materials or fine particles tends to form small agglomerates. Typically, the slope of the disc is between 40 to 65° from horizontal. The rotation speed of the disc usually is 30 to 50 rpm depending upon disc diameter and slope. Retention time typically ranges from 60 to 120 seconds (Bouffard, 2005), which can be increased by lowering the solid feed rate or disc angle. Disc agglomeration produces more uniform agglomerate size compared to other techniques.

1.2.4 Stockpile Agglomeration

Stockpile agglomeration is a simple agglomeration technique for fairly coarse particles with little clay and fines. Ores with binder are transferred on a conveyor belt and dropped down to a stockpile. At the drop point moisture is added to the ore as the ore agglomerates while cascading down the slope. A dozer may move the agglomerates up and down to help particle agglomeration. A schematic diagram of stockpile agglomeration is shown in Figure 1.11.

1.3 Binding Process and Mechanism Overview

It is essential to understand the mechanism and process of binding in agglomeration to get quality particle size enlargement and increased permeability by agglomeration.

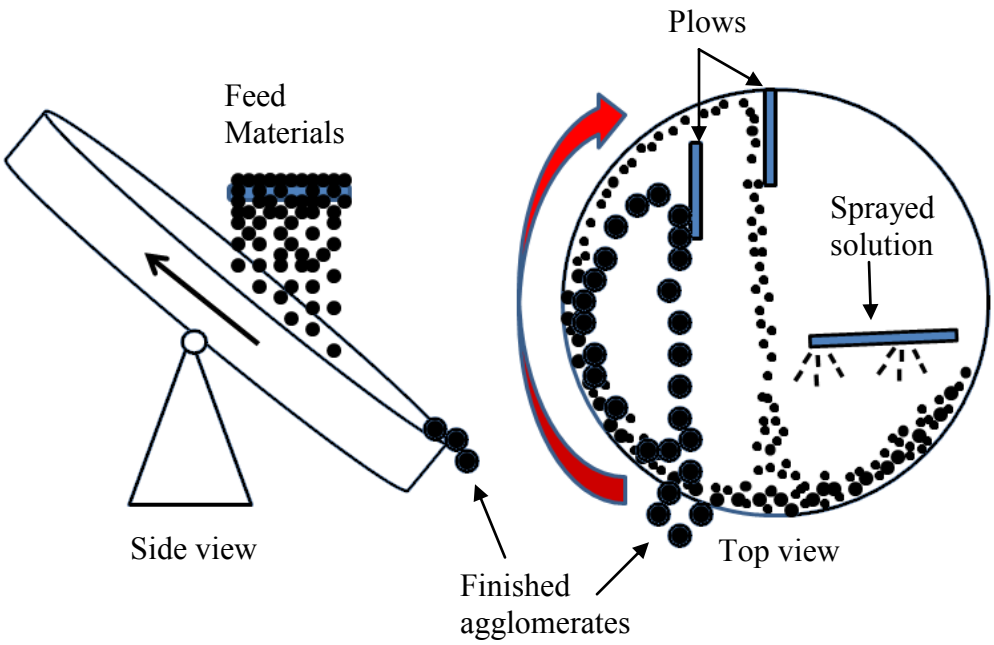

Figure 1.10 Schematic diagram of disc agglomeration [adapted from Chamberlin (1986)]

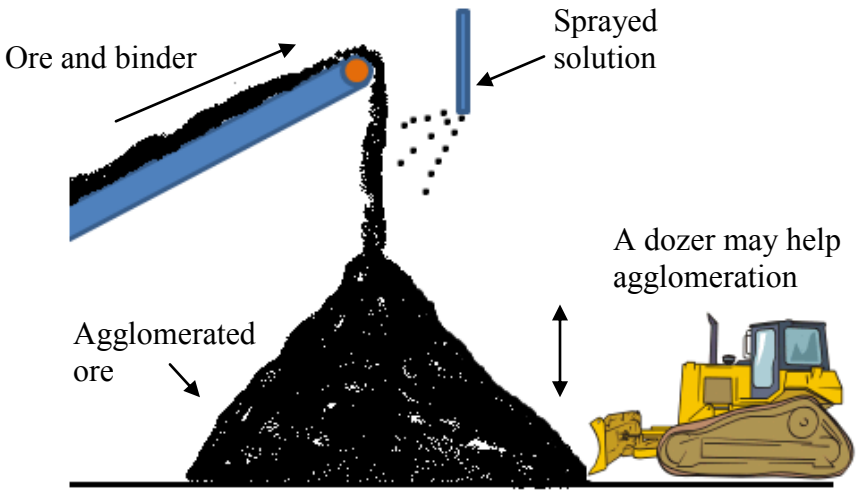

Figure 1.11 Schematic diagram of stockpile agglomeration [adapted from Chamberlin (1986)]

1.3.1 Binding Process

The binding process during ore agglomeration can be classified into 4 stages (Bouffard, 2005), which occur consecutively or simultaneously.

1. Wetting stage - In this stage, moisture is added to ore particles. The liquid coated particles start to act as nuclei for agglomerates. Figure 1.12 shows the wetting stage.
2. Growth stage - In this stage, the liquid film around the particles forms a liquid bridge with particles. Sufficient liquid content leads to attachment of new particle layers. Insufficient liquid content or excessive liquid content discontinues the growth stage. Figure 1.13 shows the growth stage.
3. Consolidation stage- In this stage, compaction pressure and agitation intensity are applied to the agglomerates. The agglomerates become more packed and porosity is reduced during this stage. Figure 1.14 shows the consolidation stage.
4. Breakage stage- In this undesirable stage, excessive compaction force is applied to the agglomerates. Fragmentation occurs and the fragments are allowed to grow if there is adequate liquid available. Poorly consolidated or oversize agglomerates are broken in this stage resulting in a more uniform agglomerate size. Figure 1.15 shows the breakage stage.

Figure 1.12 Wetting stage

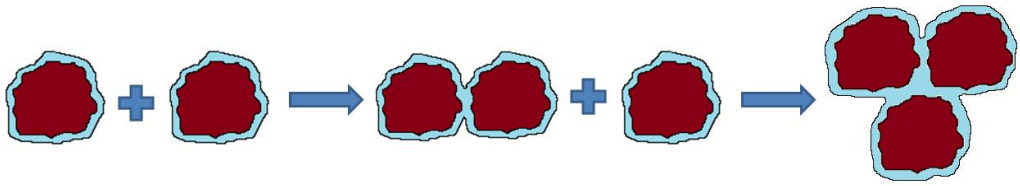

Figure 1.13 Growth stage

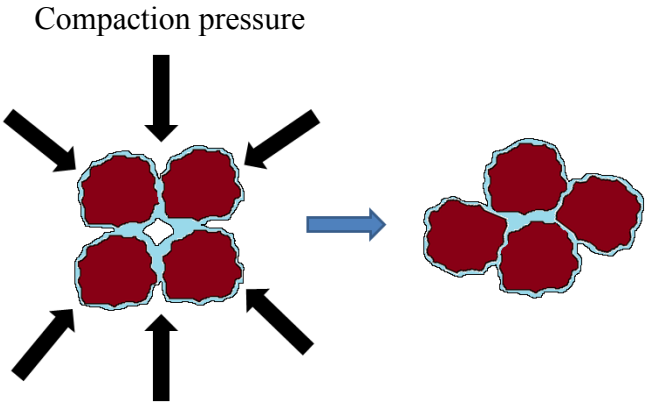

Figure 1.14 Consolidation stage

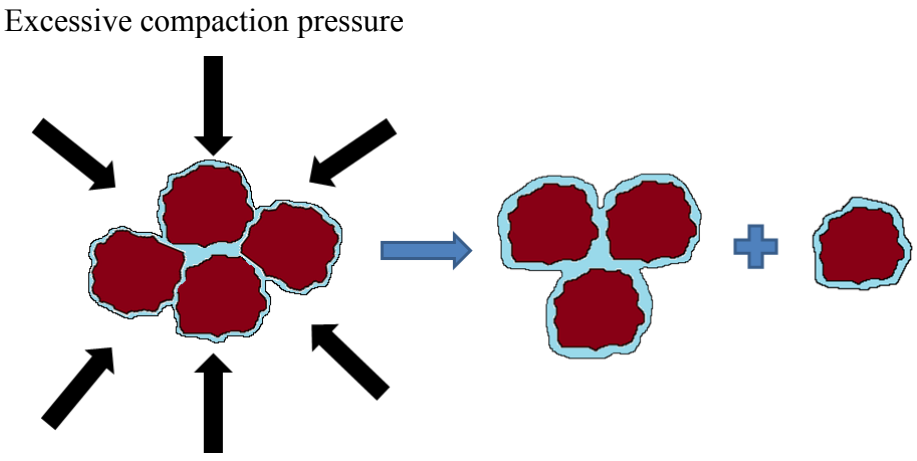

Figure 1.15 Breakage stage

1.3.2 Binding Mechanism

The binding mechanism makes ore particles stick together. The binding force varies from very weak to very strong depending on binding type, particle size, particle shape, and other particle properties such as roughness, contact angle or conductivity. There are four types of bonding mechanisms involved in the agglomeration process.

1.3.2.1 Solid Bridge Bonding Mechanism

Stable solids in ore agglomerates usually form by chemical binding using binders such as cement or polymers. Crystallization and hardening of binder bonds particles together in this binding mechanism. In some agglomeration processes, ore can react with acid to form gypsum, which may form a solid bridge. This type of binding mechanism requires curing, the period of which depends on the properties required of the binders, and the ambient conditions during curing.

1.3.2.2 Liquid Bridge Bonding Mechanism

Interfacial forces such as capillary forces are an initial binding mechanism in the agglomeration process. The capillary binding force generated by liquid bridges at coordination points between particles can be strong. Liquid bridges can be developed from free liquid or by capillary condensation. Liquid bridges can precede the formation of solid bridges that may form due to precipitation. The amount of liquid is an important key in determining the state of liquid bridges. When the amount of liquid is small, liquid bridges are formed between grains at contact points. This is called the pendular state (Figure 1.16a). If the amount of liquid is increased, multiple liquid bridges can connect to

form a local network, which is called the funicular state (Figure 1.16b). Additional liquid beyond the funicular state tends to fill some voids, resulting in the capillary state (Figure 1.16c). If the amount of liquid is greater than is needed to fill all voids, a slurry state is formed (Figure 1.16d). Some compacted agglomerates appear if liquid is added at levels near the beginning of the funicular state. As moisture is added, the compacted agglomerates are believed to increase in number until about midway in the funicular state. Additional moisture above the funicular level tends to create larger agglomerates. Increasing the bridging liquid further increases agglomerate size. Agglomerates tend to reach peak strength and obtain a spherical shape as the moisture content approaches the capillary region.

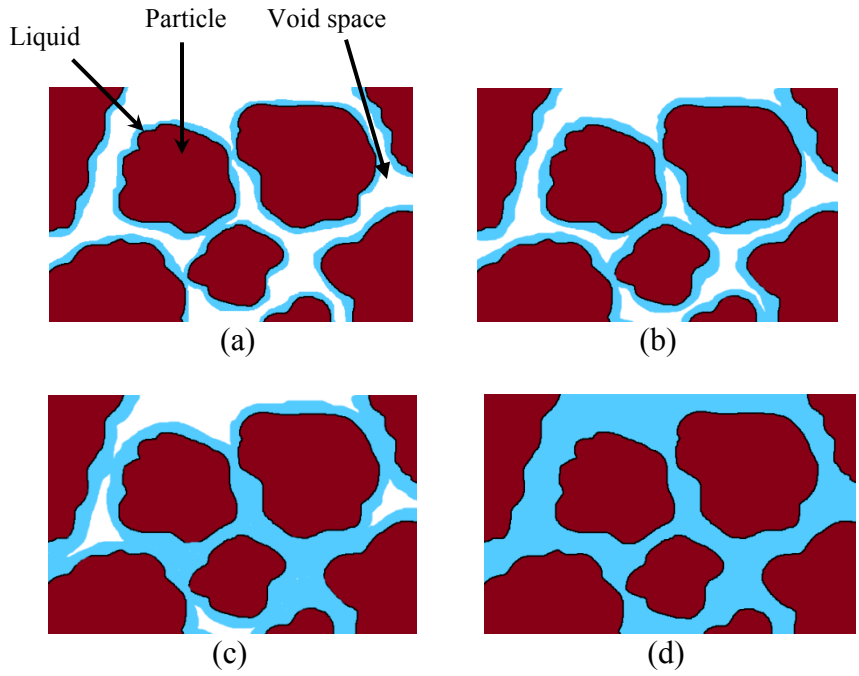

Figure 1.16 Liquid bridging states (a) Pendular state (b) Funicular state (c) Capillary state (d) Slurry state [adapt from (Kristensen & Schaefer, 1987)]

Good agglomerates can be obtained by keeping the moisture at a level that creates an optimum liquid-particle bridging state for agglomeration which is generally in the capillary state. Consequently, the amount of liquid added should not exceed that needed for the capillary state (Capes, 1980).

The simplest way to estimate binding force of the liquid bridge is the sphere and the plane model. This model assumes the plane is a hydrophilic surface and the separation distance much smaller than the particle radius (Gellert, Kustner, Hellwich, & Kastner, 1977). The maximum capillary binding force can be estimated by:

$$F_{cap} = 4\pi r\gamma \tag{1.2}$$

where r is the particle radius, and γ is the surface tension of liquid. Figure 1.17 shows a schematic diagram of a liquid bridge formed between a sphere and a plane.

1.3.2.3 Intermolecular and Electrostatic Forces

Intermolecular and electrostatic forces such as Van der Waal's force and the electrostatic force are short-range forces. These forces are responsible for adhesion between very fine particles (less than 1 μm) less than 0.1 μm apart (Kaliyan & Morey, 2010). The effectiveness of short-range forces dramatically reduces as the size of particles or separation distance increases (Rumpf, 1962). When very fine particles are close, instantaneous polarization of atoms and molecules create Van der Waal's force. The Van der Waal's force, which is nearly always attractive, can be estimated using a

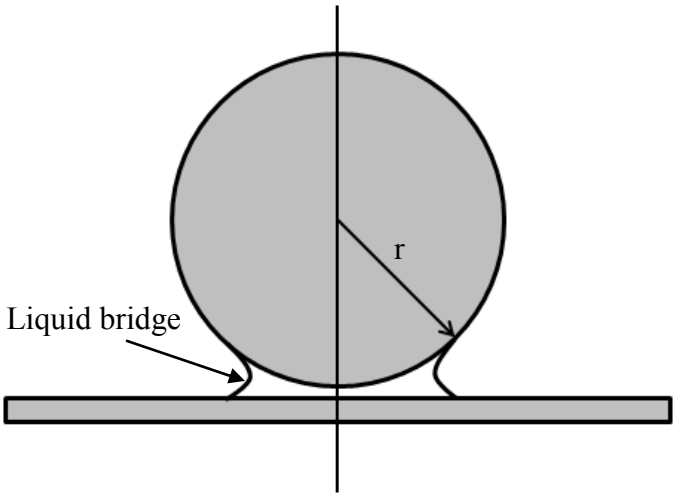

Figure 1.17 Liquid bridge formation between a sphere and a hydrophilic plane

sphere and plane model (Bowling, 1988). Assuming both surfaces have atomically smooth surfaces,

$$F_{vdw} = \frac{hr}{8\pi z^2} \tag{1.3}$$

where h is Lifshitz-Van der Waal's constant (10^{-20}), r is particle radius and z is atomic separation between the surfaces (approximately 10^{-10} m).

Electrostatic forces can be generated due to charge transfer during grinding or interparticle friction. The estimate electrostatic force between a charged sphere and conducting plane is given by

$$F_{elec} = \frac{\left(4\pi r^2 \sigma\right)^2}{4\pi\varepsilon r^2} \tag{1.4}$$

where σ is surface charge density, ε is permittivity and r is the radius of the sphere. This assumes the distance between the sphere and plane is zero.

1.3.2.4 Interlocking Bonds

Very small particles and flat particles can form interlocking bonds due to agitation or compression during the agglomeration process. The strength of the bonds depends on type of interaction and material characteristics. Examples of interlocking bonds are shown in Figure 1.18.

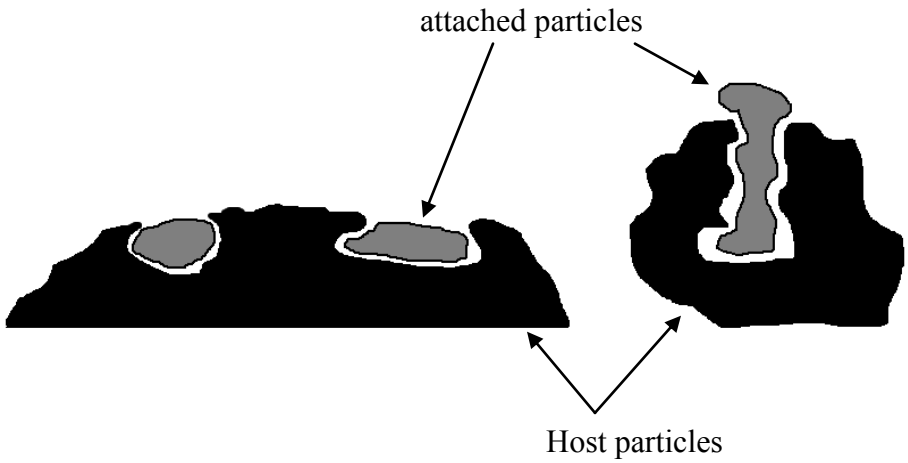

Figure 1.18 Examples of the interlocking bonds

1.4 Gold Leaching Chemistry

Cyanide has been used to recover gold during hydrometallurgical processes since the 1890s. Most gold is extracted using cyanide. Cyanide is highly soluble in water. Simple cyanide salts such as sodium cyanide (NaCN), Potassium cyanide (KCN), and calcium cyanide [$Ca(CN_2)$] are used as sources of cyanide in leaching. In the first step of leaching gold using cyanide, oxygen oxidizes gold and the cyanide reacts with the gold to form a stable complex ion [$Au(CN_2)^-$]. Oxygen is reduced and hydrogen peroxide is often formed. In the second step, the gold cyanide complex is formed by hydrogen peroxide reduction. These reactions are shown in the following chemical reactions that can proceed simultaneously.

$$2Au^+ + 4CN^- + O_2 + 2H_2O \longrightarrow 2Au(CN)_2^- + H_2O_2 + 2OH^- \quad (1.5)$$

$$2Au^+ + 4CN^- + H_2O_2 \longrightarrow 2Au(CN)_2^- + 2OH^- \quad (1.6)$$

The chemical reactions above show oxygen is required for gold leaching. Kudryk and Kellogg have shown that the rate of dissolution of gold cyanidation is directly proportional to the amount of available oxygen (Kudryk & Kellogg, 1954). Summation of these reactions are generally known as Elsner's equation presented as:

$$4Au + 8CN^- + O_2 + 2H_2O \longrightarrow 4Au(CN)_2^- + 4OH^- \quad (1.7)$$

Cyanide will also form complexes with other metals such as silver, copper, iron, and zinc, which tend to inhibit the dissolution of gold and increase cyanide consumption. Typical cyanide concentrations range from 200 to 500 ppm depending on mineralogy of the ore. Cyanide salts can be dissolved in water and ionize to free cyanide ions (CN^-) as presented below:

$$NaCN \longleftrightarrow Na^+ + CN^- \tag{1.8}$$

Cyanide ions may hydrolyze water to form hydrogen cyanide gas (HCN) which is very toxic.

$$CN^- + H_2O \longleftrightarrow HCN^- + OH^- \tag{1.9}$$

Both HCN and cyanide solution are colorless and have a scent like bitter almonds (Simeonova, 2004). Cyanide prevents cells of an organism from using oxygen. Lower doses of cyanide may lead to general weakness, headaches, difficulty in breathing, and loss of consciousness. Higher doses of cyanide cause cardiac arrest and death (Ellenhorn & Barceloux, 1988). In solutions with a pH less than 7, almost all of the cyanide will form HCN. In solution with a pH 9.3-9.5, about half of the cyanide exists as CN^- and half as HCN. In solution with a pH above 11, almost of the cyanide exists as CN^-. Hydrogen cyanide and free cyanide can be oxidized with oxygen to form cyanate (CNO^-), which reduces the available free cyanide (Marsden & House, 1992).

$$CN^- + H_2O \longleftrightarrow HCN + OH^- \quad (1.10)$$

$$4HCN + 3O_2 \longleftrightarrow 4CNO^- + 2H_2O \quad (1.11)$$

$$3CN^- + 2O_2 + H_2O \longleftrightarrow 3CNO^- + 2OH^- \quad (1.12)$$

Gold can be recovered from pregnant solution by cementation on zinc powder or by concentrating the gold using adsorption on activated carbon. The typical and cost-effective process is activated carbon adsorption (Mular, Halbe, & Barratt, 2002). There are three carbon adsorption processes generally used in gold industry, 1) carbon-in-pulp (CIP), 2) carbon-in-leach(CIL) and 3) carbon-in-columns(CIC). The main difference in CIP and CIL is gold adsorption occurring from pulp or leach solution. Both methods involve contacting the activated carbon with agitated pulp or solution. Activated carbon typically adsorbs 99.5% of the gold in 8 to 24 hours. In CIC adsorption, pregnant solution generally flows upward through a series of activated carbon columns. The gold is recovered from the carbon by elution, usually with hot caustic cyanide solution, electrowinning and then it is refined.

1.5 Research Objective

In this thesis research, agglomeration scoping experiments were performed to provide information about agglomerate properties as well as to provide information needed to appropriately determine optimum agglomeration conditions. The scoping tests included evaluations of the effects of agglomeration time, drum speed, and moisture content on agglomerates size distribution, permeability, conductivity, and fines

migration. Quality of the agglomerates was determined by agglomerate size analysis, permeability tests, column leaching tests, and visual inspection.

Agglomerate characterization and particle adhesion due to capillary forces were evaluated to provide more information about agglomerate properties of the gold ore sample. Agglomeration characterization was performed using QEMSCAN, SEM and X-ray micro CT (HRXMT) imaging and analyses to provide internal structure and agglomerate surface composition information.

A quality control (QC) tool set for controlling the agglomeration process was developed as part of this study. A part of this tool set included a tool for estimating optimal ore agglomerate moisture content for different ore types and size distributions.

1.6 Organization of Thesis

The thesis considers the effects of agglomeration time, drum speed, and moisture content on ore agglomeration as well as characterization of agglomerates. The thesis also includes the development of a tool for estimating optimal ore agglomeration moisture content for different ore types and size distributions.

In Chapter 1, ore agglomeration background information and ore agglomeration techniques are introduced as well as binding processes, binding mechanisms, and gold leaching chemistry.

In Chapter 2, gold ore mineralogy and size distribution are presented and discussed. Scoping experiments were performed and the effect of time, drum speed, and moisture content on agglomerates size distribution, permeability, conductivity, and fines

migration are evaluated. Agglomerated gold ore samples were further analyzed by QEMSCAN, SEM, and X-ray micro CT (HRXMT) imaging as discussed in Chapter 2.

In Chapter 3, liquid retention capacity was introduced as a tool for estimating optimal ore agglomeration moisture content. Liquid retention capacity measurement procedures as well as the effects of particle size distribution, ore height, liquid uptake time and fine particles on liquid retention capacity are provided. Optimal moisture content agglomeration results from Chapter 2 are also compared with the liquid retention capacity data.

In Chapter 4, Liquid retention capacity testing is applied to acidic ore agglomeration in which the liquid bridge forms in acid solution. Copper and nickel ore agglomeration were used to evaluate the liquid retention capacity in strongly acidic environments.

In Chapter 5, Gold column leaching was performed and evaluated. Different moisture and binder levels were evaluated. Detailed experimental procedures and results are presented.

Finally the conclusions and future research recommendations are presented in Chapter 6.

CHAPTER 2

EVALUATION OF GOLD ORE AGGLOMERATION

2.1 Introduction

Scoping tests were performed to provide information about agglomerate properties as well as to provide information needed to appropriately select agglomeration conditions to prepare ore material for column leaching. The scoping tests included evaluations of the effects of agglomeration time, drum speed, and moisture content on prospective quality control measurements which are particle size distribution, permeability, conductivity, and fines migration.

Particle size and permeability have been studied by many geologists and soil scientists. Particle size distribution is a fundamental independent variable controlling permeability (Graton & Fraser, 1935). In this study, sieve analysis was used to assess the particle size distribution. Cured agglomerates were gently screened by hand. A constant-head method was used to assess the permeability (Bowles, 1992).

In 2003, Fernandez reported that the electrical conductivity increases as the amount of moisture in the agglomerates increases. He related this conductivity reading to the optimal moisture content. In this study, electrical conductivity test equipment has been created as a quality control tool. Conductivity data were obtained by applying a voltage between two electrodes through a bed of packed particles.

Fine particle migration is an important parameter for evaluating agglomerate durability. A "soak test" has been developed to measure the percentage of fine particle migration of agglomerated ore. In this study, agglomerates were place on a screen in stagnant solution for 30 minutes. Then the screen was gently lifted and the fines passing through the screen were weighted after drying. Agglomerates which release less material are generally desirable.

2.2 Gold Ore Characteristics

There are two samples of gold ore evaluated in this study. Most of the minerals in the ore are quartzite and silica. The average ore grade is 0.68 g/t. The first sample of gold ore was used for studying the effect of agglomeration time, drum speed, and moisture content on quality of the agglomerates. The second sample of gold ore originated from high pressure grinding roll (HPGR) product. This sample of gold ore (D_{50} = 4.2 mm) had a slightly smaller size than the first sample (D_{50}= 6.1 mm). In this study, the first sample of gold ore is referred as gold ore (sample I) and the second sample is referred as gold (sample II). The size distributions of the gold ore (sample I) and gold ore (sample II) are shown in Figure 2.1.

2.3 Experimental Procedures

2.3.1 Agglomeration Procedure

Four-kilogram samples of gold ore (sample I) were agglomerated in a 5-gallon plastic drum in batch mode. The plastic drum was closed at one end with a central port in the other end to allow the introduction of ore and liquids. The drum had 5-mm plastic

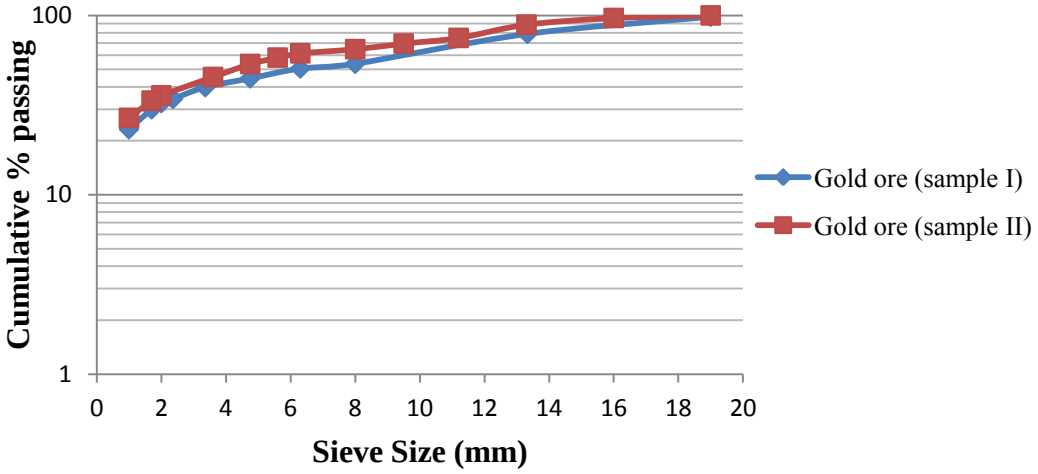

Figure 2.1 Gold ore (sample I) and gold ore (sample II) size distribution.

lifters installed inside along the drum to assist the tumbling motion. Ore samples were dry mixed for 30 minutes with 16 grams of Portland cement (Type II) as binder prior to agglomeration to insure that solids were well-mixed prior to agglomeration. 1000 ppm NaCN solution (pH 11.5) was introduced into the agglomeration drum through a tube with small spray holes facing downward. The solution flow rate and amount was controlled using a peristaltic pump to achieve the desired moisture content. Liquid was introduced for the first 1/3 of the retention time. The remainder of the agglomeration time was used to allow the agglomerates to grow without additional moisture. The drum operated at the desired critical speed. The small batch agglomerator utilized a ball mill shell, a sealable plastic sleeve, and two separated solution injection tubes as shown in Figures 2.2a and 2.2b.

(a) (b)

Figure 2.2 Picture of agglomerator (a) and solution injection tubes (b)

2.3.2 Electrical Conductivity Tests

After 1 hour of curing, 800 g of agglomerated gold ore (sample I) was split from the 4 kg batch and placed in the testing cell. A DC power supply was connected to the leads on each side of the cell. Inside the cell, the leads connect to stainless steel plates which contact the agglomerated sample. A schematic diagram of the electrical conductivity testing cell is shown in Figure 2.3. A series of voltages (1, 1.5, 2, 2.5 and 3 Volts) were applied to the circuit and the response current was measured with a handheld multimeter connected in series between the power supply and testing cell. After finishing the first conductivity test, a second conductivity test was performed at a load of 20.4 kg (45 lb), which simulates the weight that the agglomerates face in a 2 m high heap. A schematic diagram of the electrical conductivity set up is shown in Figure 2.4, and the electrical conductivity testing cell and system are shown in Figure 2.5.

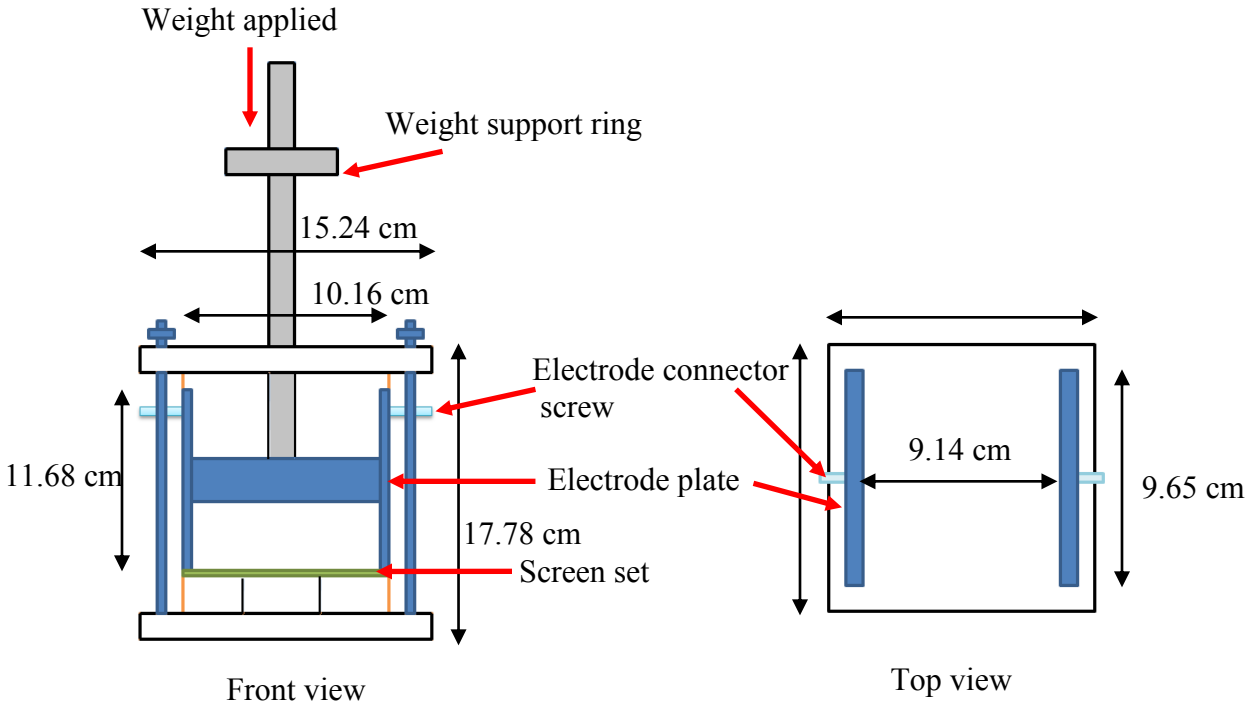

Figure 2.3 Schematic diagram of the electrical conductivity testing cell

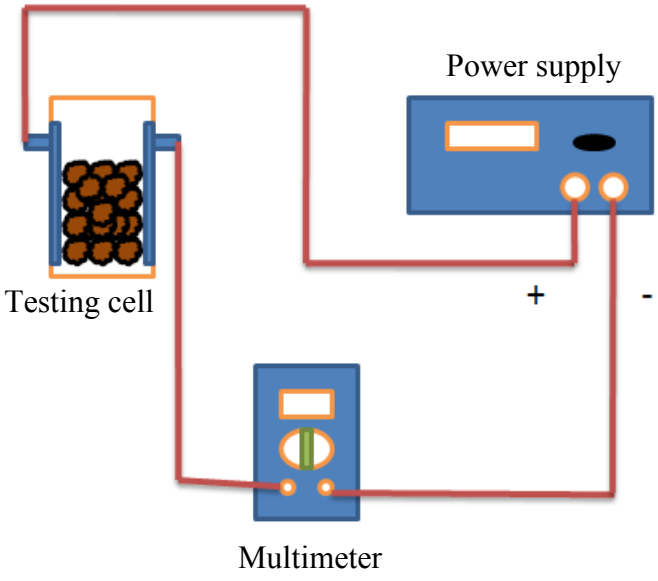

Figure 2.4 Schematic diagram of the electrical conductivity setup

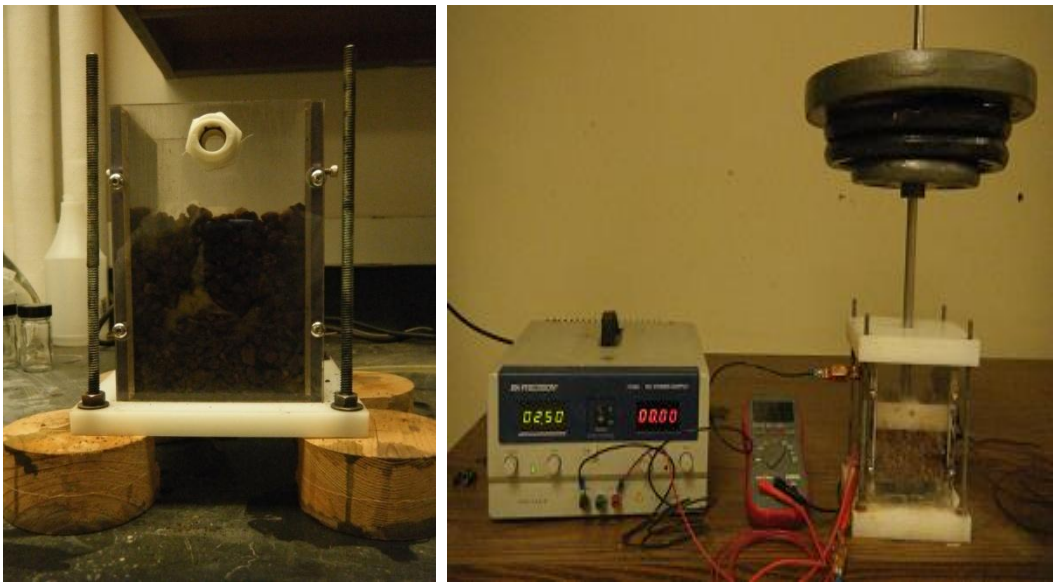

(a) (b)

Figure 2.5 Electrical conductivity testing cell (a) and electrical conductivity test system (b)

Resistance values are obtained from the slope of the voltage vs. current graph (V-I). The resistivity and conductivity of agglomerated samples were obtained using the equations (Ohring, 1995):

$$\rho = \frac{RA}{l} \tag{2.1}$$

$$\sigma = \frac{1}{\rho} \tag{2.2}$$

where ρ = resistivity (Ω m), R = resistance (Ω), A = cross sectional area of the bed (m^2), l = distance between electrodes (m), and σ = conductivity in S m^{-1}.

2.3.3 Hydraulic Permeability and Turbidity

After finishing each electrical conductivity test, hydraulic permeability and turbidity tests were performed in the testing column (see Figure 2.6). Four and a half kg (10 lbs) of load is applied to the sample to keep the height of the sample consistent from test to test. Deionized water was introduced to the cell from the bottom. Water flowed from a reservoir, which was set at a particular hydrostatic head or height, by gravity through the cell and exited through the outlet; then 1, 4, 7 and 10 cm hydraulic heads were applied. At each head level, the water exiting the cell was allowed to stabilize, and then it was collected for 3 minutes to determine the volume and flow rate. Stabilization takes about 3 minutes at each head height.

The area of the bed and the height of agglomerated ore bed were measured. Hydraulic permeability is calculated using Darcy's Equation:

$$Q = AK\frac{h}{L} \tag{2.3}$$

where Q = volumetric flow rate (cm^3/s), A = flow area perpendicular to L (cm^2), K = hydraulic permeability (cm/s), L = flow path length (cm), h = change in hydraulic head (cm)

For turbidity measurements, a 20 ml sample was collected during the permeability measurement. The turbidity test measures the amount of light transmitted through the stream sample. Turbidity test results are reported in FAU (Formazin Attenuation Units).

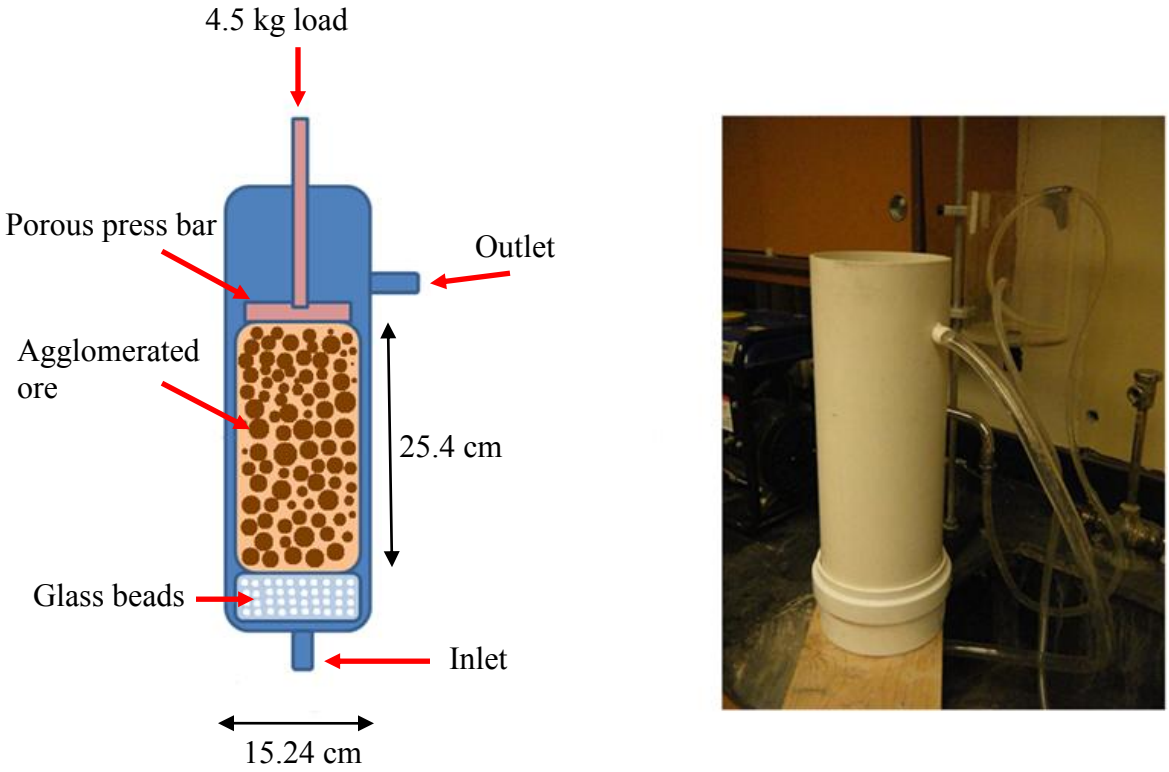

Figure 2.6 Hydraulic permeability and turbidity testing column

2.3.4 Soak Tests

Five hundred grams of agglomerated and cured ore sample was transferred to a 10 Mesh screen then lowered into a 300 ppm NaCN solution. The experimental setup is shown in Figure 2.7. After 30 minutes, the screen was carefully removed. The fines passing through the screen as it was removed were collected, dried, and weighed.

2.3.5 Evaluation of Mixing

Before agglomeration, gold ore (sample I) and cement binder were dry mixed in the agglomeration drum for 30 minutes. To make sure that the size distribution of the feed does not change during this mixing process, a size distribution analysis was performed before and after mixing. Figure 2.8 shows the gold ore (sample I) size distribution before and after mixing. The data in Figure 2.8 show there is no significant difference in size distribution before and after mixing.

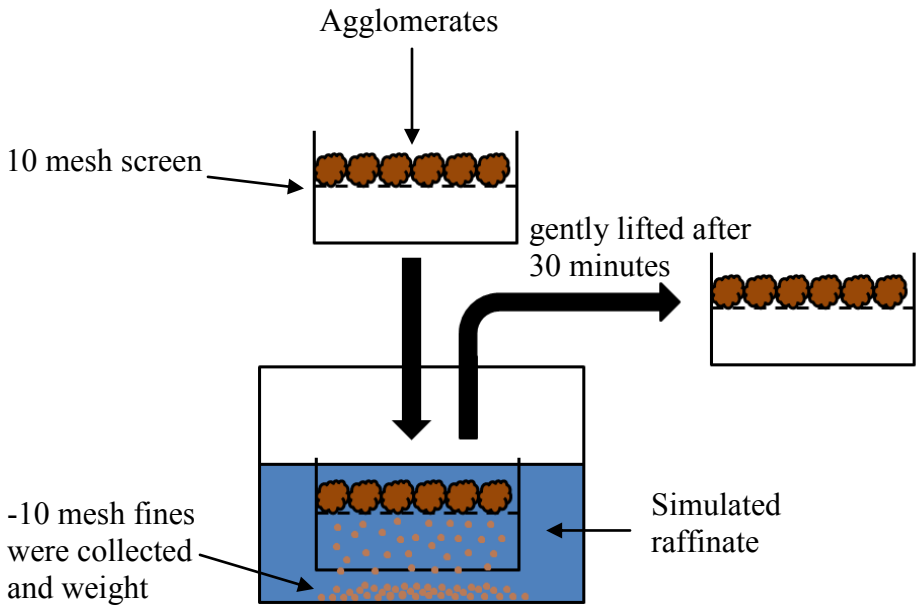

Figure 2.7 Soak test process

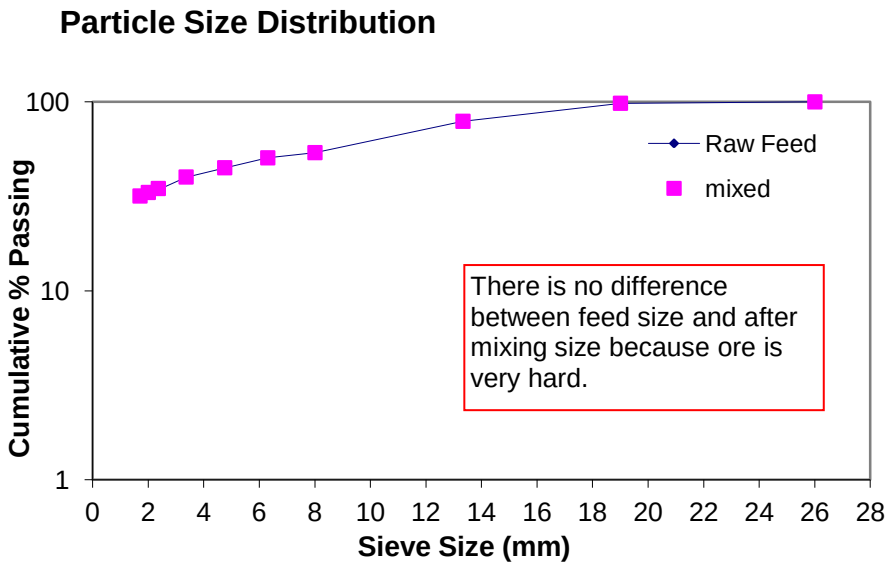

Figure 2.8 Gold ore (sample I) size distribution before and after mixing

2.4 The Effects of Agglomerate Moisture Content [gold ore (sample I)]

2.4.1 Size Distribution

Agglomerated gold ore (sample I) was taken out from the agglomeration drum and air dried for 1 hour before beginning additional testing. Pictures of the agglomerates and the associated size distributions are shown in Figures 2.9 to 2.12.

Figures 2.10 to 2.12 illustrate that the agglomerated ore starts forming agglomerates with 4% agglomerate moisture content. The agglomerates became more mud like above 10% agglomerate moisture content. The size distribution and D_{50} of the agglomerates are shown in Figures 2.13 and 2.14.

Figure 2.9 Gold ore (sample I) before agglomeration

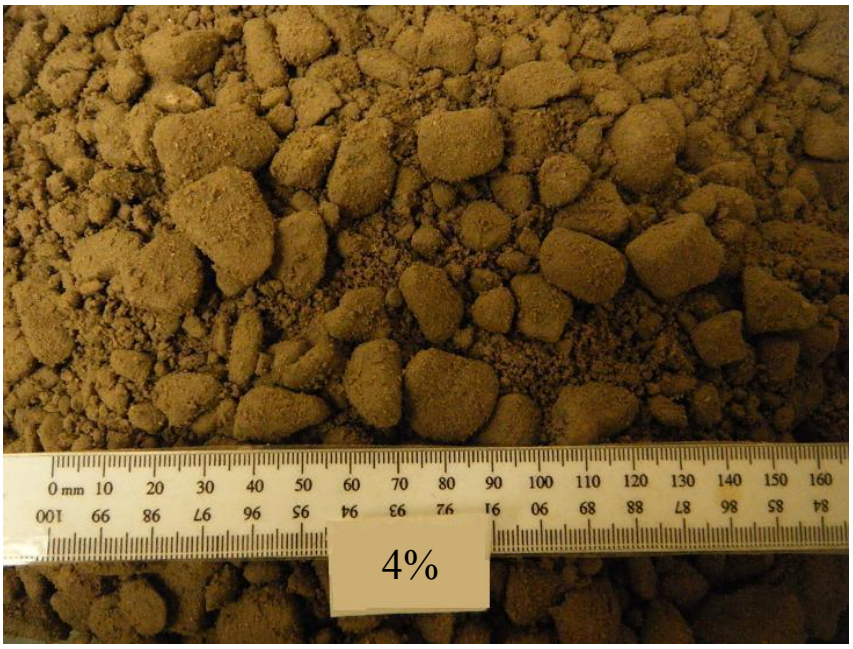

Figure 2.10 Gold ore (sample I) agglomerated with 4% moisture content

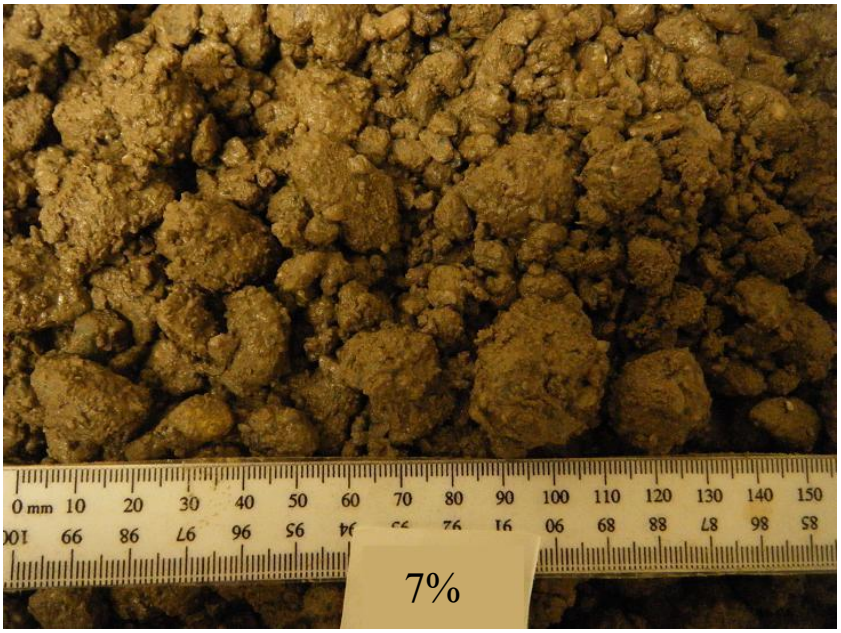

Figure 2.11 Gold ore (sample I) agglomerated with 7% moisture content

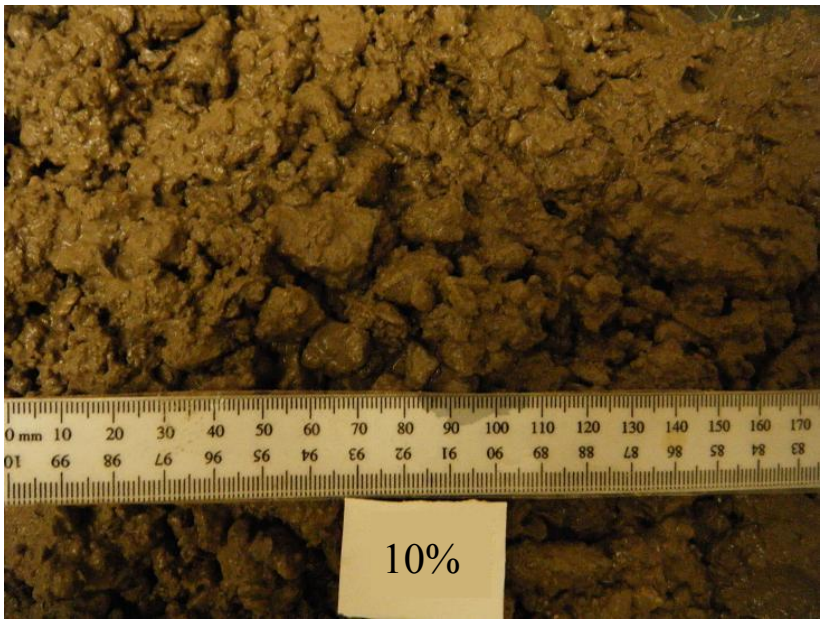

Figure 2.12 Gold ore (sample I) agglomerated with 10% moisture content

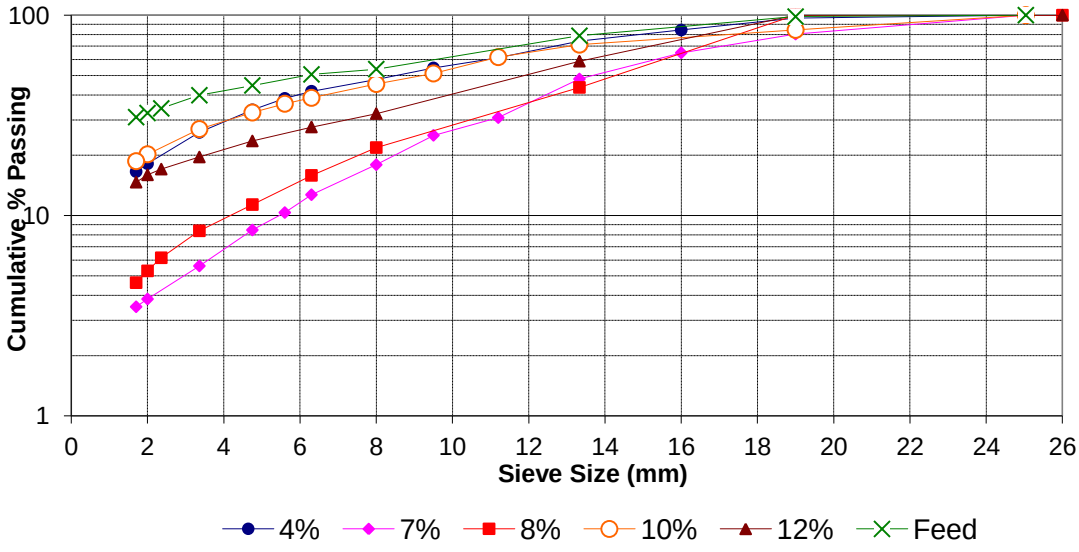

Figure 2.13 Particle size distribution of agglomerated gold ore (sample I) at different agglomeration moisture levels as noted in the legend.

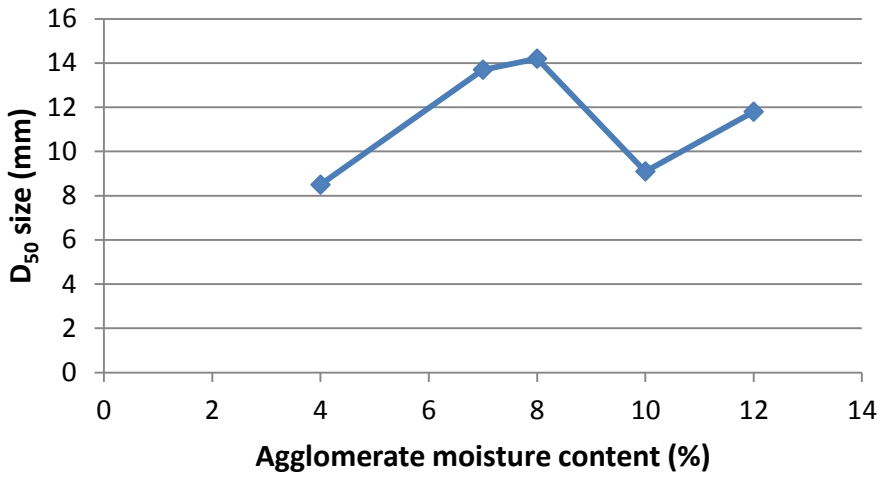

Figure 2.14 D_{50} size distribution of agglomerated gold ore (sample I) for different agglomeration moisture levels as indicated.

As Figures 2.13 and 2.14 show, the size of the agglomerates starts to increase with increasing moisture content until 8% agglomerate moisture content is reached. The D_{50} size starts to drop above 8% agglomerate moisture content and increases again at 12% agglomerate moisture content. However, at the 12% agglomerate moisture content, the agglomerates form a mud-like material that settle and dry into larger pieces that are formed by mud settling and consolidation rather than agglomeration.

2.4.2 Conductivity

As the graph in Figure 2.15 shows, it is obvious that when the wet ore was evaluated the conductivity increased as the moisture content increased. When 20.4 kg (45 lb) of load was placed on the top of the ore in the conductivity cell, the conductivity increased due to increased compaction of the ore particles and the associated increase in contact between the ore particles.

2.4.3 Permeability

The permeability increased as the moisture content increased up to 7% agglomerate moisture content as shown in Figure 2.16. This trend is somewhat similar to the associated size distribution data trend in Figure 2.14. Large agglomerates produce better permeability than small agglomerates.

2.4.4 Turbidity

Turbidity is an indicator of fine particle release during the permeability test. Figure 2.17 shows the agglomeration process reduces turbidity. The lowest turbidity was associated with 7% agglomerate moisture content, which resulted in very good agglomerates.

2.4.5 Soak Test

Soak tests gave information about agglomerate stability. Fine particles released from agglomerates during soak tests are not securly attached, and they are quantified by the amount of fine particle migration through the soak test screen. The lowest fines migration occurred with 7% agglomerate moisture content as shown in Figure 2.18.

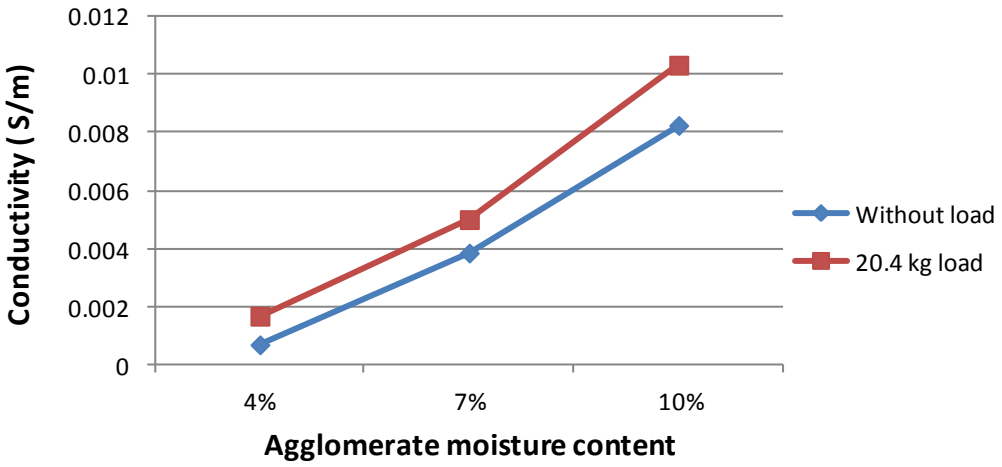

Figure 2.15 Conductivity at different moisture levels as indicated.

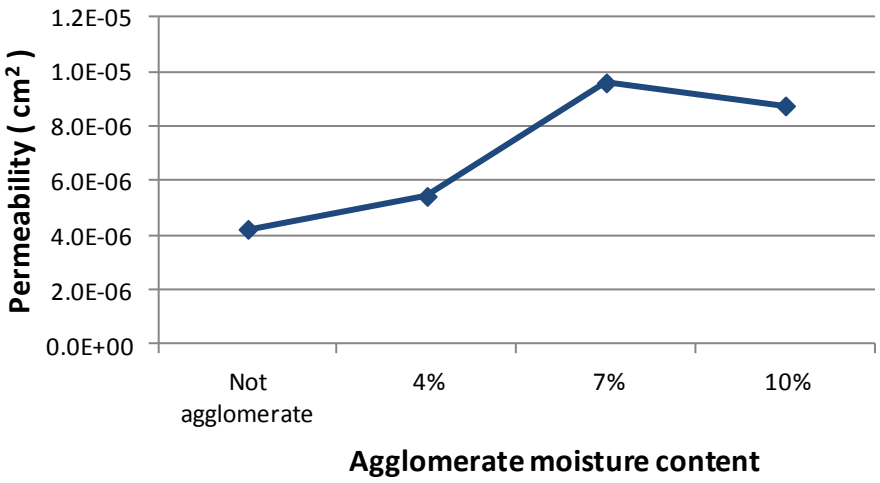

Figure 2.16 Permeability at different moistures as indicated

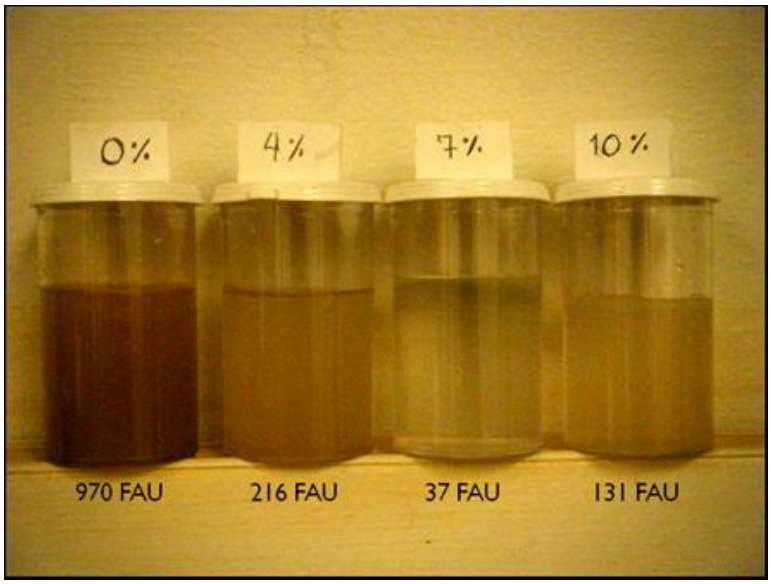

Figure 2.17 Turbidity of liquid from permeability tests of agglomerates at different moisture levels as indicated

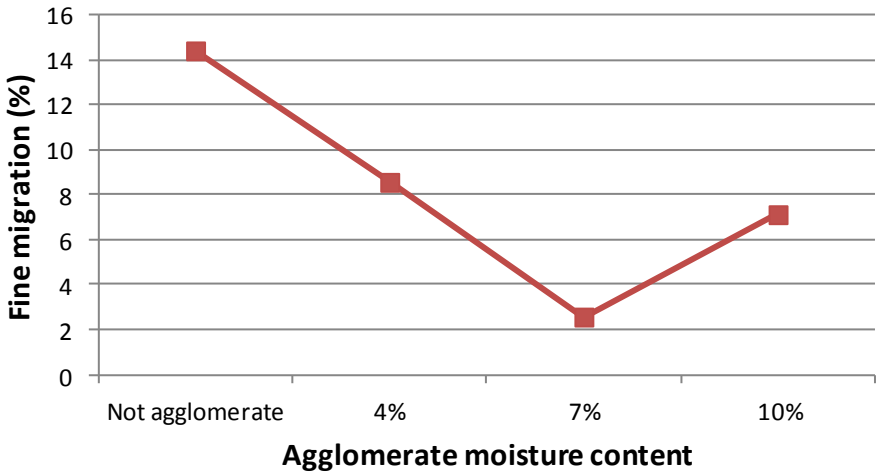

Figure 2.18 Fines migration at different moisture levels as indicated

2.5 Effects of Agglomeration Time [gold ore (sample I)]

2.5.1 Size Distribution

This test evaluated the effect of agglomeration time on size distribution. Seven percent agglomerate moisture content was used because it produced the highest permeability, lowest turbidity, and lowest fine particle migration. Agglomerate pictures and the associated size distributions are shown in Figures 2.19 to 2.24. The relationship between size and agglomeration time is presented in Figure 2.25.

As the results of the agglomeration time tests show, 3, 4 and 5 minutes agglomeration times produced very similar size distributions. At 5 minutes of agglomeration the agglomerates have smooth and round surfaces. At 1 minute of agglomeration time the highest D_{50} value was observed because the mixing was insufficient to homogenize the agglomerates.

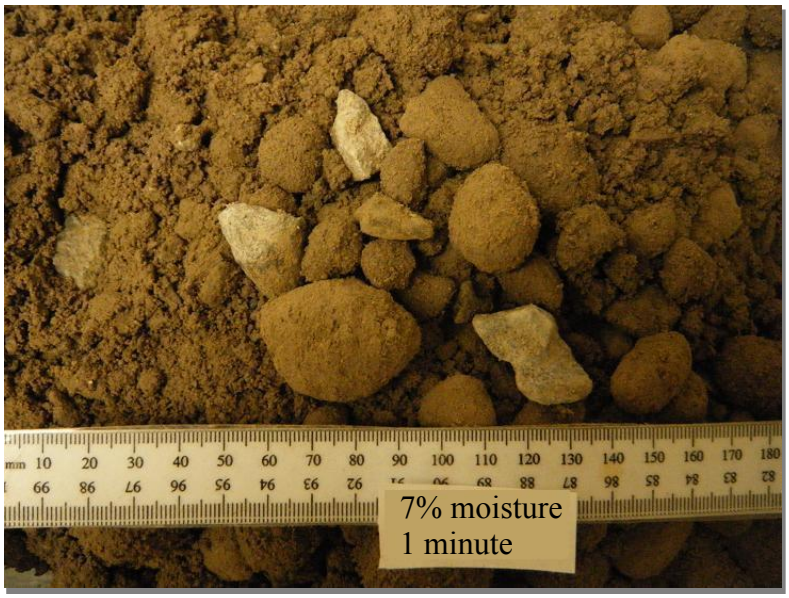

Figure 2.19 Gold ore (sample I) agglomerated with 7% moisture content for 1 minute of agglomeration time

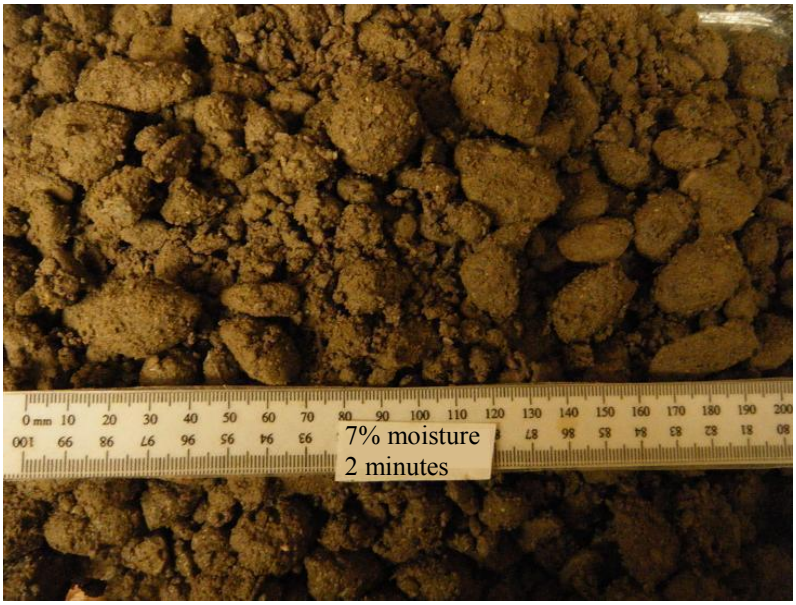

Figure 2.20 Gold ore (sample I) agglomerated with 7% moisture content for 2 minutes of agglomeration time

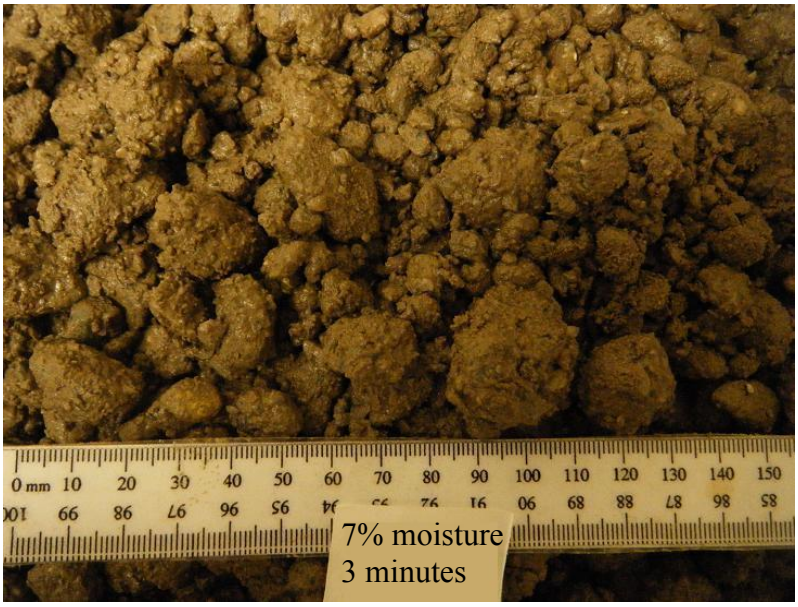

Figure 2.21 Gold ore (sample I) agglomerated with 7% moisture content for 3 minutes of agglomeration time

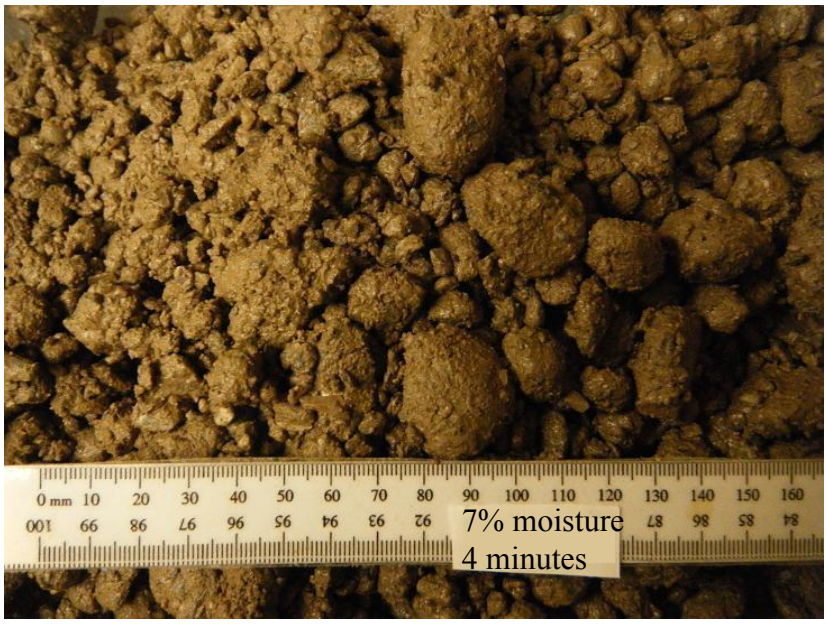

Figure 2.22 Gold ore (sample I) agglomerated with 7% moisture content for 4 minutes of agglomeration time

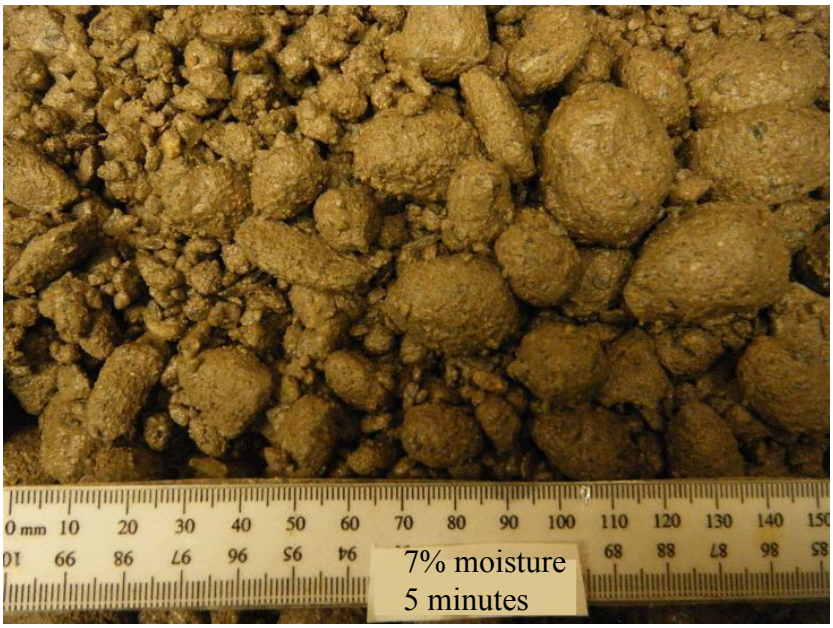

Figure 2.23 Gold ore (sample I) agglomerated with 7% moisture content for 5 minutes of agglomeration time

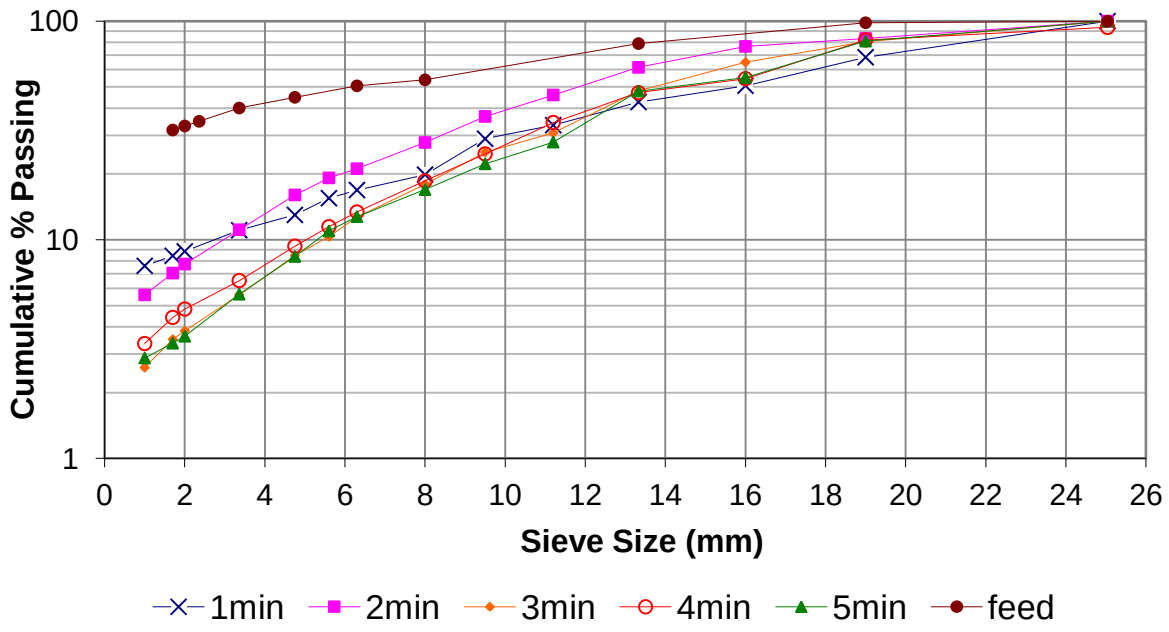

Figure 2.24 Size distribution of gold ore (sample I) with 7% agglomerate moisture content and different agglomeration times as noted in the legend

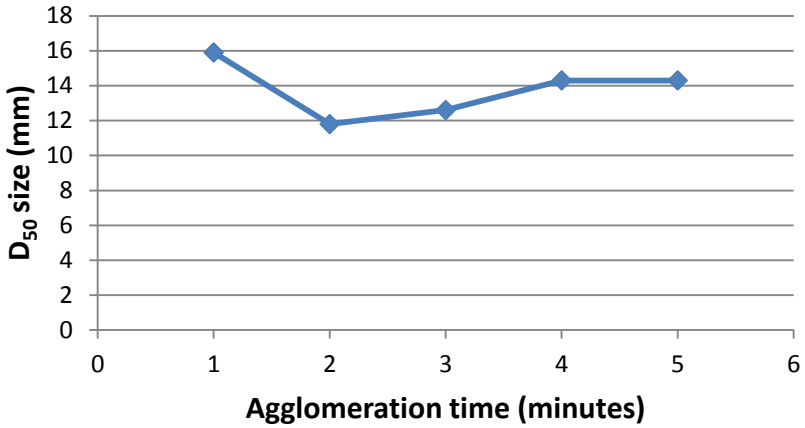

Figure 2.25 D_{50} size of agglomerated gold ore (sample I) with 7% agglomerate moisture content, at different agglomeration times as indicated.

2.5.2 Conductivity

Conductivity does not change by a large quantity as a function of agglomeration time. 1-minute agglomeration time results in lowest conductivity. Conductivity increased generally as the time increased as shown in Figure 2.26.

2.5.3 Permeability

Permeability increased slightly as the agglomeration time increased as shown in Figure 2.27. The 1-minute agglomeration time has the lowest permeability due to a lot of fine particles and inadequate mixing.

2.5.4 Soak Test

Results from the soak tests indicate that the migration of fine particles decreased as the agglomeration time increased and fine migration reaches a plateau as time exeeds 3 minutes of agglomeration as shown in Figure 2.28.

2.5.5 Turbidity

Turbidity is a measure of very fine particle migration during flow through agglomerates. Turbidity generally follows the same trend with respect to agglomeration time as soak test fines migration. Turbidity at different agglomeration times is shown in Figure 2.29.

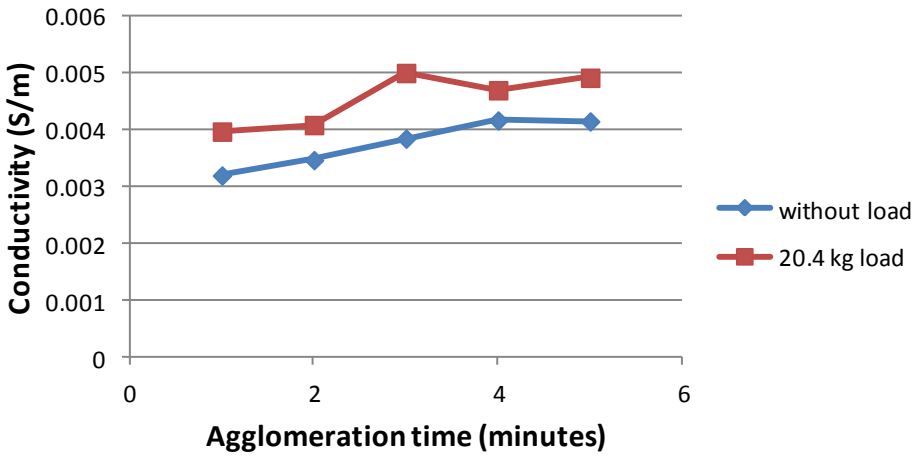

Figure 2.26 Conductivity of agglomerated gold ore (sample I) with 7% agglomerate moisture content, at different agglomeration times as indicated

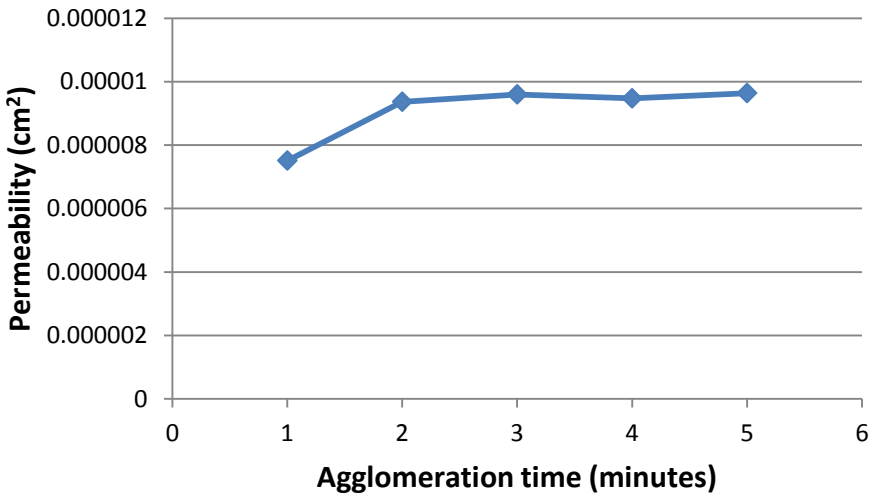

Figure 2.27 Permeability of agglomerated gold ore (sample I) with 7% agglomerate moisture content, at different agglomeration times as indicated

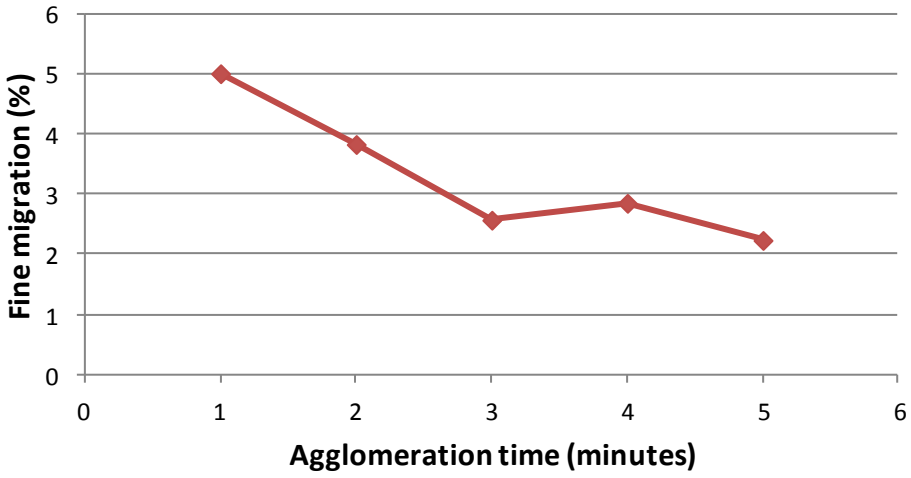

Figure 2.28 Fine migration of agglomerated gold ore (sample I) with 7% agglomerate moisture content, at different agglomeration times as indicated.

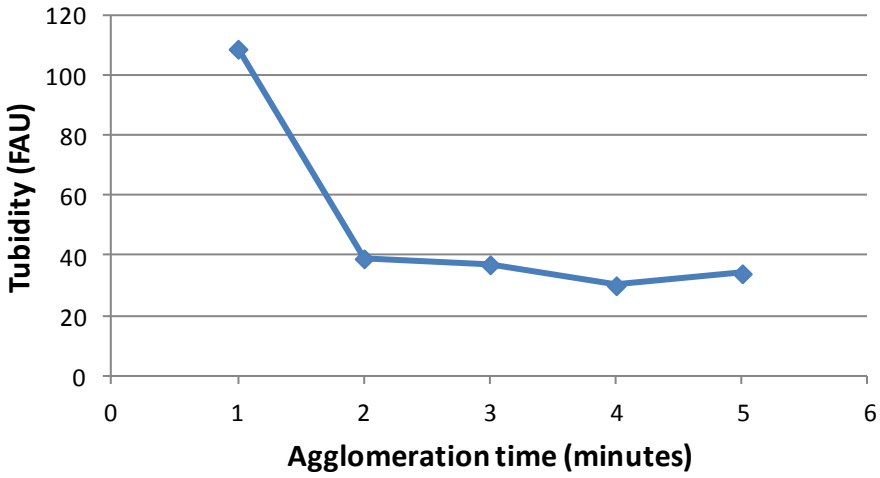

2.29 Turbidity of agglomerated gold ore (sample I) with 7% agglomerate moisture content, at different agglomeration times as indicated.

2.6 Effects of Drum Speed [gold ore (sample I)]

2.6.1 Size Distribution

Results from the drum speed tests are presented in Figures 2.30 to 2.37. The drum speed evaluation tests were performed using 7% agglomerate moisture content and 3 minutes of agglomeration time. Tests were performed between 10 and 60% of the critical speed, where the critical speed is defined as the speed at which centrifugal forces balance gravitational forces.

At 60% of the critical speed fine particles stick to the drum's wall due to the centrifugal force as shown in Figure 2.35. The fine particles were taken off the drum wall and dried with the other agglomerates. At 30% critical speed more coarse agglomerates were produced than at the other speeds as indicated by the size distribution information presented in Figures 2.36 and 2.37.

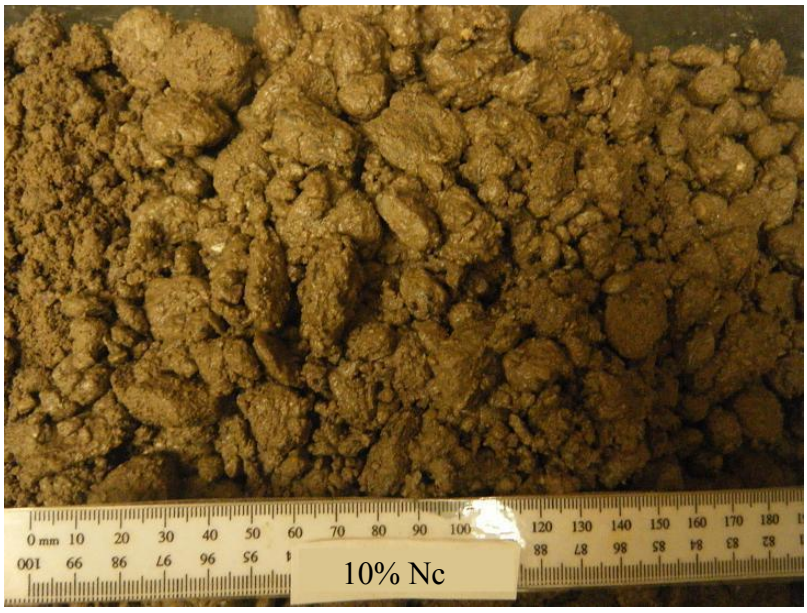

Figure 2.30 Gold ore (sample I) agglomerated with 7% moisture content, 3 minutes of agglomeration time, and 10% critical speed

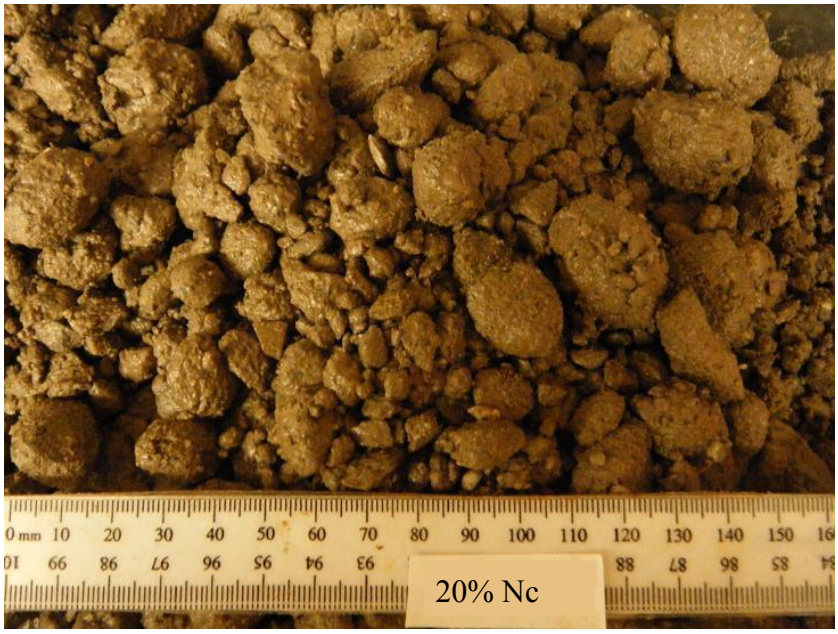

Figure 2.31 Gold ore (sample I) agglomerated with 7% moisture content, 3 minutes of agglomeration time, and 20% critical speed

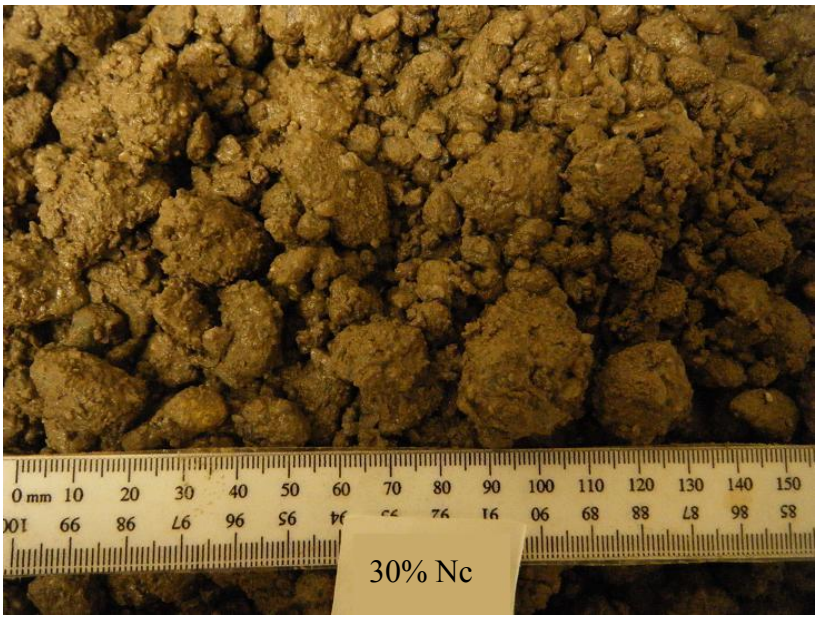

Figure 2.32 Gold ore (sample I) agglomerated with 7% moisture content, 3 minutes of agglomeration time, and 30% critical speed

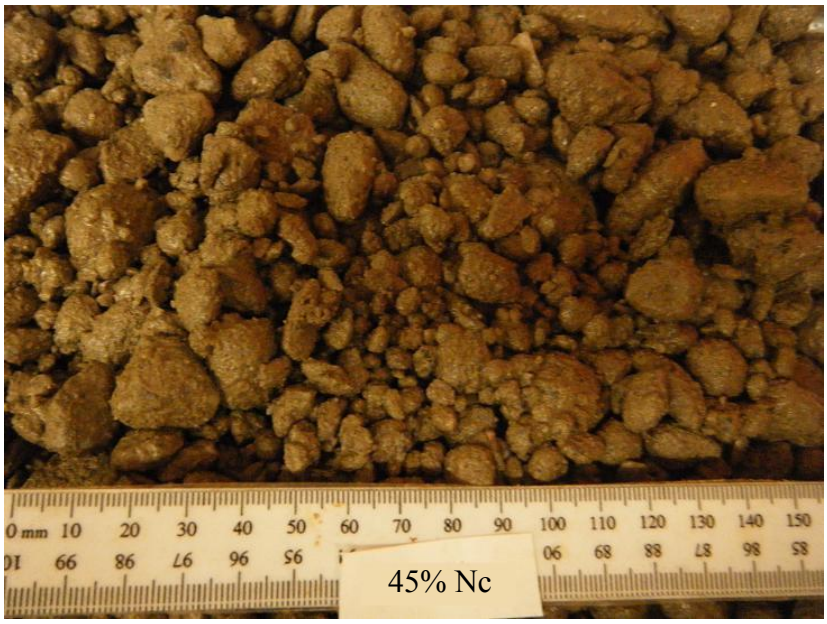

Figure 2.33 Gold ore (sample I) agglomerated with 7% moisture content, 3 minutes of agglomeration time, and 45% critical speed

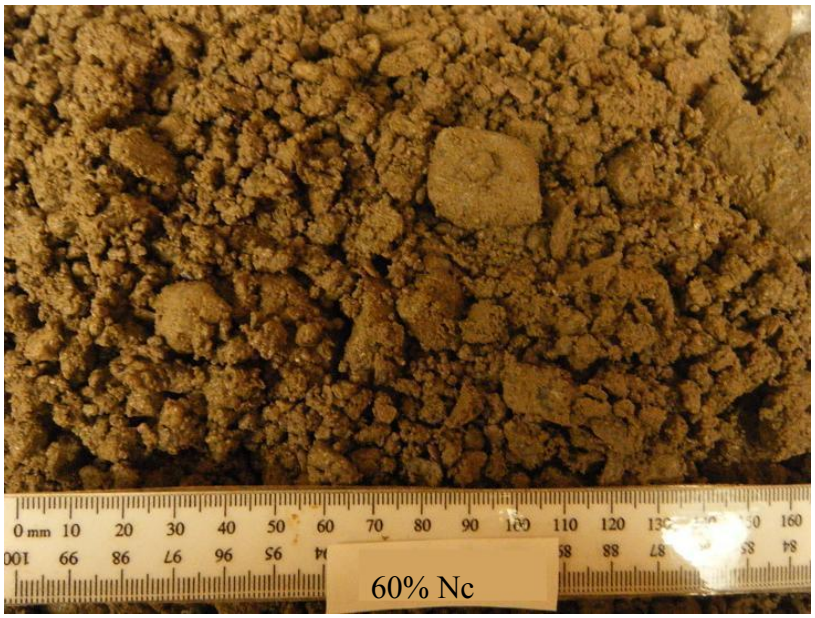

Figure 2.34 Gold ore (sample I) agglomerated with 7% moisture content, 3 minutes of agglomeration time, and 60% critical speed

Figure 2.35 Fines particles on the drum wall after agglomeration at 60% of the critical speed

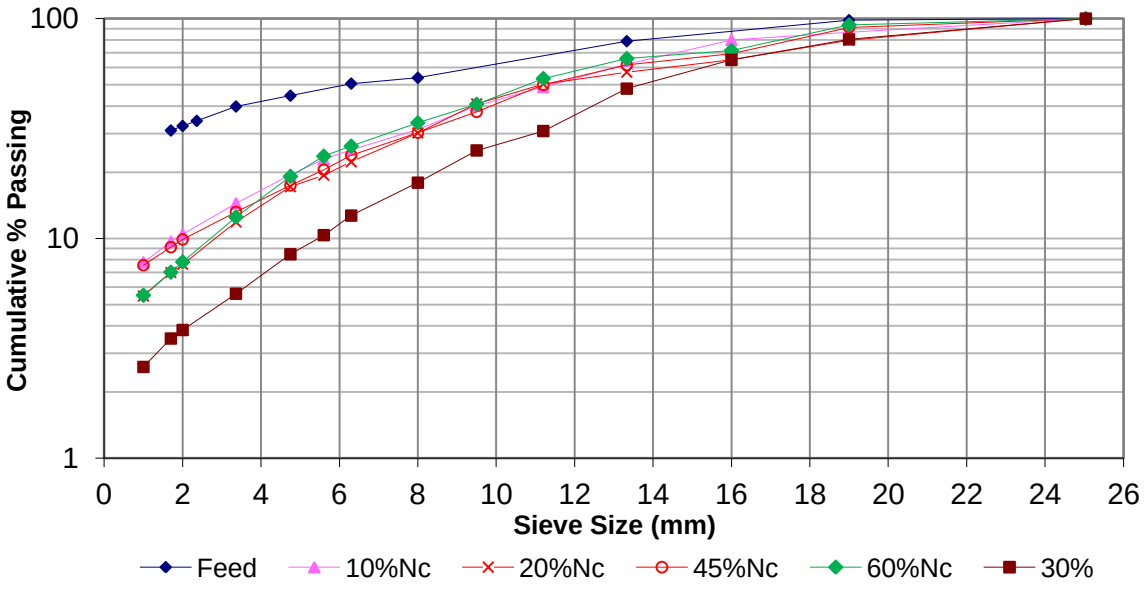

Figure 2.36 Size distribution of gold ore (sample I) agglomerated with 7% moisture content, 3 minutes of agglomeration time, at different drum speeds as noted in the legend

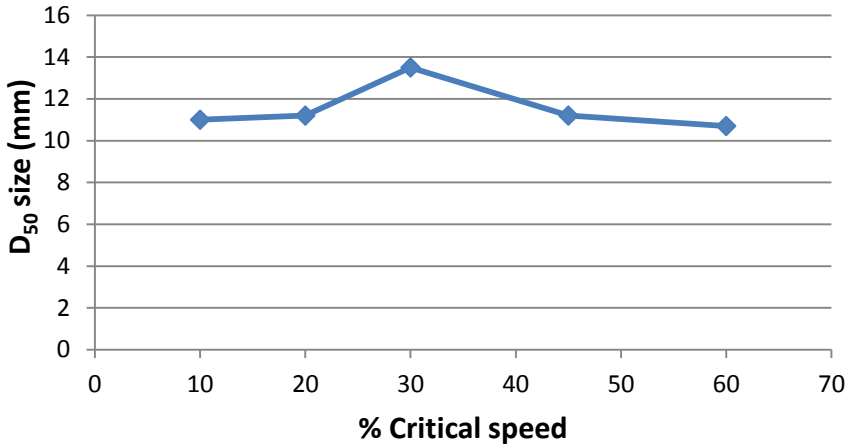

Figure 2.37 D_{50} size distribution of gold ore (sample I) agglomerated with 7% moisture content, 3 minutes of agglomeration time, at different drum speeds as indicated.

2.6.2 Conductivity

The effect of drum speed was also evaluated to determine its effect on conductivity. Because conductivity is most strongly affected by moisture and ionic strength of the solution, and the moisture content in this series of tests was constant at 7%. The conductivity was not significantly affected by drum speed as shown in Figure 2.38.

2.6.3 Permeability

At 45% and 60% of the critical speed, a lot fine particles did not agglomerate with larger particles so the permeability decreased at the higher speeds as shown in Figure 2.39.

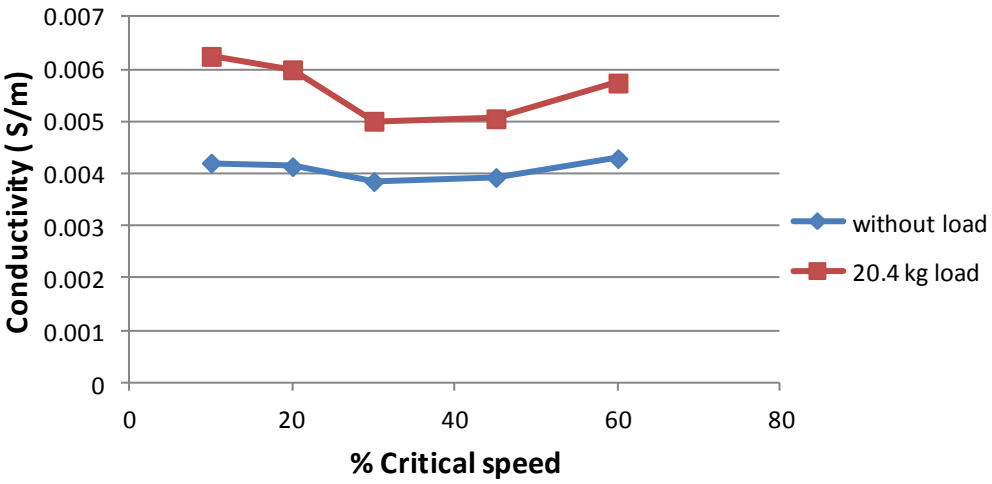

Figure 2.38 Conductivity of gold ore (sample I) agglomerated with 7% moisture content, 3 minutes of agglomeration time, at different drum speeds as indicated.

2.6.4 Soak Test

Fine migration data, presented in Figure 2.40, show that fines are reduced to low levels at 30% of the critical speed relative to either higher or lower drum speeds.

2.6.5 Turbidity

Turbidity, which utilized solution that had flowed through a column of agglomerated ore during permeability tests, was related to the fine migration percentage. The turbidity decreased as the critical speed increased up to 30% of the critical speed. The turbidity increased above 30% of the critical speed as shown in Figure 2.41.

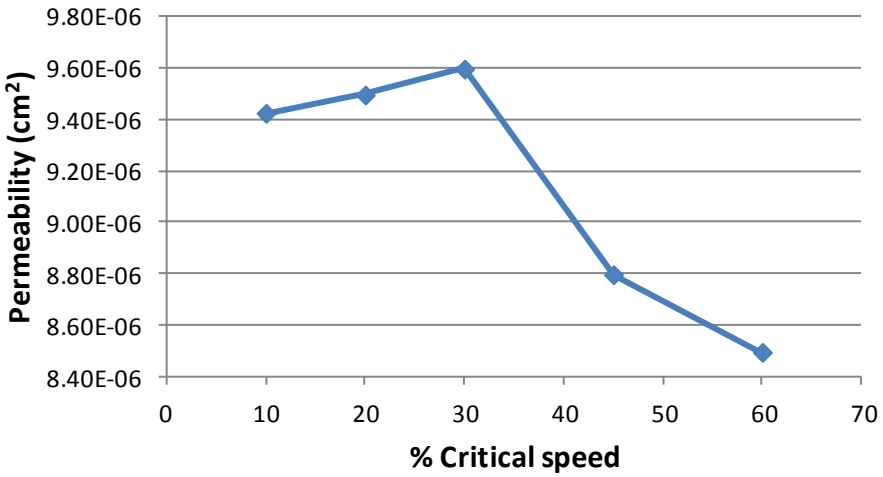

Figure 2.39 Permeability of gold ore (sample I) agglomerated with 7% moisture content, 3 minutes of agglomeration time, at different drum speeds as indicated.

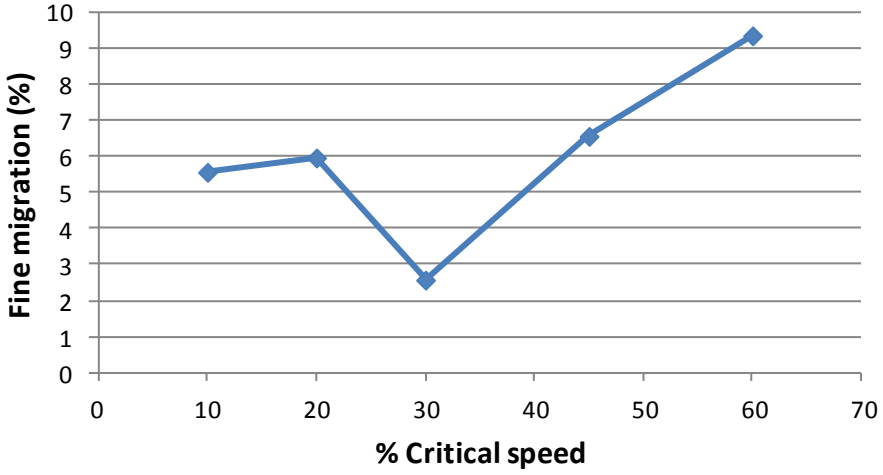

Figure 2.40 Fine particle migration percentage of gold ore (sample I) agglomerated with 7% moisture content, 3 minutes of agglomeration time, at different drum speeds as indicated.

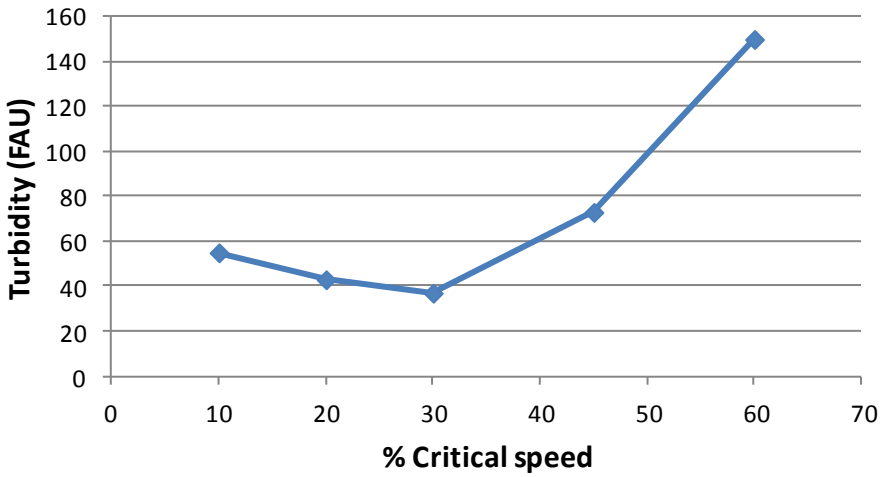

Figure 2.41 Turbidity of gold ore (sample I) agglomerated with 7% moisture content, 3 minutes of agglomeration time, at different drum speeds as indicated.

2.7 Gold ore (sample II) Scoping Test Prior to Column Leaching

Scoping tests were performed using gold ore (sample II) to provide information about agglomeration parameters and agglomerate properties. The resulting information was used to appropriately select agglomeration conditions to prepare ore material for column leaching. A small agglomerator was used to reduce the amount of sample needed for scoping tests relative to the amount needed for previous scoping tests. Other experimental procedures remained the same as discussed in connection with the scoping tests performed on the gold ore (sample I).

2.7.1 Agglomeration Procedures for Gold Ore (sample II)

Five hundred-gram samples of gold ore (sample II) were agglomerated in a 1-liter plastic drum in batch mode. The drum is 9 cm in diameter and 17 cm long. The plastic drum was closed at one end with a central port in the other end to allow the introduction of ore and

liquid. The drum has three 5-mm thick, 2 cm wide and 14.3 long cm plastic lifters installed 120° apart inside to assist the tumbling motion. The samples were dry mixed for 5 minutes with the needed amount of Portland cement (Type II) as binder prior to the agglomeration to insure that the solids were well-mixed prior to agglomeration. Moisture was added using a 1000 ppm NaCN solution, which was introduced into the agglomeration drum through a syringe and tube with small spray holes facing downward. The pH of the mixture was greater than 11 due to the alkalinity of the cement. The solution flow rate and amount was controlled using a 60 ml syringe. Liquid was introduced for the first 1/3rd of the retention time. The drum operated at the desired speed. An image of the small agglomerator and the syringe with spraying tube is shown in Figure 2.42.

2.7.2 Particle Size Distributions of Agglomerated Gold Ore (sample II)

Agglomerated ores were taken out from the agglomeration drum and air dried for one hour before additional testing. Size distribution information as well as pictures of the agglomerates are shown in Figures 2.43-2.48.

(a) (b)

Figure 2.42 Image of small agglomerator (a) and the syringe with spraying tube (b)

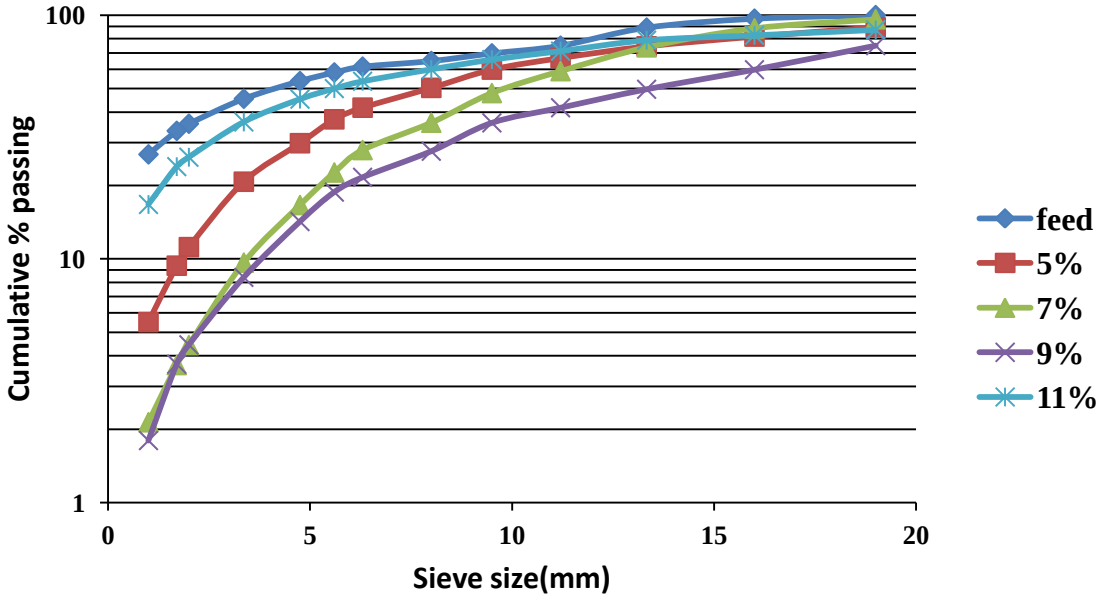

Figure 2.43 Particle size distribution of agglomerated gold ore (sample II) at different agglomerate moisture levels with 8 kg of cement per tonne of ore

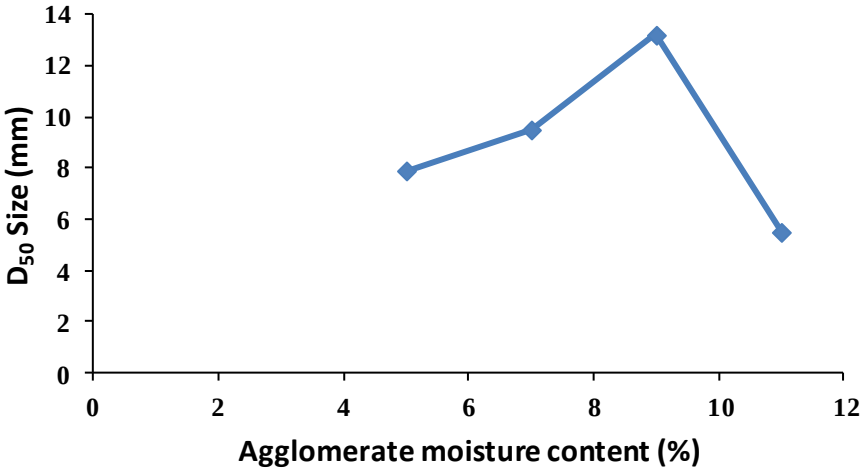

Figure 2.44 D_{50} size of agglomerated gold ore (sample II) at different agglomerate moisture levels with 8 kg of cement per tonne of ore

(a) (b)

Figure 2.45 Gold ore (sample II) agglomerated with 5% moisture content [fresh agglomerates (a), and dried agglomerates (b)] with 8 kg of cement per tonne of ore.

(a) (b)

Figure 2.46 Gold ore (sample II) agglomerated with 7% moisture content [fresh agglomerates (a), and dried agglomerates (b)] with 8 kg of cement per tonne of ore.

(a) (b)

Figure 2.47 Gold ore (sample II) agglomerated with 9% moisture content [fresh agglomerates (a), and dried agglomerates (b)] with 8 kg of cement per tonne of ore.

(a) (b)

Figure 2.48 Gold ore (sample II) agglomerated with 11% moisture content [fresh agglomerates (a), and dried agglomerates (b)] with 8 kg of cement per tonne of ore.

Figures 2.45 to 2.48 illustrate that the agglomerated ore starts forming agglomerates with 5% agglomerate moisture content. Figures 2.43 and 2.44 show that the D_{50} of the agglomerates starts to increase with increasing moisture content until 9% agglomerate moisture content is reached. The D_{50} decreases above 9% agglomerate moisture content. Figure 2.48 shows that the agglomerates with 11% agglomerate moisture content formed a mud-like agglomerate material. When dried, the mud-like material formed larger pieces than were originally formed by agglomeration as determined by hand sieving. It is believed that the mud settles or consolidates to form larger particles than were made by agglomeration.

2.7.3 Conductivity of Agglomerated Gold Ore (sample II)

As Figure 2.49 shows, conductivity data for 5%, 7%, 9% and 11% agglomerate moisture content contents consistently increase as moisture content increases. The gold ore (sample II) tests had conductivity values similar to those measured for the gold ore (sample I) as shown in Figure 2.49. Conductivity is strongly related to moisture above the 4 % agglomerate moisture content as shown. This trend is consistent with data for other ores that also show that conductivity is a good indicator of moisture content within appropriate ranges.

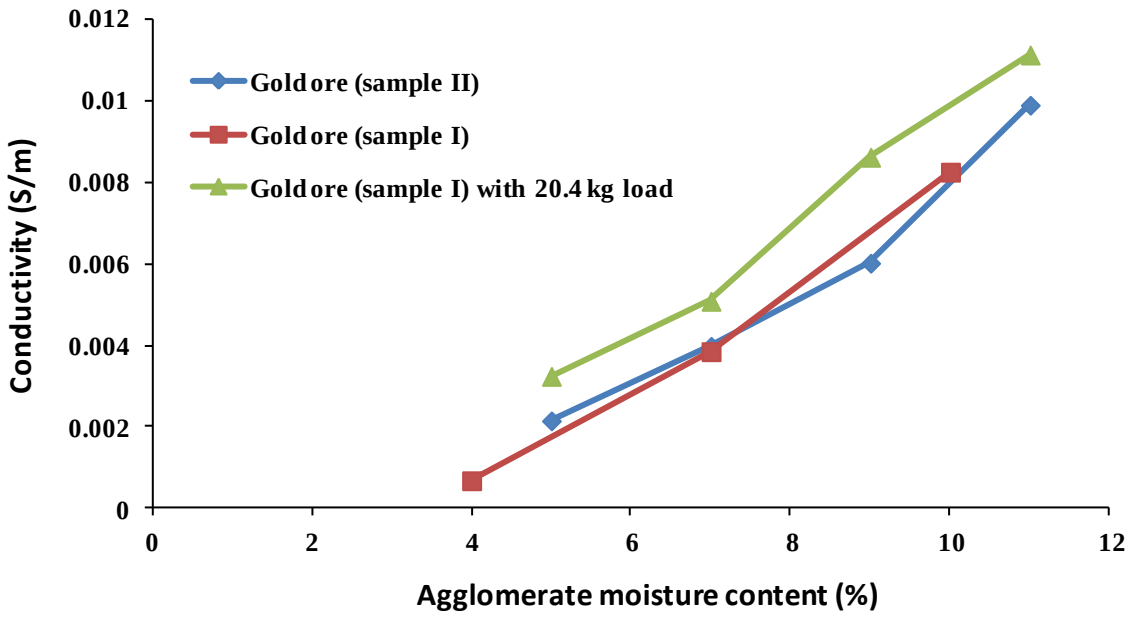

Figure 2.49 Conductivity of agglomerated ore as a function of moisture with 8 kg of cement per tonne of ore

2.7.4 Fines Migration of Agglomerated Gold Ore (sample II)

Soak tests provided information about agglomerate stability. Fine particles released from agglomerates during soak tests are not securely attached. The released or migrated particles that fall through the screen are quantitatively tracked as "fines migration" as a fraction of the ore sample. The size distribution and the fines migration of the agglomerates are shown in Figures 2.50 and 2.51 as a function of binder addition. Increasing cement binder from 6 to 8 kg/ton reduced fines migration from 5.3% to 2.6%. However, increasing cement binder from 8 to 10 kg/ton reduced fines migration by only 1%. Thus, a reasonable amount of binder is very effective, but additional binder above a useful level is not effective in reducing fines migration.

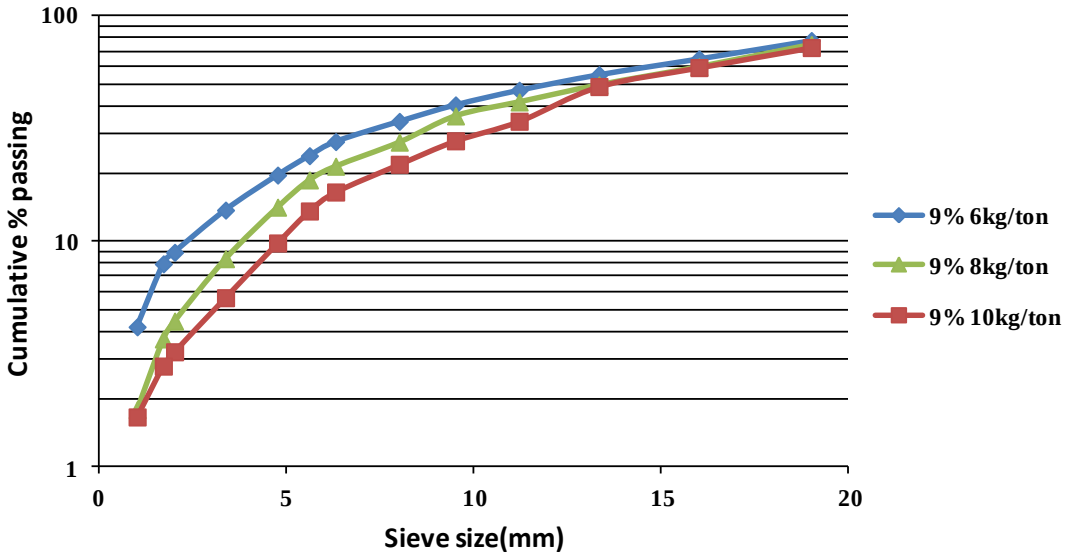

Figure 2.50 Particle size distribution of gold ore (sample II) agglomerated with 7% moisture content, 3 minutes agglomeration time for different amounts of cement binder.

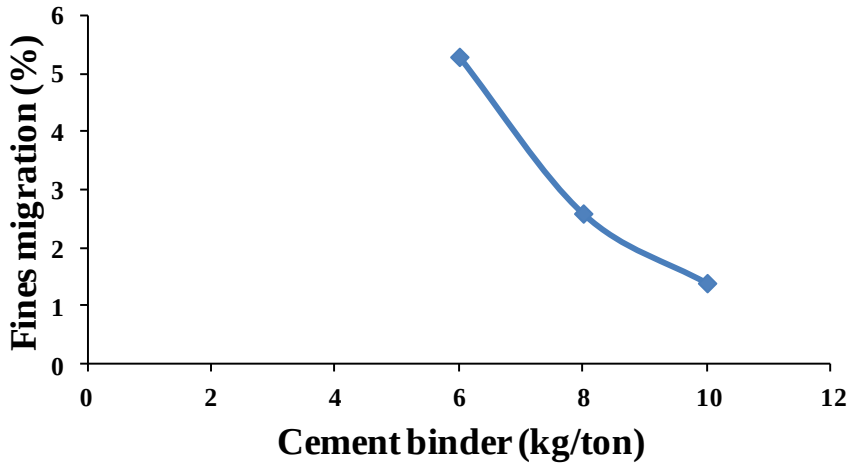

Figure 2.51 Fines migration of gold ore (sample II) agglomerated with 7% moisture content, 3 minutes agglomeration time for different amounts of cement binder.

Scoping test results for the gold ore (sample II) showed that the best agglomerates were formed at 9 % agglomerate moisture content and 8 kg/ton cement binder addition. Electrical conductivity measurements showed a consistent increase in conductivity with increasing moisture in a trend that is very similar to the gold ore (sample I). Column leaching was designed based on a factorial design of experiments using agglomeration conditions discussed in this study.

2.8 Gold Ore Agglomerates Structure Analysis

Agglomerate characterization and particle adhesion due to capillary forces were evaluated to provide more information about agglomerate properties of the gold ore (sample I). Agglomeration characterization was performed using X-ray computerized tomography (CT), quantitative evaluation of minerals by scanning electron microscopy

(QEMSCAN), and scanning electron microscope (SEM) imaging and analyses to provide internal structure and agglomerate surface composition information.

2.8.1 X-ray Computerized Tomography (CT)

X-ray computerized tomography is an X-ray- based method which gathers 2D X-ray images of the sample in different directions and reconstructs the data in a 3D image. Originally, X-ray computerized tomography was used for medical services. However, this technique has also been applied to nonmedical and industrial applications. A simple step to computed 3D images is illuminating the sample. A projection of the attenuation coefficients is measured for each direction. Then the image is reconstructed based on mathematical computations.

For quantitative examination, cone-beam X-ray Micro Tomography (XMT) is appropriate due to high resolution. As technology advances, it becomes more feasible to map greater details in mineralogical textures of ore particles. High-resolution X-ray micro CT (HRXMT) can be used to analyze multiphase particles ranging from 40 mm to a few hundred microns. Samples are rotated and a two-dimensional projection is used to reconstruct a 3D image. Figure 2.52 shows a schematic diagram for a cone-beam X-ray micro-CT system.

X-rays from the micro focus point are attenuated by the sample. One rotation of the sample is adequate for a whole 3D data set. Transmitted X-rays are detected by a planar 2D detector. A 3D image is reconstructed from the collected set of projection images by the image processing system. The gold ore (sample I) agglomerated with 4, 6 and 8% agglomerate moisture contents were analyzed by cone-beam X-ray micro-CT. A

comparison of the sliced images from the agglomerated gold ore (sample I) particles are shown in Figures 2.53a-2.53c.

From Figures 2.53a-2.53c, gold ore (sample I) agglomerated with 4% agglomerate moisture content shows thin layer of fines coated on coarser particles. Growth of the agglomerates was not observed, which indicated that there was not enough liquid present to promote a liquid bridge between particles. Fine particles were still loose and scattered. At the 6% agglomerate moisture content, a thicker fine particle layer was formed due to more available liquid. At the 8% agglomerate moisture content, which is the optimal moisture level from scoping experiment, an appropriate amount of moisture was present to form liquid bridges, holding not only fines, but also coarser particles while fine particles were connected between coarser particles. The 3D split views of agglomerates with 4, 6 and 8% of agglomerate moisture content are shown in Figure 2.54a-2.54c. Void spaces between agglomerated ore can be observed from the 3D split views of the agglomerates. At the 4% agglomerate moisture content, there are a lot of tiny spaces which lead to poor permeability. The larger void spaces are available at the 6% and 8% agglomerate moisture content, which greatly improves the permeability and helps distribute leaching solution through the material during leaching.

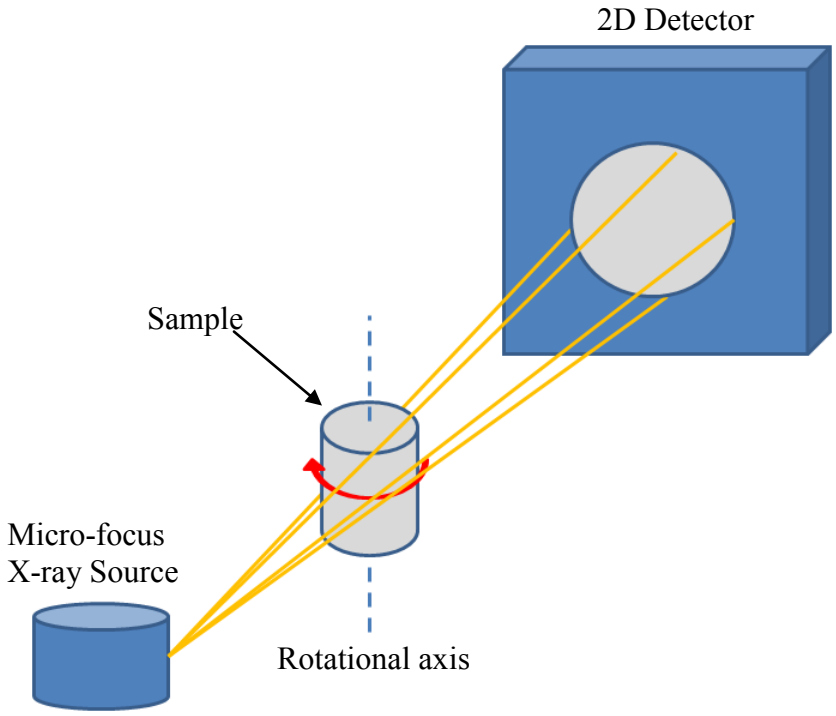

Figure 2.52 a schematic diagram for the cone-beam geometry X-ray micro-CT system [adapted from (Miller & Lin, 2003)]

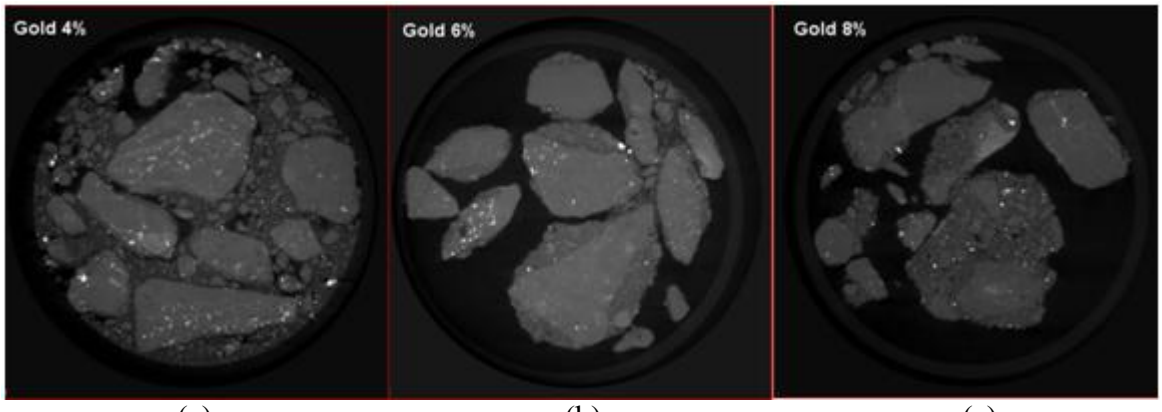

(a) (b) (c)

Figure 2.53 Comparison of the sliced images from the gold ore (sample I) agglomerated with 4% (a), 6% (b), and 8% (c) agglomerate moisture content using X-ray CT.

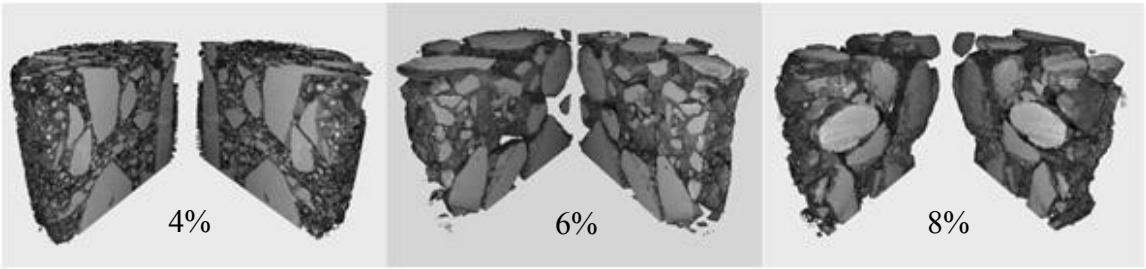

(a) (b) (c)

Figure 2.54 The 3D split views of agglomerates with 4% (a), 6% (b) and 8% (c) agglomerate moisture content

2.8.2 Scanning Electron Microscope (SEM) and Quantitative Evaluation of Minerals by Scanning Electron Microscopy (QEMSCAN)

SEM and QEMSCAN generally share the same electron microscope mechanics. Electron microscopes use electrons instead of light, which provides advantages such as a large depth of field and much higher resolution. In a vacuum chamber, a beam of electrons released from an electron gun at the top of microscope travels through electromagnetic fields and lenses. The electron beam is focused and projected on carbon or gold coated sample. Detectors collect X-rays, backscattered electrons and secondary electrons which are released from the sample and then convert them to an image. Figure 2.55 shows a schematic diagram for scanning electron microscope.

QEMSCAN shares the same mechanics as SEM. QEMSAN identifies most rock and minerals from back scattered electron and secondary electron signals then analyzes mineral proportion and chemical assay based on backscattered electrons (BSE) and energy dispersive spectroscopy (EDS). The advantage of QEMSCAN is the ability to map the sample surface based on mineral and phase classification.

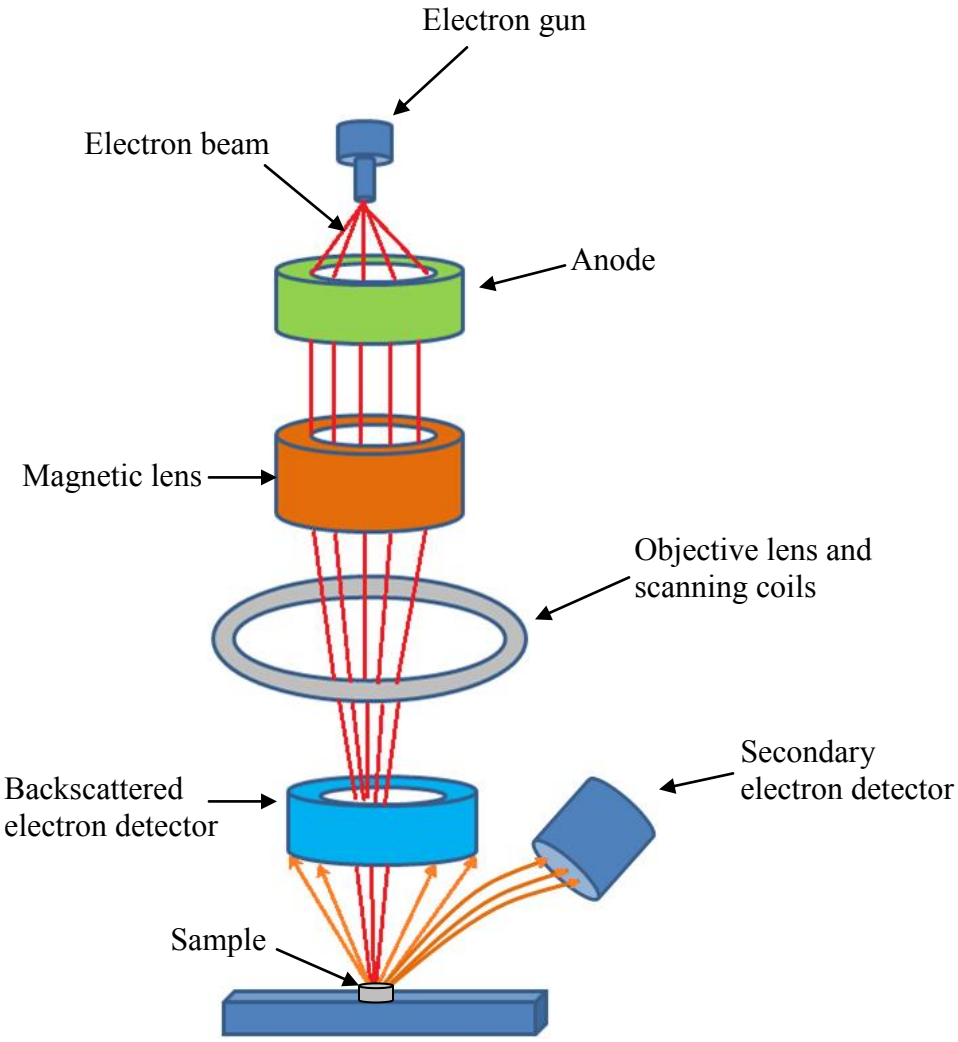

Figure 2.55 A schematic diagram for scanning electron microscope [adapted from (Bertin, 1978)]

After the agglomeration, which involved the addition of 7% agglomerate moisture content using a 1000 ppm cyanide solution, fine particles were attached to coarser particles in sphere-like structures. Several of the resulting agglomerates were mounted in epoxy, cross-sectioned, and polished to facilitate surface analyses. Figure 2.56 shows a mounted agglomerate sample. The highlighted area in Figure 2.56 shows the area of the agglomerate that was evaluated by QEMSCAN. The sample was carbon coated to facilitate subsequent analyses.

Figure 2.57 shows a back scattered electron (BSE) image that was acquired in a portion of the highlighted region of Figure 2.56. Figure 2.57 shows that fine particles were packed along with the coarser particles. However, there are small spaces between particles. The big particles at the bottom of the Figure 2.57 are actually a composite of many particles as shown in Figure 2.58. Thus the BSE image did not effectively resolve most of the finer, agglomerated particles.

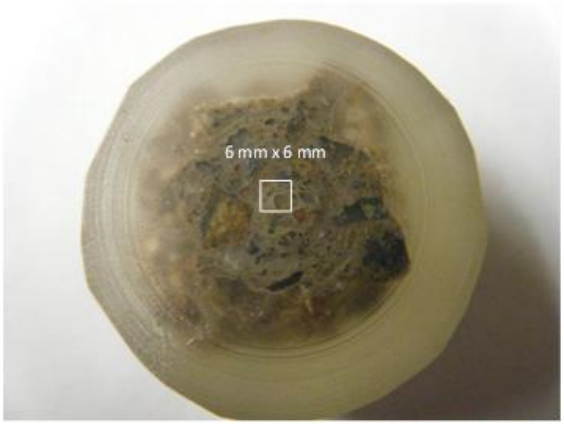

Figure 2.56 View of a mounted agglomerate specimen with a highlighted 6 mm x 6 mm QEMSCAN analysis area [gold ore (sample I) agglomerate prepared with 7% agglomerate moisture content]

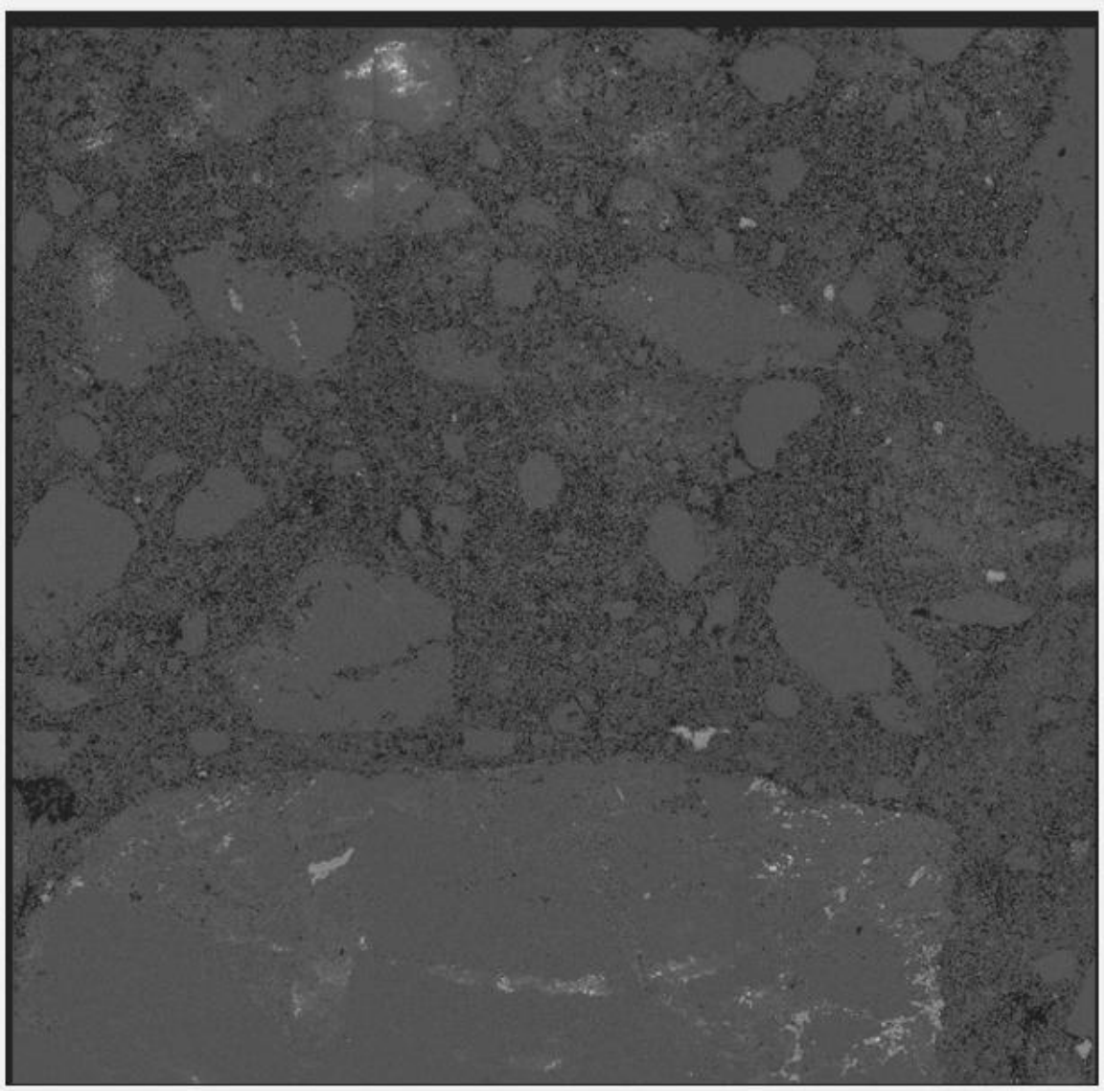

Figure 2.57 Back scattered electron (BSE) image of the agglomerate analysis area in Figure 2.56

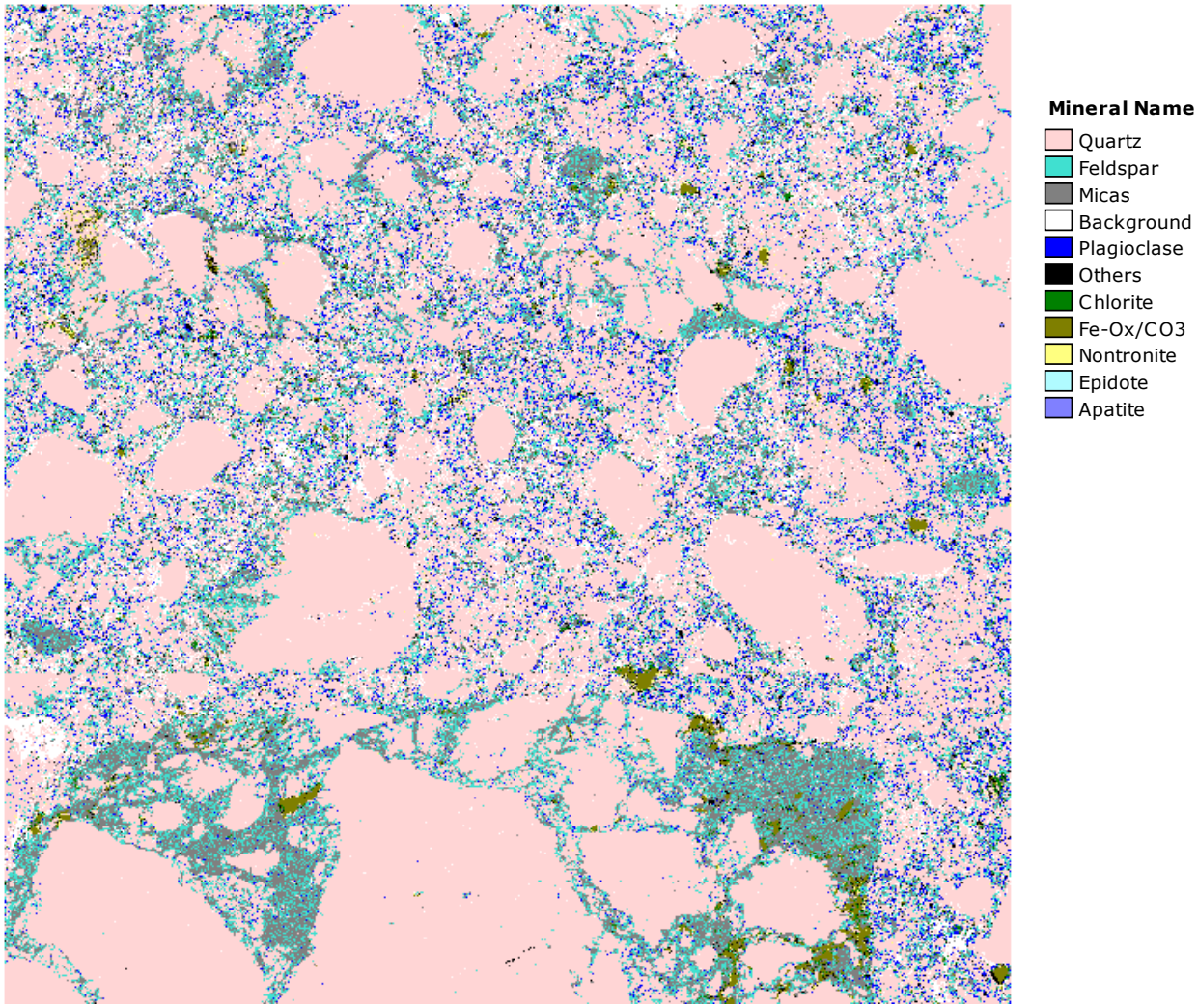

Figure 2.58 QEMSCAN image of the gold ore (sample I) agglomerate analysis area of Figure 2.56

The QEMSCAN image (Figure 2.58) shows that most of the coarse particles were quartz, and that most of the fine particles were plagioclase and feldspar. The porosity can be determined by measuring the background area which is shown as the white areas in Figure 2.58. The picture was analyzed using Image J® software. The analysis indicates that the porosity of the agglomerate was 8.57% based on the background white areas. The black color is associated with the other minerals.

High resolution SEM/EDS images of the agglomerate surface were acquired to evaluate local composition and structure. The agglomerate samples were prepared the same way as the QEMSCAN samples, and the same agglomeration conditions were used.

The first SEM/EDS analysis area was the middle of the agglomerate which consisted of many small and larger particles that formed a small agglomerate ball. The SEM image of a portion of the highlighted analysis area of Figure 2.59 is presented as Figure 2.60.

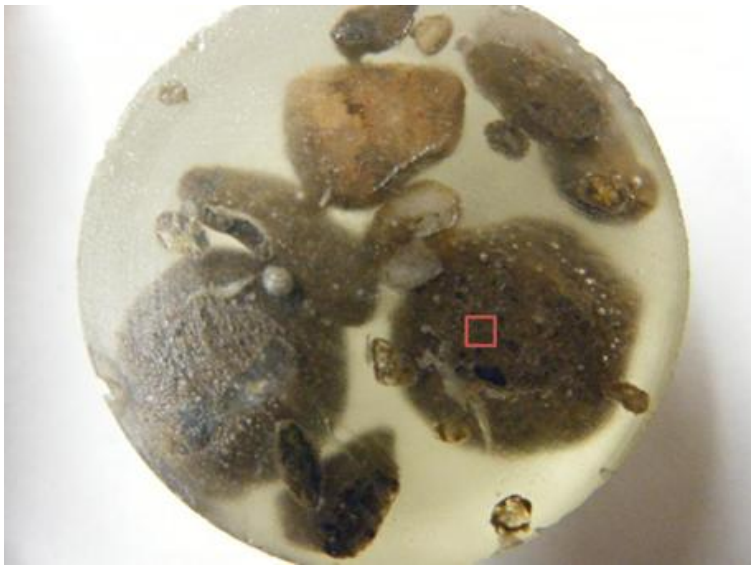

Figure 2.59 Mounted agglomerates [7% agglomerate moisture content gold ore (sample I) agglomerates] for SEM analysis. The highlighted square shows the first area analyzed by the SEM

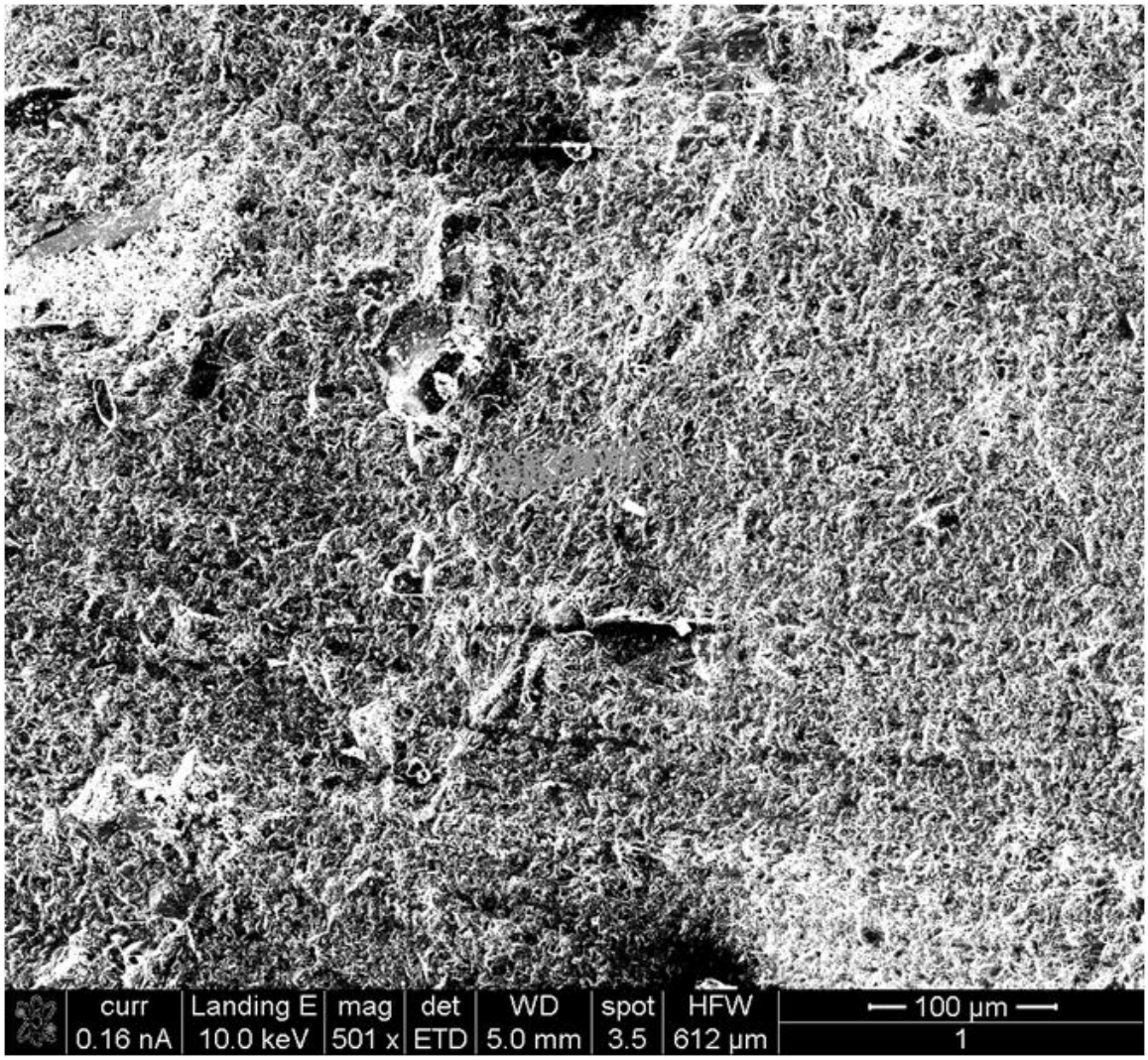

Figure 2.60 SEM image of a small portion of the first analysis area that is highlighted in Figure 2.59.

As shown in Figure 2.60 the ore has a rough surface due to the difficulty of precision polishing that is associated with particle plucking during polishing of the agglomerates. The associated EDS imaging data used for identification of chemical composition of a specimen are presented in Figure 2.61.

Figure 2.61 shows significant amounts of oxygen and silicon, which are the main constituents of quartz. The presence of 19.91% by weight of carbon resulted from the carbon coating process. No other elements were present in significant amounts in this specific specimen area analysis.

The SEM analysis area was changed to a second location as shown by the highlighted square in Figure 2.62 for a second analysis. The second SEM analysis area is a large particle coated with many fine particles, which is different from the first area that consisted of many fine particles packed together to form a much larger ball. A magnified view of a portion of the second analysis area is shown in Figure 2.63.

It is difficult to resolve individual particles in Figure 2.63, although the distinctive trench near the middle of the figure is likely a boundary between two particles. EDS analysis of the highlighted area of Figure 2.63 is presented in Figure 2.64. The EDS information provides insight into the chemical composition of the surface. Oxygen, silicon, and aluminum, which is a minor component of Portland cement were found in this area. Due to the small amount of Portland cement added to the agglomerates (8 kg/ton), it is not anticipated that large concentrations of aluminum will be present due to cement binder. It is possible that the aluminum in this analysis is due to either cement or an aluminum bearing mineral. Additional analysis would be necessary to confirm whether or not it is due to the cement binder.

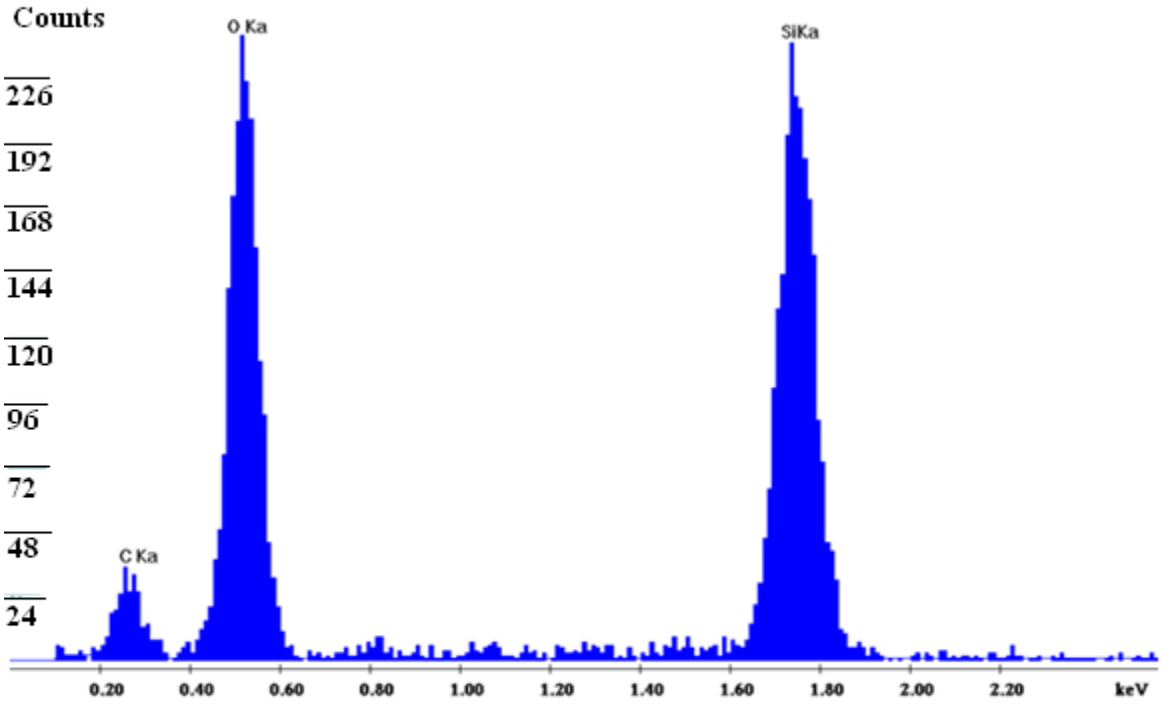

Elem	Wt %	At %	K-Ratio
C	19.91	29.04	0.0503
O	44.60	48.83	0.2265
Si	35.48	22.13	0.3210

Figure 2.61 EDS chemical composition for the material shown in Figure 2.60

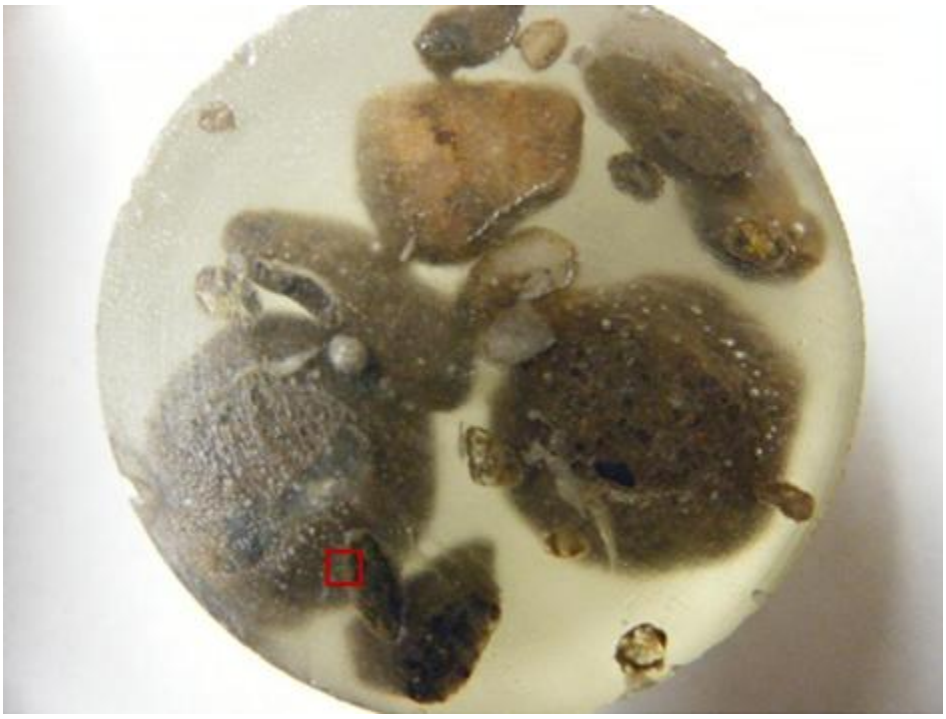

Figure 2.62 Mounted agglomerates [7% agglomerate moisture content gold ore (sample I) agglomerates] for SEM analysis. The highlighted square shows the second area analyzed by the SEM.

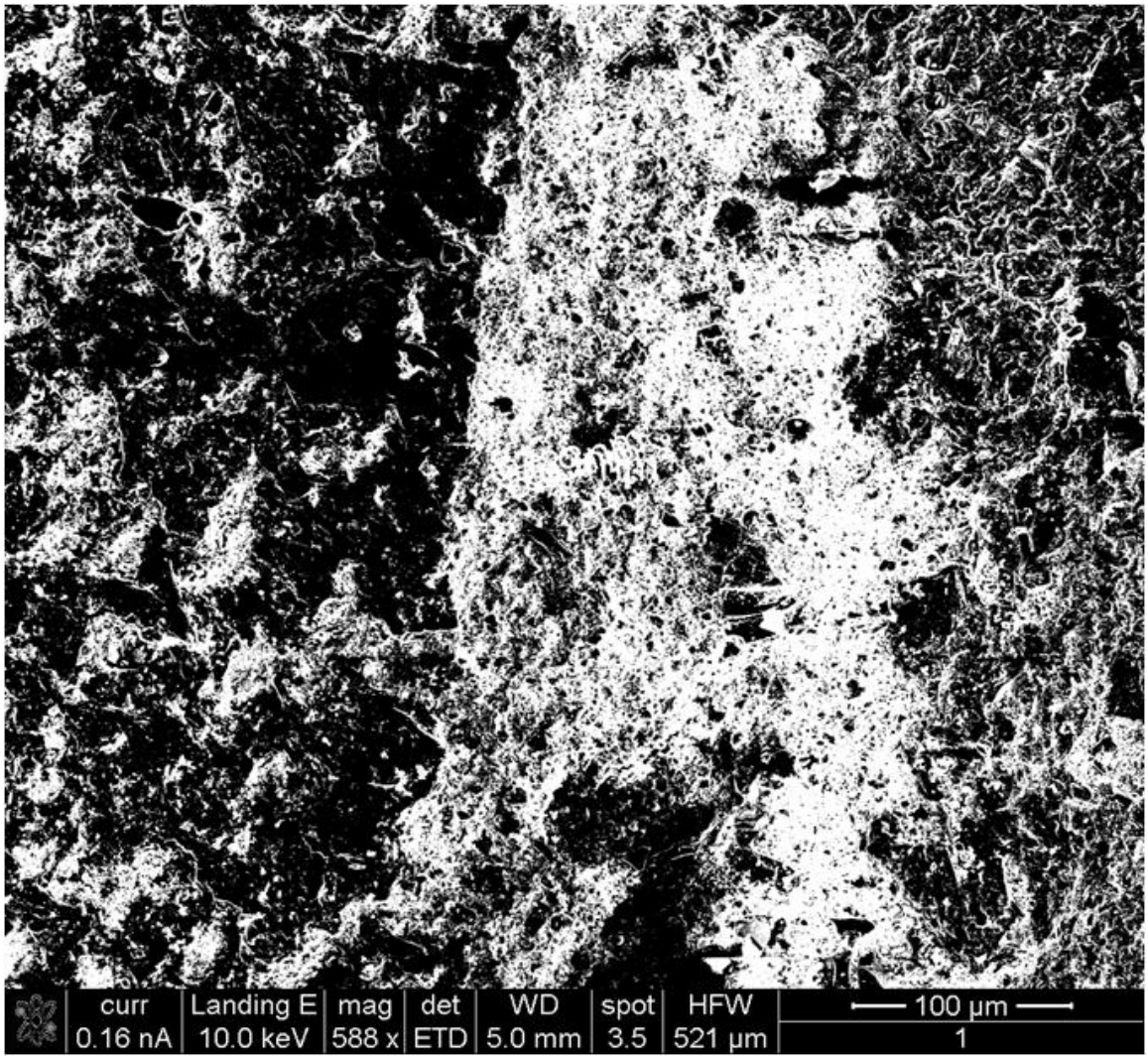

Figure 2.63 SEM image of a portion of the second SEM analysis area

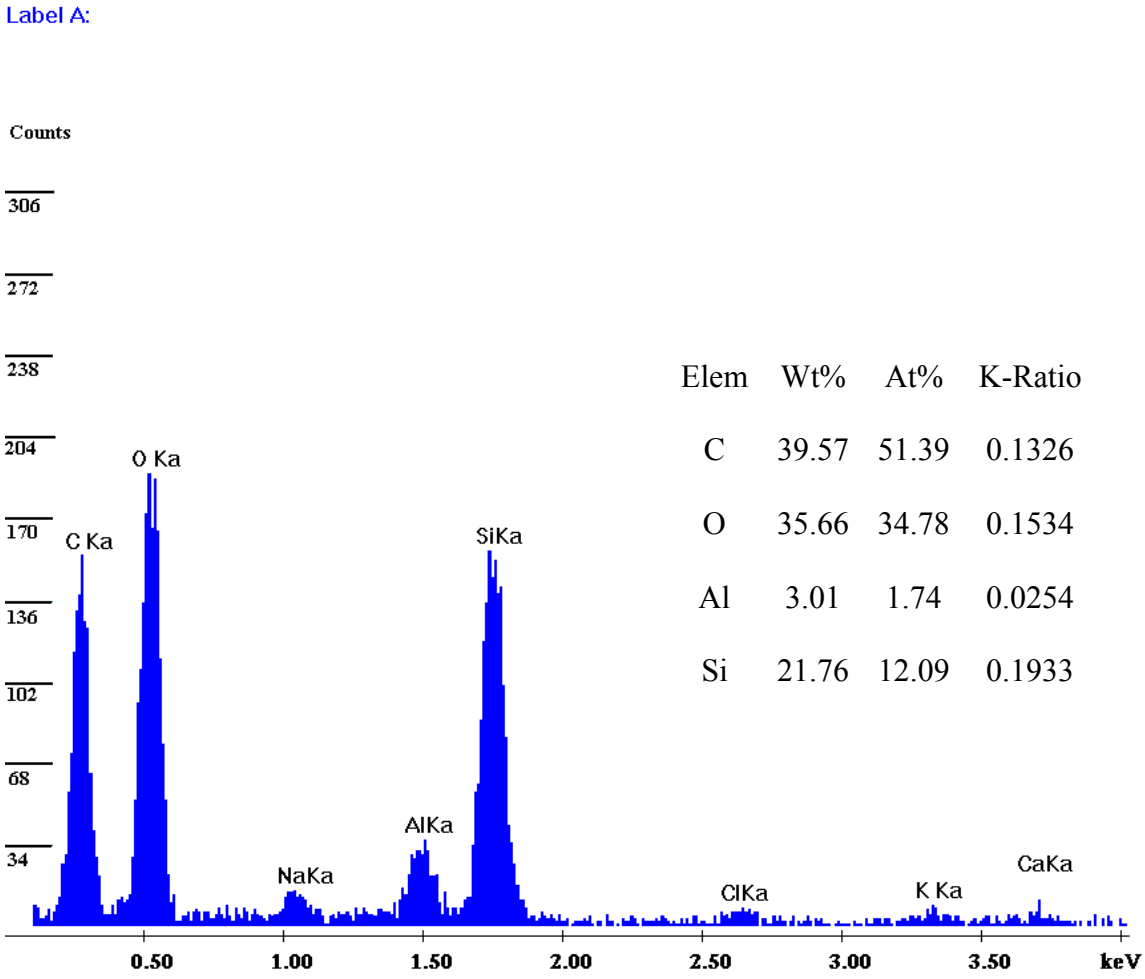

Figure 2.64 EDX showing the chemical composition of the second analysis area.

-

A sample of mounted gold ore (sample I) agglomerates containing 4% agglomerate moisture content is shown in Figure 2.65. This figure shows most of the agglomerates are larger particles coated with fine particles. A magnified SEM view of a portion of the highlighted section in Figure 2.65 is presented in Figure 2.66.

The light colored region between the darker regions is a region of fine particles between two larger particles. An image with increased magnification of the fine particles is shown in Figure 2.67. The EDS analysis of the area presented in Figure 2.67 is shown in Figure 2.68.

The results shown in Figure 2.68 are similar to the second analysis area. However, calcium and aluminum are observed. Because Portland cement contains calcium and aluminum, this finding provides some evidence that Portland cement may have been present at the edge of the agglomerates, which is expected for the gold ore (sample I) agglomerates, such as the one in the analysis, that have Portland cement as a binder.

QEMSCAN data showed that most of the large particles in the agglomerates were quartz and most of the fine particles are plagioclase and feldspar. The internal porosity of the 7% agglomerate moisture content gold ore (sample I) agglomerates was measured by QEMSCAN images to be about 9 %.

SEM/EDS data provided some evidence that Portland cement binder can be detected in isolated areas, although it is clearly not detectable on all surfaces.

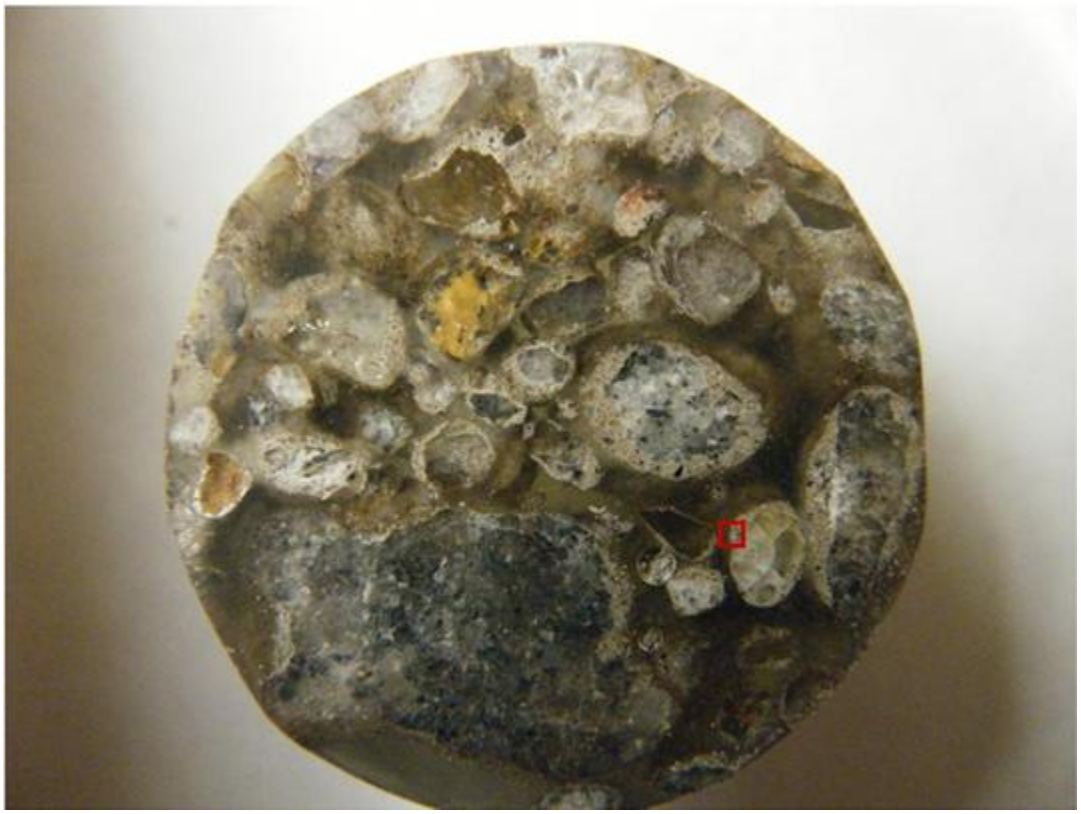

Figure 2.65 Mounted agglomerates [4% agglomerate moisture content gold ore (sample I) agglomerates] for SEM analysis. The highlighted square shows the third area analyzed by the SEM.

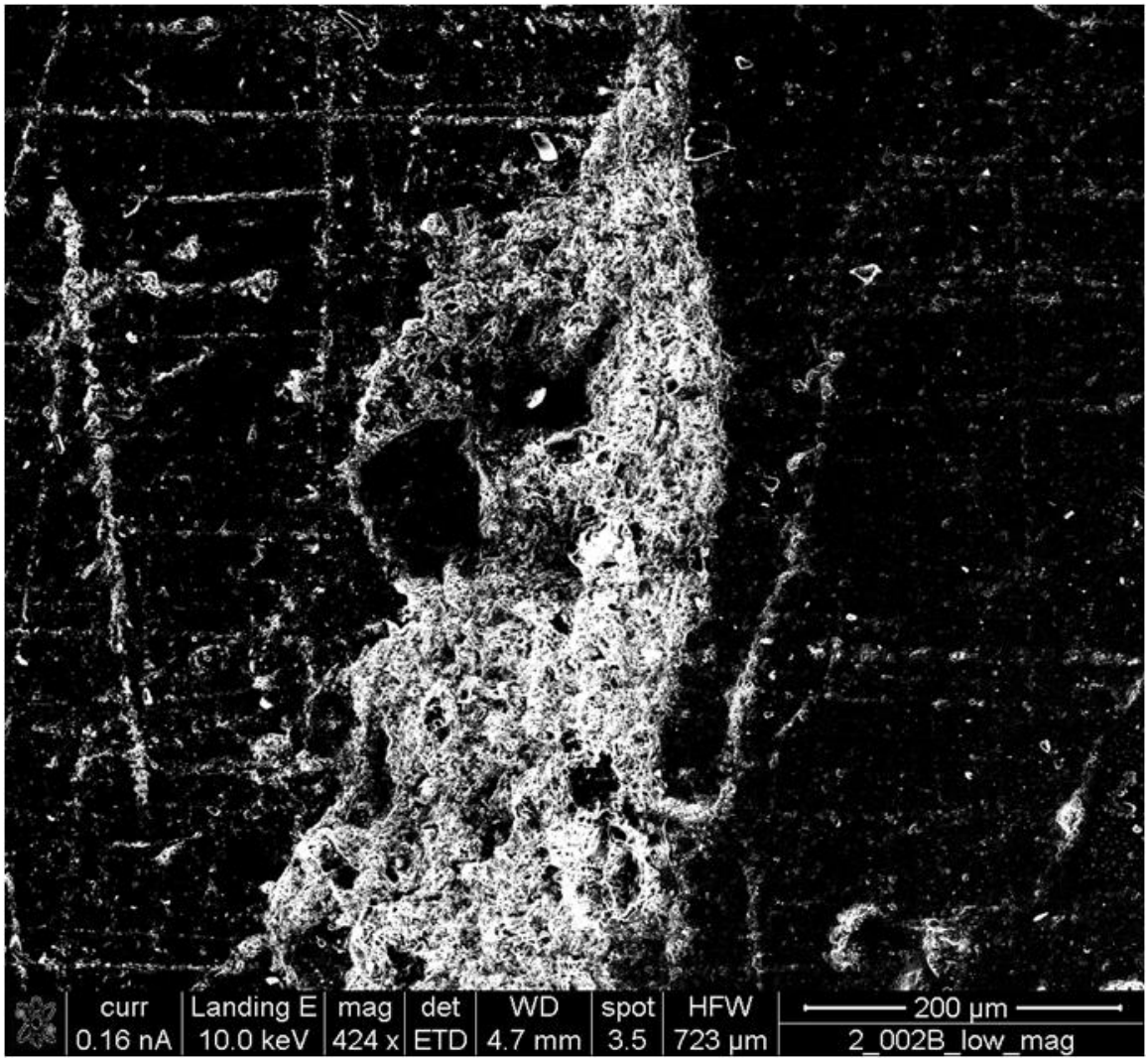

Figure 2.66 SEM image of a portion of the third SEM analysis area.

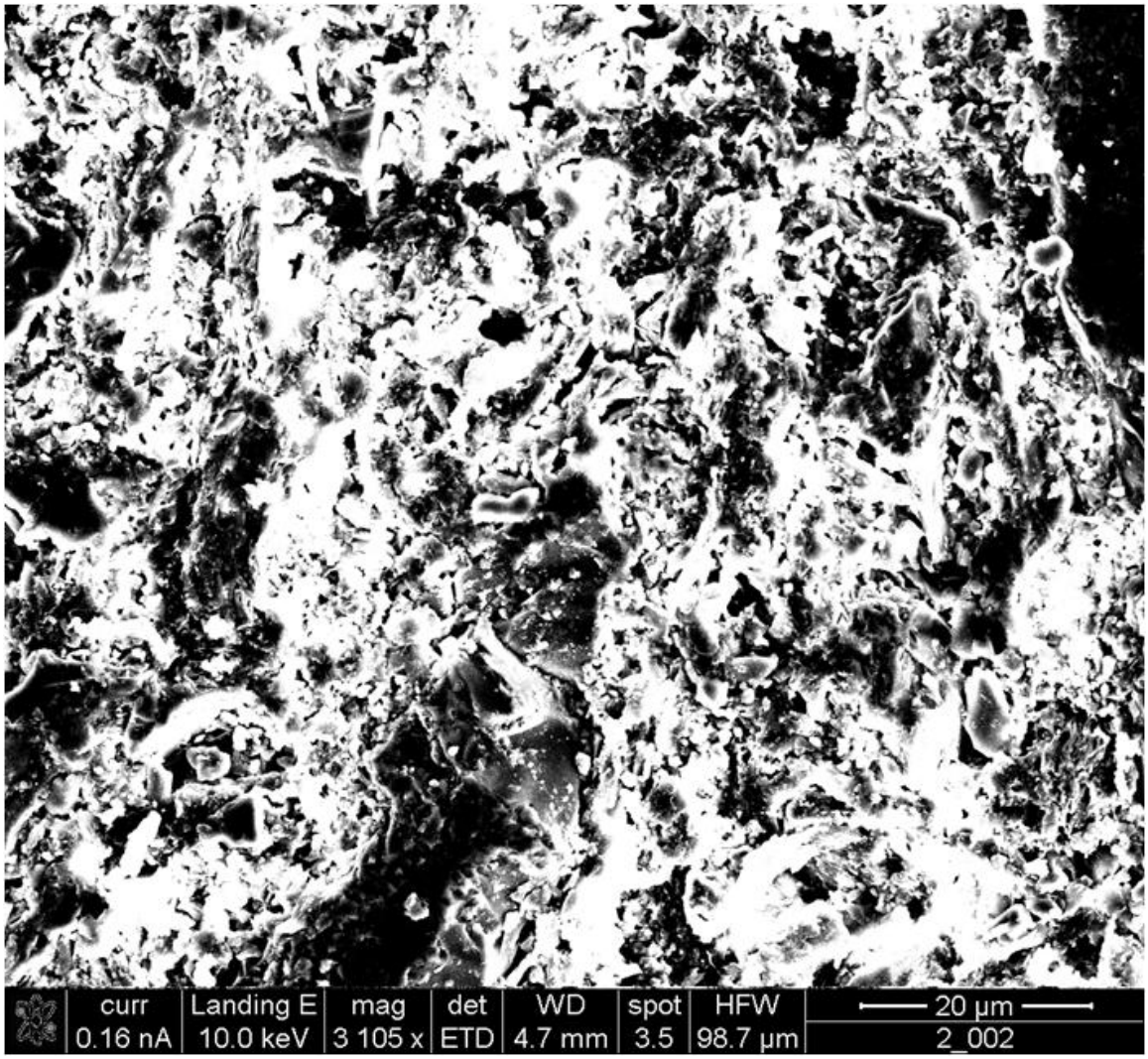

Figure 2.67 High magnification SEM image of a small portion of the light area in Figure 2.66 that contains fine particles.

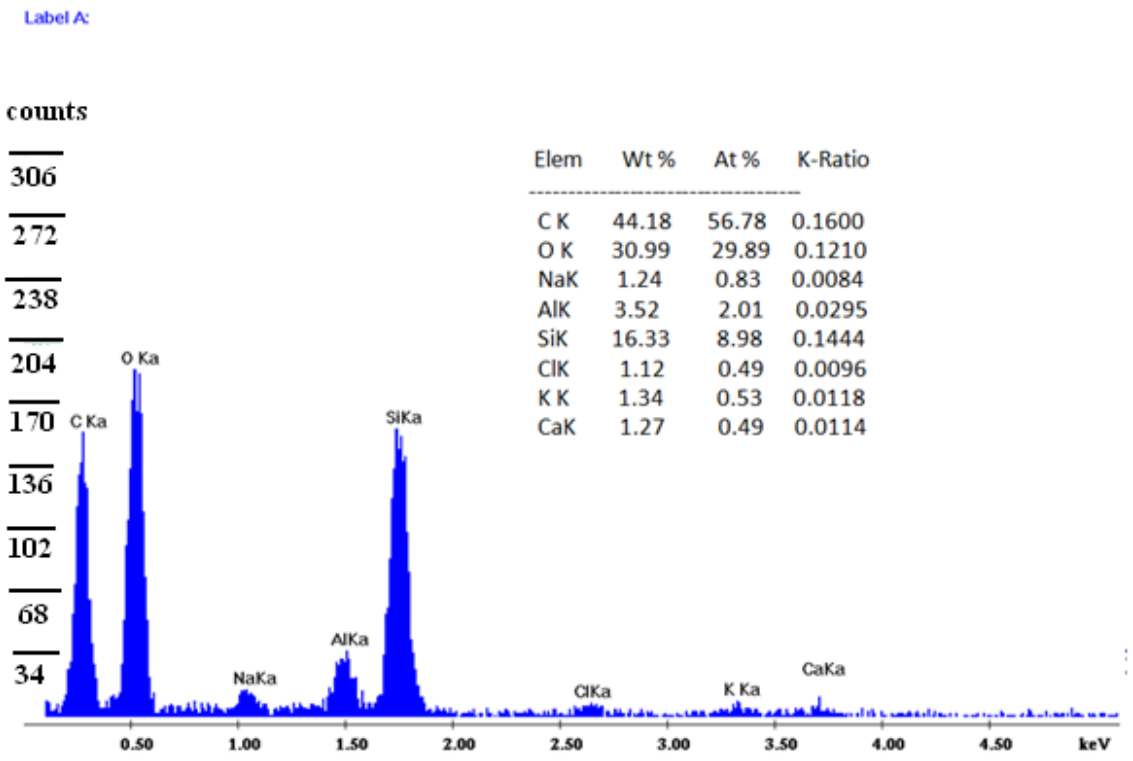

Figure 2.68 EDS result of the chemical composition of the material in Figure 2.67.

2.9 Summary and Conclusions

Permeability data from all of the scoping tests were gathered and compared at each condition tested as presented in Figures 2.69-2.72. The red color represents moisture content at 4 %, the orange represents 10 % agglomerate moisture content, and the blue and green colors represent 7 % agglomerate moisture content content test data. The blue color represents data when agglomeration time was the changing variable and the green color represents data when drum speed was changed as shown in Figure 2.69.

Permeability is the primary parameter of interest in most heap leaching operations and is one of the prime reasons for agglomeration. Moisture content has the greatest effect on the permeability for the variables evaluated in these tests. The highest permeability values are obtained using 7 % agglomerate moisture content, at least 2-3 minutes of agglomeration time, and 30% critical speed.

Conductivity is controlled by moisture and ionic strength of the solution used to add moisture. Loading is also a factor that affects conductivity, and the higher load gave greater conductivity. In this series of scoping tests, conductivity was affected primarily by moisture. The associated data are presented in Figure 2.70.

For the fine particle migration percentage, every condition had a diferent result. Fines migration reached a minimum at 7 % agglomerate moisture content for a 5-minute agglomeration time at a drum speed of 30 % of the critical speed. Fines migration data are shown in Figure 2.71.

Turbidity data shown in Figure 2.72 indicate that agglomeration with 7% agglomerate moisture content for more than 2 minutes resulted in the lowest turbidity which correspond to the same trend presented for fines migration data shown previously in Figure 2.71.

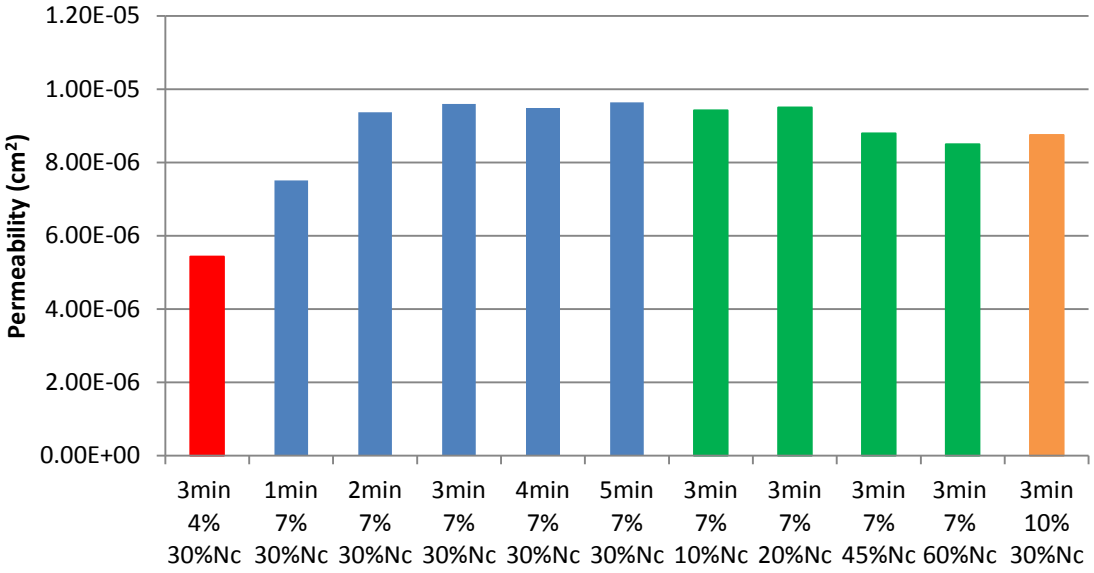

Figure 2.69 Permeability results for different agglomeration conditions

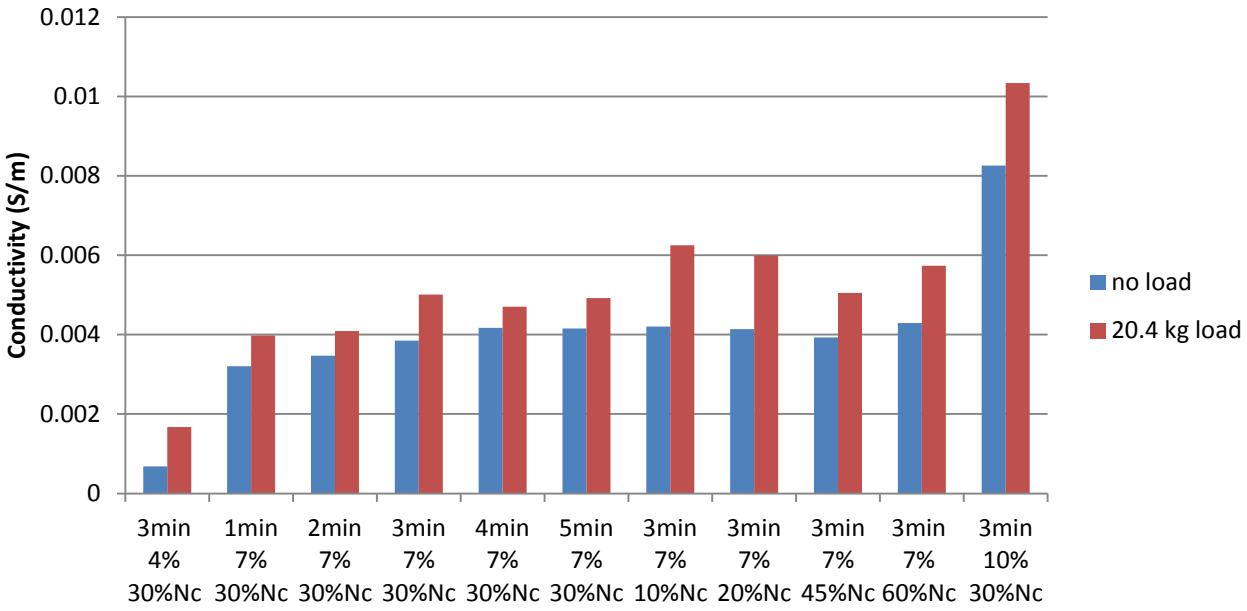

Figure 2.70 Conductivity results for different agglomeration conditions

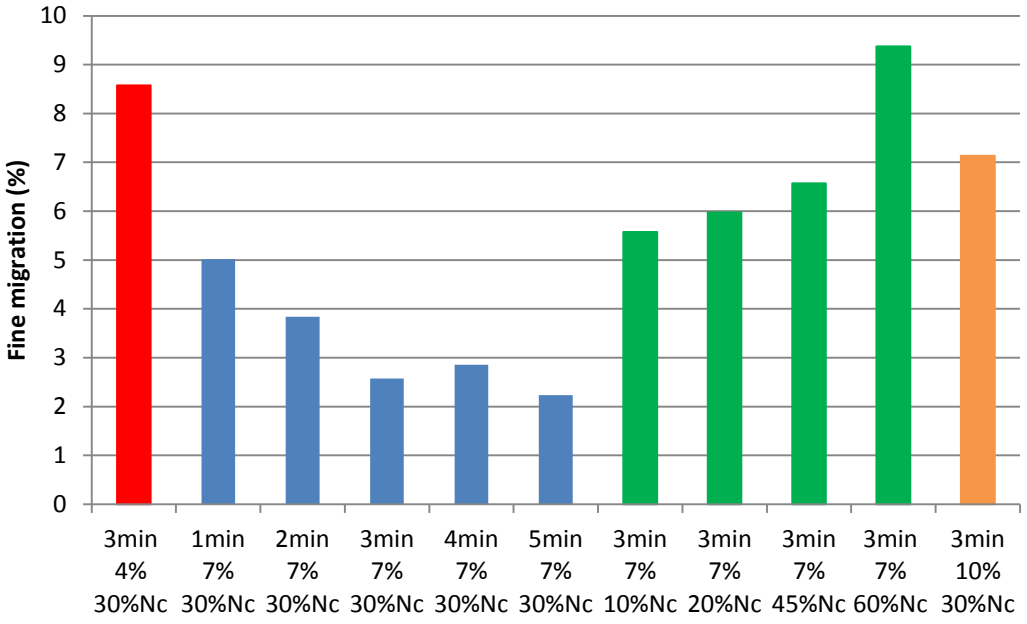

Figure 2.71 Fine particle migration under different agglomeration conditions

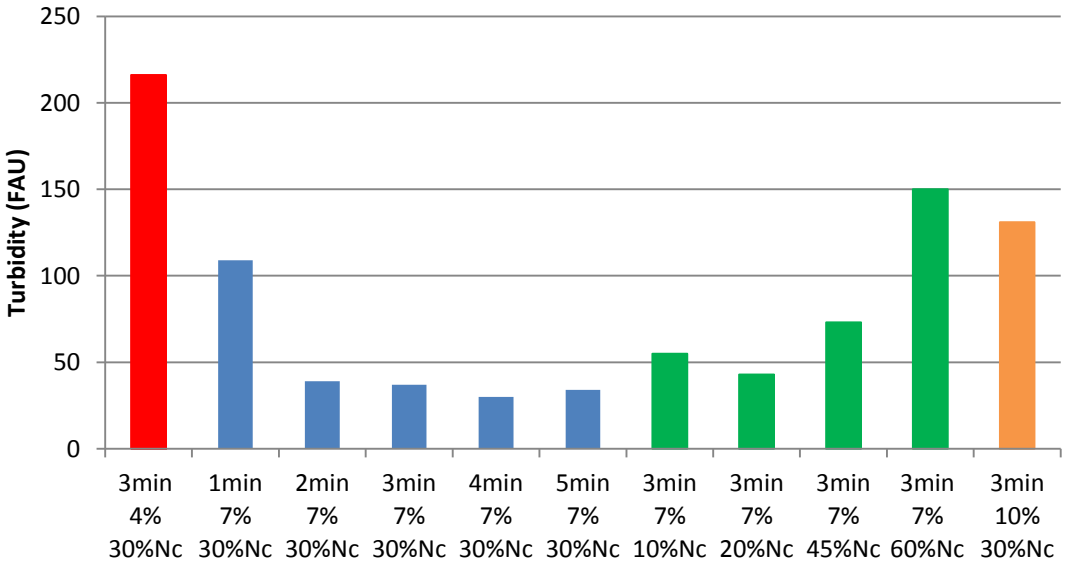

Figure 2.72 Turbidity of liquid from permeability tests of agglomerates in different conditions

CHAPTER 3

LIQUID RETENTION CAPACITY

3.1 Introduction

Good agglomerates can be obtained by keeping the moisture at a level that creates an optimum liquid-particle bridging state for agglomeration which is generally the capillary state. Consequently, the amount of liquid added should not exceed that needed for the capillary state to form desirable agglomerates. This amount of liquid is termed the liquid retention capacity.

Liquid retention capacity is the amount of moisture held in soil or ore particles after excess liquid has drained away. It is known in soil science as the field capacity(Israelson & West, 1922). This amount of moisture is related to the capillary state for agglomeration. If significant moisture is added beyond this state, slurry will form, making agglomeration a mud forming operation, rather than an agglomeration process. Moisture levels below the liquid retention capacity may not produce sufficient capillary bonding for desired agglomeration.

Feed ore for agglomeration consists of particles of uneven size and shape. Therefore, a variety of voids will be left between ore particles in a bed. A schematic diagram of packed ore particles is shown in Figure 3.1a. Liquid is held in void spaces by adhesion (absorbed) liquid and capillary force as shown in Figure 3.1b. When a moisture

saturated ore bed is drained, liquid in larger pores will drain by gravity, leaving air-filled voids inside when the system is unsaturated following initial saturation with liquid. Thus, if ore is saturated with liquid, then allowed to drain in an unsaturated condition without flowing liquid, the drainage will temporarily result in the capillary state for liquid bridging, which is desirable for agglomeration. Consequently, liquid exposure in excess of that needed for agglomeration, followed by drainage can lead to a condition comparable to desired agglomeration moisture content.

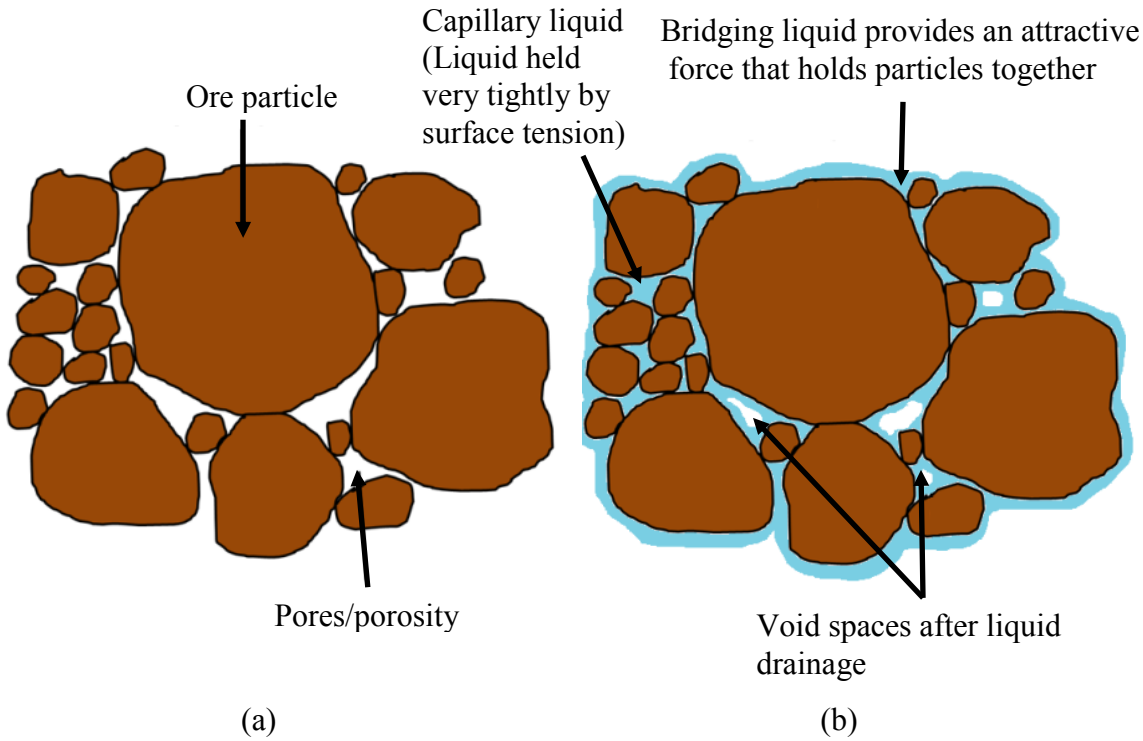

Figure 3.1 Picture illustrates pores/porosity between particles (a). illustration of liquid retention capacity in a bed of packed ore particles (b).

3.2 Liquid Retention Capacity Measurements

A simple measurement procedure has been developed to measure the liquid retention capacity of an ore. This technique uses a capillary rise method to determine the amount of liquid retained in an ore sample. A 2-kg sample of crushed dry feed ore was placed in a 15.25 cm diameter column which is 6 times larger than the largest diameter ore particle to minimize wall effects. A perforated plastic sheet and a plastic screen are used at the bottom to hold the ore particles as shown in Figure 3.2. A glass tray and a perforated plastic sheet were used to facilitate liquid uptake. The perforated sheet was used as a support at the bottom of the column to allow liquid uptake and to maintain the solid contents in the column when the experiment was finished. The column with the ore and perforated plastic sheet were weighed before the liquid retention capacity testing was initiated. After weighing, the column, screen, and perforated sheet were placed in the tray which was filled with enough liquid to cover the bottom of the column as shown in Figure 3.2. After the column was assembled, liquid was added into the tray. The liquid level was maintained approximately 1 cm above the perforated plastic sheet and bottom of the column. (The excess liquid in the saturated zone at the very bottom of the column drained quickly when the column was removed from the liquid in the glass tray)

The time the column remained in the liquid until complete liquid uptake occurred depended on the particle size distribution. The range of liquid uptake time for the ores tested was 20 to 120 minutes. After sufficient time was allowed for liquid uptake, the column was lifted with the perforated sheet securing the column contents. The column was held above the liquid for 10-15 seconds to let excess liquid drain out from the bottom of the column. The wet column was then weighed to determine the liquid uptake

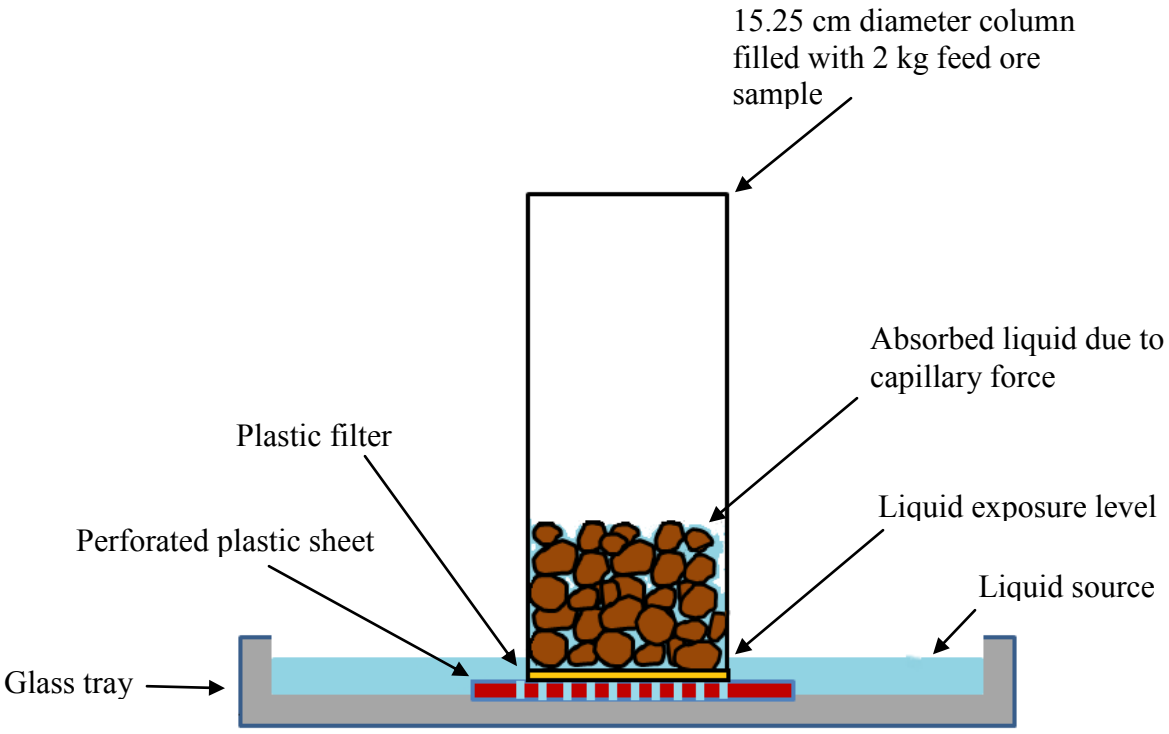

Figure 3.2 Schematic diagram of liquid field capacity measurement apparatus

3.3 Effect of Particle Size Distribution

Particle size and surface area are very important parameters that are closely related to the amount of liquid that can be held by an ore. The importance of this relationship led to an evaluation of the effect of size on retention liquid using gold ore (sample II) particles. Samples of minus 1.5 mm gold ore (sample II) were wet screened and size classified. The uptake of liquid into individual columns containing monosize ore particles was measured using one-half-inch diameter tubes. Moisture content was calculated based on a mass balance and the weights of the capillary column, liquid retained by ore, the initial column, and dry ore. Results from these tests are shown in Figure 3.3.

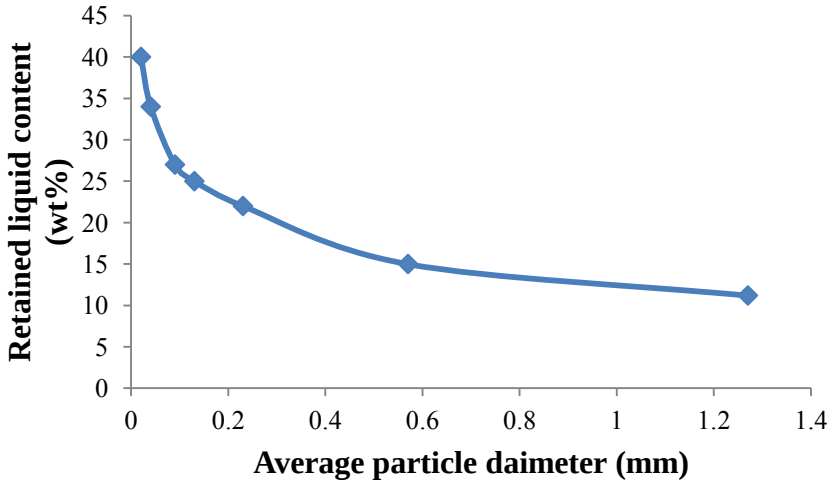

Figure 3.3 Effect of particle size on saturated moisture content.

The data in Figure 3.3 show the expected result that smaller particles retain more liquid than larger particles. The saturated moisture content increases dramatically for particle sizes less than 0.15 mm. Particles that are 0.05 mm in diameter held 40% liquid by weight. Thus, from an agglomeration perspective it is expected that fine particles require more moisture for optimum agglomeration.

Three different types of ore [gold ore(sample II), nickel ore and copper ore] were used to evaluate the liquid retention capacity and optimum agglomeration moisture. The size distribution of the samples is shown in Figure 3.4.

The nickel ore contained more fine particles than the gold and copper ores, which have similar size distributions. The size distribution of minus 2 mm particles also is shown in Figure 3.5. Data in Figure 3.5 show fine particles (minus 2 mm) of nickel ore are much smaller those in than the gold and copper ores used in this study. These minus 2 mm particle fractions were 38 wt% of nickel ore, 35 wt% and 33 wt% for gold and copper ore, respectively.

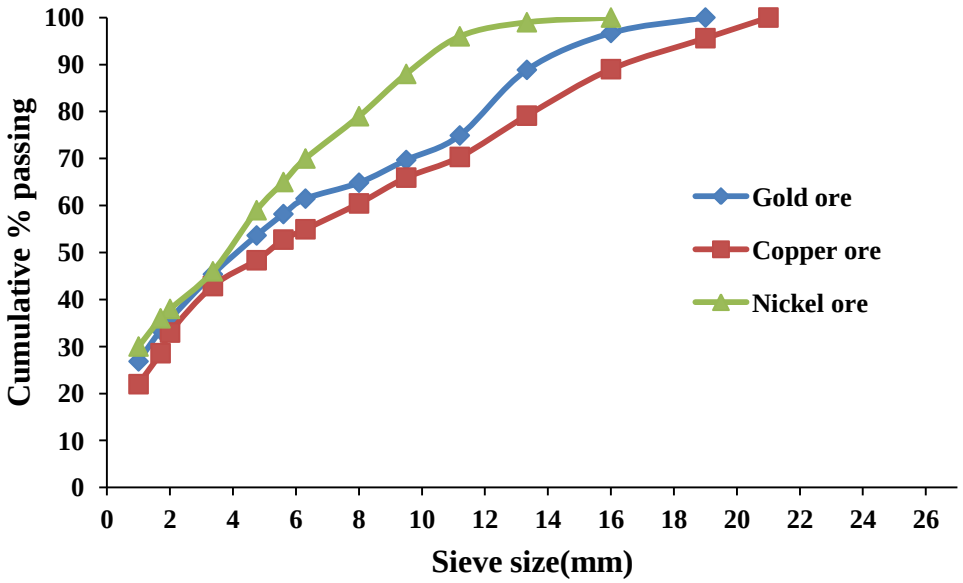

Figure 3.4 Particle size distribution of gold (sample II), copper and nickel ore

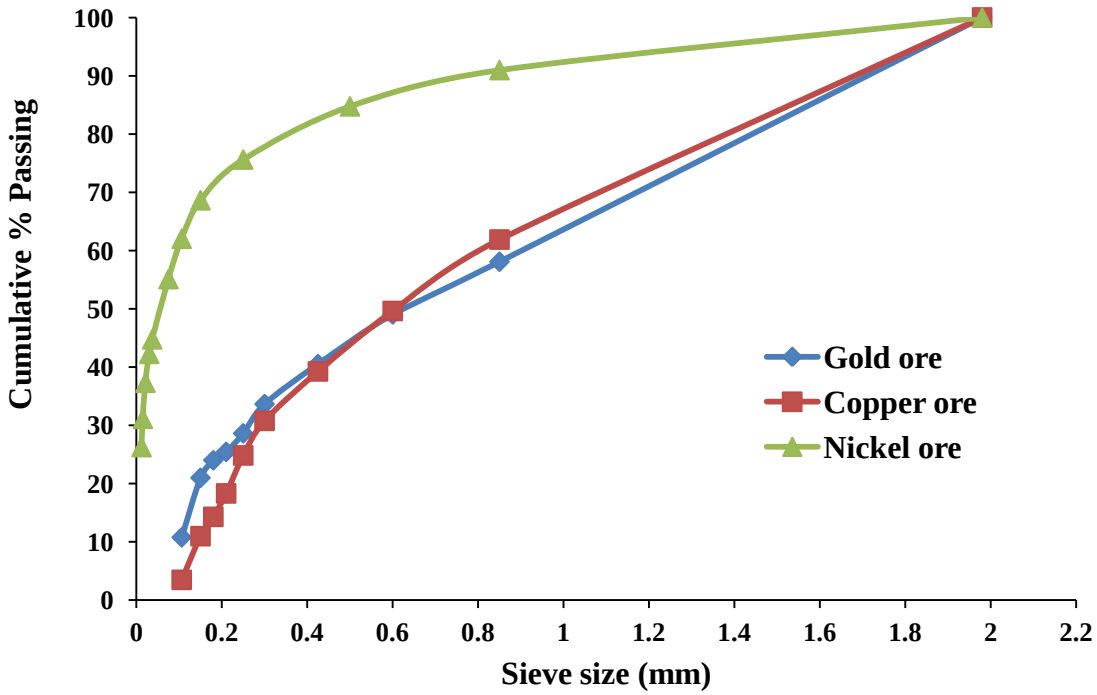

Figure 3.5 Minus 2 mm particle size distribution of gold (sample II), copper and nickel ore

3.4 Effect of Ore Height on Liquid Retention Capacity Measurement

Capillary rise tests provide information on the liquid retention capacity of the ore. Capillary height at equilibrium for monosize particles can be calculated by

$$h = \frac{4\gamma \cos\theta}{g\rho d_c} \tag{3.1}$$

where h is capillary rise height at equilibrium, d_c is average capillary diameter, γ is surface tension of the liquid, g is gravity, θ is contact angle and ρ is density of the liquid. Based on W.J. Schlitt (1983) and R. W. Bartlett (1997) for typical leach solutions, γ is 73 dyne/cm, ρ is 1.08 g/cm^3, $cos\ \theta$ is 1, and g is 981 cm/s^2. Thus, h can be reduced to

$$h \approx \frac{0.28}{d_c} \tag{3.2}$$

The average capillary diameter d_c is related to effective particle diameter d_p. Based on 37% void space for random packing of uniform spheres based on (Yang, 2003), the relationship between particle size and the ratio of volume of void space (V_l) to volume of solid phase (V_s).

$$\frac{d_c}{d_p} \approx \left(\frac{V_l}{V_s}\right)^{1/3} \tag{3.3}$$

This relation gives

$$d_c \approx 0.84 d_p \tag{3.4}$$

Substitution of d_c in the equation above gives

$$h \approx \frac{0.33}{d_p} \tag{3.5}$$

This theoretical relationship is calculated based on uniform sphere random packing. This relationship compares with experimentally observed data for capillary rise using mono-size ore particles. The relationship shows smaller particles absorb more liquid and facilitate a greater capillary height as shown in Figure 3.6.

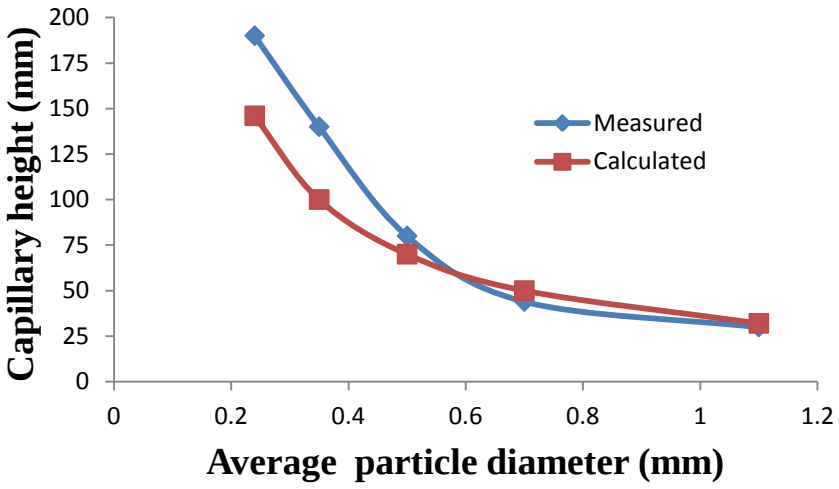

Figure 3.6 Experimentally observed data for capillary rise compared with theoretical values based on approximations by W.J. Schlitt (1983) and R. W. Bartlett (1997)

For non-uniform particles, the height of capillary rise can be separated into three zones, which are categorized differently than liquid bridging states as shown in Figure 3.7. First, at the bottom of the column, there is a saturated zone in which porosity in the ore sample is filled with liquid. This saturated layer may extend a few centimeters above the liquid exposure level. This saturated moisture level exceeds the desired level for agglomeration because filled voids remove capillary attractive binding forces by eliminating the necessary solid-air-liquid interface that provides the attractive capillary force. Although some liquid drains from this zone when the column of ore is removed from the liquid source, some saturation remains. Above the saturated moisture level, liquid seeps up from the saturated zone to fill many pores by capillary action until tension saturation is reached (Abdul & Gillham, 1984) and capillary and funicular liquid bridging states form between most particles. These conditions are suitable for agglomeration. At the upper funicular bridging region, the pendular bridging state is form. Most of the particles in this liquid-bridging state are coated with a thin layer of liquid and few liquid bridges are formed. This pendular state is inadequate for agglomeration. A schematic view of liquid bridging states and relative column height effects is shown in Figure 3.7. Figure 3.7 also shows the associated moisture levels in each zone. The distribution of the moisture content and height of each zone above the liquid level are related to the particle-size distribution(Lane & Washburn, 1947)The saturated zone can be extended to a few feet if the particle size is uniform and very small, or it may be near zero if the particle size is large and non-uniform

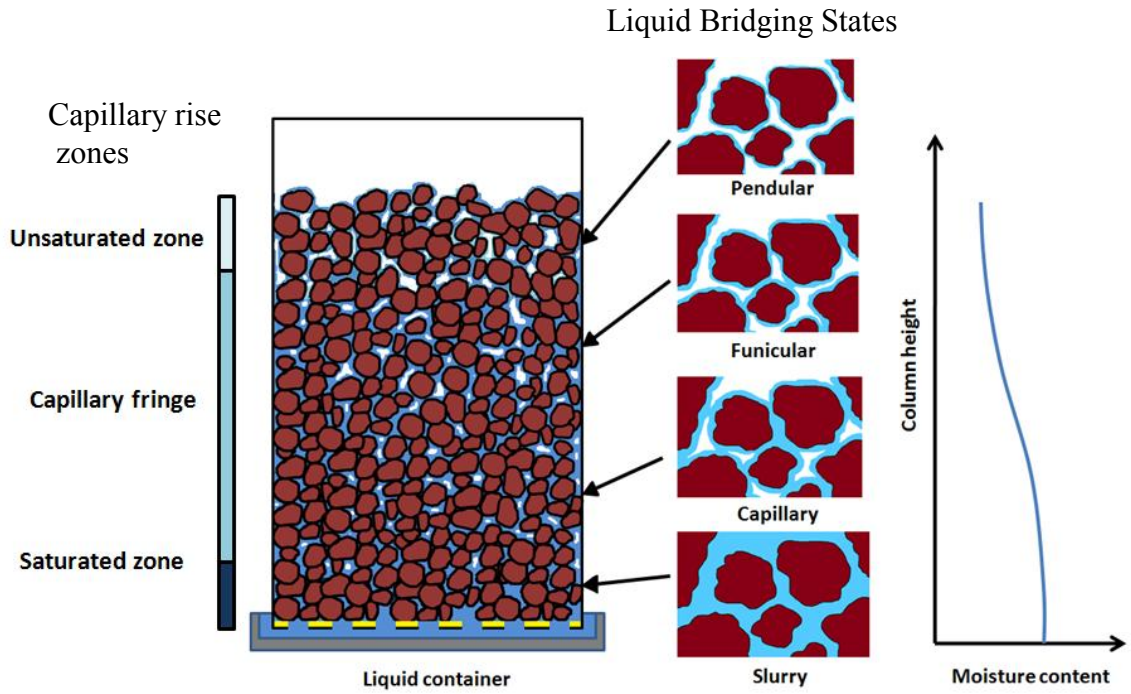

Figure 3.7 A schematics view of capillary rise zones [adapted from (Kristensen & Schaefer, 1987) and (Godt & Mckenna, 2008)]

Experiments to determine the effect of ore height on liquid retention capacity were performed using 1, 2 and 4 kg of nickel and gold ore (sample II). It should also be noted that the moisture retention is measured after removing the liquid source, so most of the saturated slurry zone is removed from the material. The results from the liquid retention measurements are shown in Table 3.1.

The results in Table 3.1 show that the liquid retention is greater in shorter column tests. The greater liquid retention in short columns shows column height is important. It is expected that for short columns, most of the liquid retained after removing the column from the liquid source will be in the capillary and funicular liquid bridging states with some potential retention in short columns in the slurry state. Because the slurry state

Table 3.1 The effect of ore height on liquid retention capacity

Sample	Height (cm)	Liquid retention capacity
1-kg gold	4.1	11.2%
2-kg gold	8.2	9.3%
3-kg gold	12.3	7.6%
4-kg gold	16.4	6.4%
1-kg nickel	4.5	26.8%
2-kg nickel	9.0	24.4%
3-kg nickel	13.5	23.6%
4-kg nickel	18.0	22.5%

zone may include a small but significant fraction of the total ore height in the short column tests, the overall moisture retention is higher. As the height of the ore bed increases, the relative contribution of the funicular and pendular liquid bridging zones to the overall column liquid retention increases, and the liquid retention correspondingly decreases. The gold ore (sample II) liquid retention capacity values decrease more than those of nickel ore (D_{80} is 8.2mm) due to the coarser particle size of the gold ore (sample II) (D_{80} is 12.4mm).

Another approach to obtain the liquid retention capacity data is to flood the column and drain the excess liquid. Two-kg of nickel and gold ore (sample II) samples were flooded in a 15.25 cm column and the excess liquid was drained. The results from this approach are shown in Table 3.2.

Table 3.2 Liquid retention capacity results obtain by flooding the column followed by draining the excess liquid.

Ore Type	15-second drain time	20-minute drain time	Capillary rise data
Gold	11.5%	10.6%	9.3%
Nickel	26.6%	25.2%	24.4%

The results in Table 3.2 show that after a 15-second drain time, the liquid retention capacity is very similar to the liquid retention capacity data obtained using the capillary rise method with 1-kg samples. After a 20-minute drain time, the liquid retention capacity was reduced further by about 1%. Thus, flooding, followed by draining, results in similar liquid retention relative to the capillary rise method for short columns (less than 10 cm) and short drain times (less than 20 minutes).

3.5 Effect of Liquid Uptake Time on Liquid Retention Capacity Measurement

Figure 3.8 shows liquid uptake increases as liquid exposure time increases. As seen in Figure 3.8 gold and copper ores approach the maximum liquid uptake after 20 minutes. The liquid uptake/capillary rise rate for gold and copper ore is very similar due to similar sizes (D_{80} is 12.4mm for gold and D_{80} is 13.4mm for copper). However, the nickel ore, which has much finer particles (D_{80} is 8.2mm), continues to increase in liquid content until it approaches saturation after about 90 minutes.

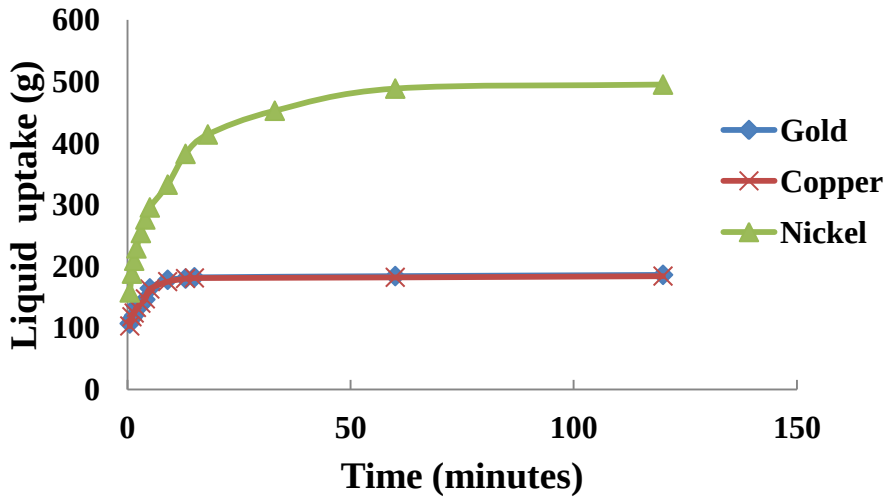

Figure 3.8 Liquid uptake versus time for 2-kg samples of feed ore in a 15.25 cm diameter column during liquid retention capacity measurements.

3.6 Effect of Pressure on Liquid Retention Capacity Measurement

Experiments were performed to understand the effect of pressure on liquid retention capacity. A 20.4-kg load was placed on the top of the 2-kg ore sample in the vessel while the water retention capacity test was performed as shown in Figure 3.9. The results from the pressure tests are presented in Table 3.3.

Table 3.3 shows that load has only a small influence on the liquid retention capacity. The 20.4-kg load (1,117 kg/m^2) compacted the ore slightly and reduced the amount of void space between particles. The reduced void space reduced liquid retention slightly for the short columns used in these tests. Although little difference in moisture content was measured due to the load provided, the associated pressure is low compared to loads in leaching practice, so the effect of loading at high levels in leaching pads is not known.

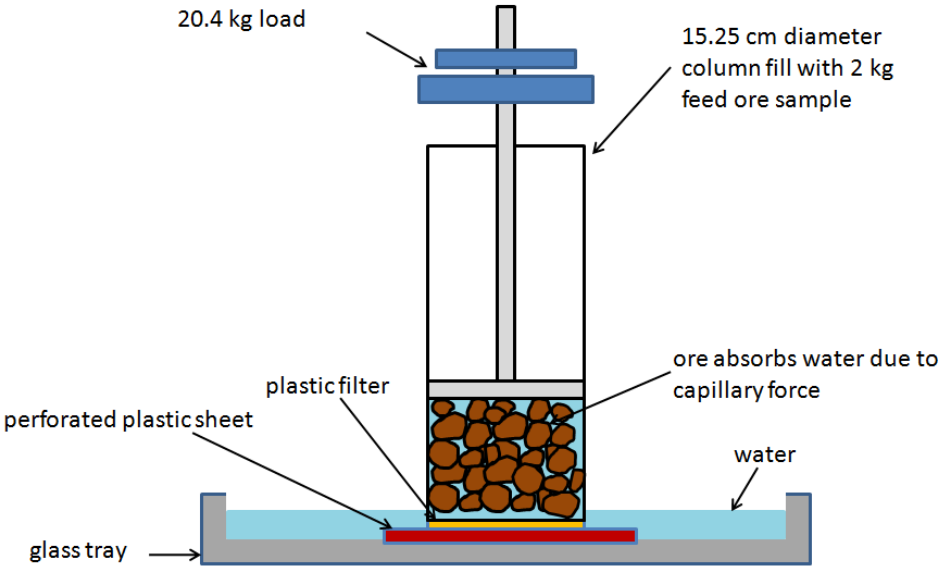

Figure 3.9 Schematic diagram of liquid retention capacity measurement with load apparatus.

Table 3.3 Comparison of moisture content from liquid retention capacity measurement tests.

Ore Type	Moisture without load	Moisture with 20.4 kg load
Gold (main ore)	9.3%	8.5%
Nickel (first received)	24.4%	23.5%

3.7 Effect of Fine Particles on Liquid Retention Capacity Measurement

Experiments were performed to improve the understanding of the effect of fines particles on liquid retention capacity. The fraction of gold ore (sample II) fine particles (-1mm) in an ore sample was increased and decreased by 50%, and liquid retention capacity were measured. The size distribution and results are presented in Table 3.4. The results show that increasing and decreasing the amount of fine particles have a strong effect on liquid retention capacity. Increasing the amount of fine particles by 50% results in increasing the liquid retention capacity by 2%. Decreasing the amount of fine particles by 50% results in decreasing the liquid retention capacity by 2%.

Table 3.4 Effect of fine particles on liquid retention capacity.

Size	Weight (%)		
	Original	50% less fines	50% more fines
+12.5 mm	19.40	22.25	16.60
-12.5 mm to +6.3 mm	19.40	22.25	16.60
-6.3 mm to +3.35 mm	19.40	22.25	16.60
-3.35 mm to +1 mm	20.90	22.80	18.85
-1 mm	20.90	10.45	31.35

Gold ore	Liquid retention capacity
Original gold ore	9.1%
50% less fines	6.8%
50% more fines	11.2%

3.8 Small - Scale, Scoping Test Agglomeration Procedures

Five hundred-gram samples of gold ore (sample II) were agglomerated in a 1-liter plastic vessel in batch mode. The plastic vessel was closed at one end with a central port in the other end to allow the introduction of ore and liquid. The vessel or drum has four 5-mm plastic lifters installed inside to assist the tumbling motion. The gold ore (sample II) samples were dry mixed for 5 minutes with the needed amount of Portland cement (Type II) as binder. Copper and nickel ore were dry mixed for 5 minutes prior to the agglomeration to insure that the solids were well-mixed prior to agglomeration. Liquid was introduced into the agglomeration drum through a tube with small spray holes facing downward. The solution flow rate and amount was controlled using a 60 or 120 ml syringe. Liquid was introduced for 1 minute of the 3 minutes of total agglomeration time. The drum operated at 30% of the critical speed. The remainder of the agglomeration time was used to allow the agglomerates to grow without further moisture addition.

3.9 Ore Agglomeration

Agglomeration of gold ore (sample II) involved 4 grams Portland cement (Type II) as a binder and 1000 ppm NaCN solution as the feed solution. Agglomerated copper and nickel ore, used respectively, 100 and 500 grams of sulfuric acid per liter of solution as feed solution. Agglomerated ores were taken out from the agglomeration drum and air dried for 1 hour before additional testing. Size distribution information obtained by hand sieving as well as pictures of the agglomerates are shown in Figures 3.10-3.13. Figure 3.10 shows the size of gold ore (sample II) increases as moisture increase to the feed ore

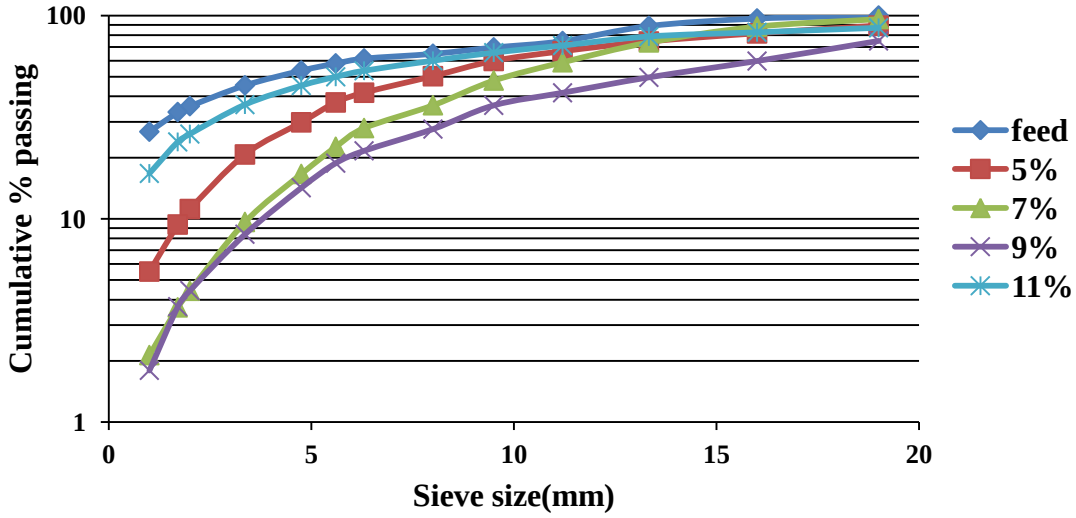

Figure 3.10 Particle size distribution of agglomerated gold ore (sample II) at different moisture levels.

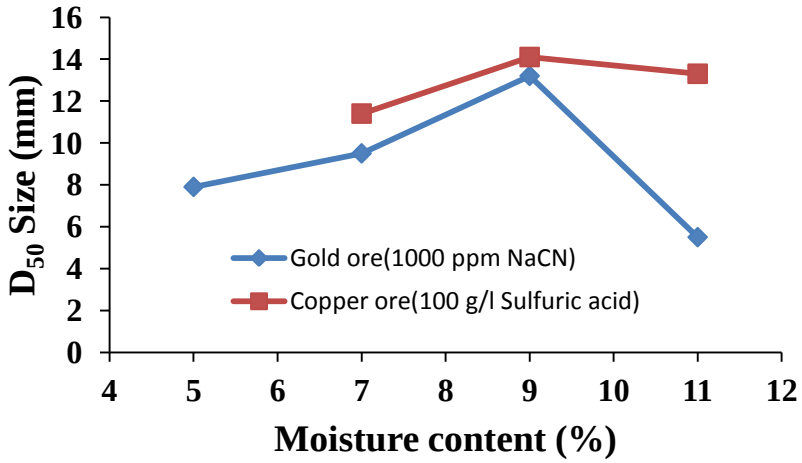

Figure 3.11 D_{50} size of agglomerated gold ore (sample II) with 1000 ppm NaCN and cement binder compared to agglomerated copper ore with 100 grams of sulfuric acid per liter of solution at different moisture levels

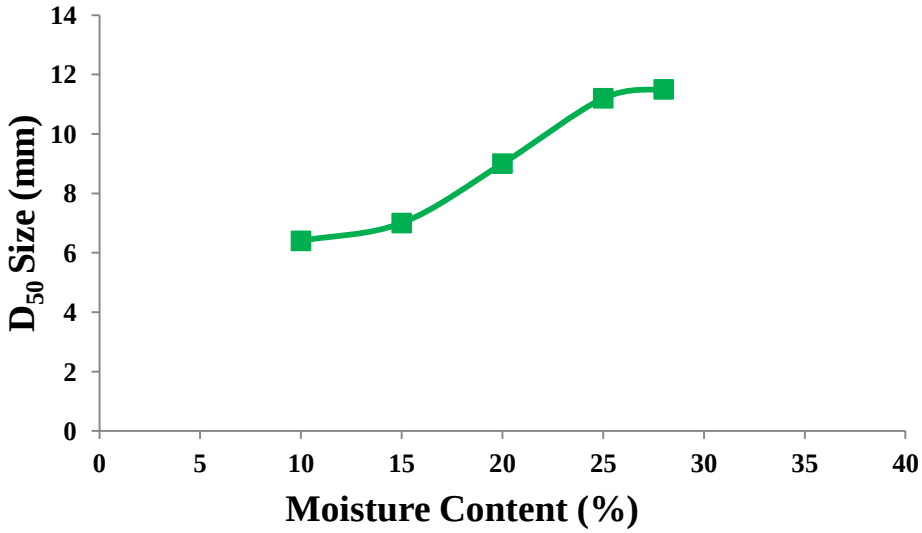

Figure 3.12 D_{50} size of agglomerated nickel ore with 500 grams of sulfuric acid per liter of solution at different moisture levels

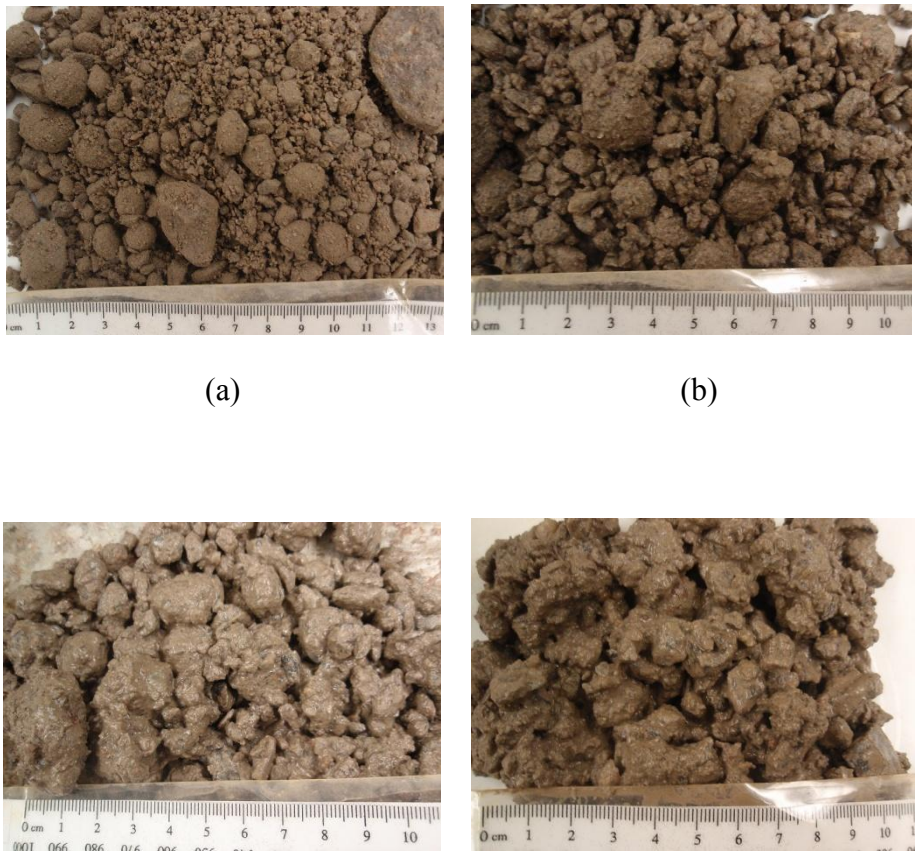

(a) (b)

(c) (d)

Figure 3.13 Agglomerated gold ore (sample II) 5% agglomerate moisture content (a), 7% agglomerate moisture content (b), 9% agglomerate moisture content (c), 11% agglomerate moisture content (d)

up to the 9% levels and then a noticeable decrease is observed. The D_{50} of gold ore (sample II) and copper ore versus moisture content are shown in Figure 3.11.

The D_{50} of Nickel ore is plotted versus moisture content shown in Figure 3.12. Figure 3.12 shows the nickel ore achieves an appropriate agglomerate size with 25% agglomerate moisture content. If agglomerate moisture is increased further than 28% the material starts to form a thin muddy layer.

Images of gold agglomerates are shown in Figures 3.13a – 3.13d. Figures 3.13a-3.13d illustrate that the agglomerated ore begins forming agglomerates with 5% agglomerate moisture content. Agglomeration of the finer particles occurs as moisture is increased. At 9% agglomerate moisture content, particles have a distinctive sheen indicting that water is not completely contained within the pores of the agglomerates. Figure 3.13d shows that the agglomerates with 11% agglomerate moisture content formed a mud-like agglomerate material, which is undesirable for agglomeration. Thus, the ideal agglomeration moisture content for the gold is 9%. Likewise, similar observations were made with the copper ore, indicating an ideal agglomeration moisture content of 9%. The ideal agglomeration moisture content for nickel ore agglomeration was 25% to 28%. moisture beyond 28% formed mud-like agglomerates for nickel ore.

3.10 Comparison of Liquid Retention Capacity and Agglomeration Moisture

Liquid retention capacity data show that the nickel ore retained more liquid than the gold and copper ores. The liquid retention capacity data acquired from the capillary rise method using 2 kg ore samples are 9.3%, 9.2% and 24.4% agglomerate moisture content for the gold, copper, and nickel ores, respectively. The optimum agglomeration moisture is determined by visual observation and size distribution. The largest particle size and no formation of mud were set as the criteria for optimum agglomerate moisture. The associated optimum agglomeration moisture content is shown for comparison in Table 3.5. Liquid retention capacity moisture is very similar to optimum agglomeration moisture for each ore. This encouraging result suggests that a simple liquid retention capacity test can be used to estimate the optimum agglomeration moisture content for an ore.

Table 3.5 Comparison of liquid retention capacity

Ore Type	Liquid retention capacity (%dry weight basis)	Measured optimum agglomeration moisture**	Measured optimum agglomeration liquid
Gold	9.3%	9%	9.0 ml per 100 g of ore (1000 ppm NaCN)
Copper	9.2%	9%	8.7 ml per 100 g of ore (100g/l H_2SO_4)*
Nickel	24.4%	28%	23.5 ml per 100 g of ore (500 g/l H_2SO_4)*

*Acid has some effect that is discussed in more detail in Chapter 4

** Optimum agglomeration moisture is based on visual inspection, no mud formation, and the largest D_{50} size.

Agglomerates with higher moisture content than liquid retention capacity are likely to create mud-like agglomerates and be difficult to transport to the heap. Lower moisture content agglomerates do not have enough moisture to agglomerate all of the fines and cannot form the appropriate liquid bridges. This could lead to fines transport during lift building and result in poor percolation during leaching.

CHAPTER 4

EVALUATION OF LIQUID RETENTION CAPACITY ON ACIDIC SOLUTION BASED ORE AGGLOMERATION

4.1 Introduction

Capillary rise experiments with acid solution with real ore sample can be difficult because acid solution can react with the ore sample. In some cases reactions can generate gas and bubbles underneath the pack bed. Such reactions can interfere with the liquid retention capacity measurements. In this study, a series of liquid retention capacity measurements were performed with glass beads to avoid unknown reactions with particles. Then, a series of agglomeration tests with acid solution were performed and evaluated.

Capillary and surface tension are the primary adhesive forces in agglomeration. In acidic solution based agglomeration, acid solution forms the liquid bridge instead of water. Changes in acid concentration result in slight changes in surface tension as shown in Table 4.1

Table 4.1 The surface tension of aqueous sulfuric acid solutions at 25°C based on literature data (Suggitt, Aziz, & Wetmore, 1949)

Acid %	Surface tension (dyne/cm)
0 (water)	71.97
4.11	72.21
8.26	72.55
12.18	72.80
17.66	73.36
21.88	73.91
29.07	74.80
33.63	75.29

Capillary height at equilibrium for monosize particles can be calculated by equation (3.1). The capillary force arises if the liquid bridge form between the spheres. Assuming hydrophilic surface and separation distance much smaller than the object radius the maximum capillary force can be calculated by this expression

$$F_{cap} = 4\pi r\gamma \qquad (4.1)$$

where r is the radius of sphere and γ is the surface tension. From equation (3.1) and (4.1) slight changes in surface tension result in slight changes in capillary force and capillary height which have a small effect on the liquid bridge network in liquid retention capacity tests.

4.2 Estimation of Acid Solution Retention Capacity

(Glass Bead Tests)

Acid solution retention capacity tests using glass beads were used for comparison with water. Four sizes of glass beads (3, 1, 0.5, and 0.1 mm diameter particles mixed in equal weight proportions for each size class) were used for these tests. A 1-kg sample was prepared from the mixture of glass beads to simulate a nonreactive ore. Liquid retention capacity tests were performed with water, 100, 500, and 900 g/l sulfuric acid solutions. Results from these tests are shown in Figure 4.1 and Table 4.2.

As the results show, at higher acid concentrations the weight based moisture content retained in the glass beads increases. The increase in liquid weight retained is associated with the increase in density of the acid solution. The calculated liquid volume retained in the glass beads remained at similar levels in each of the tests despite the significant rise in solution density as indicated in Table 4.2. Thus, the moisture retention in these tests is based on liquid volume rather than weight percent moisture.

The data in Table 4.2 show that the acid solution retention in the glass beads increases as acid concentration increases. Measurements for the 900 g/l acid solution show the weight of solution retained is 47 % greater than the control test using water. Because moisture content is weight based, the resulting difference in retained moisture between 900 g/l acid and water is large. Liquid volume retained in the glass beads remains within 5% of at around 143 cm^3 even though the acid concentration changes by a large fraction (47.3%). Thus, the volume of liquid needed for agglomeration can be estimated using either water or acid solution retention data. This is an important finding that will be further substantiated with additional data in a subsequent section.

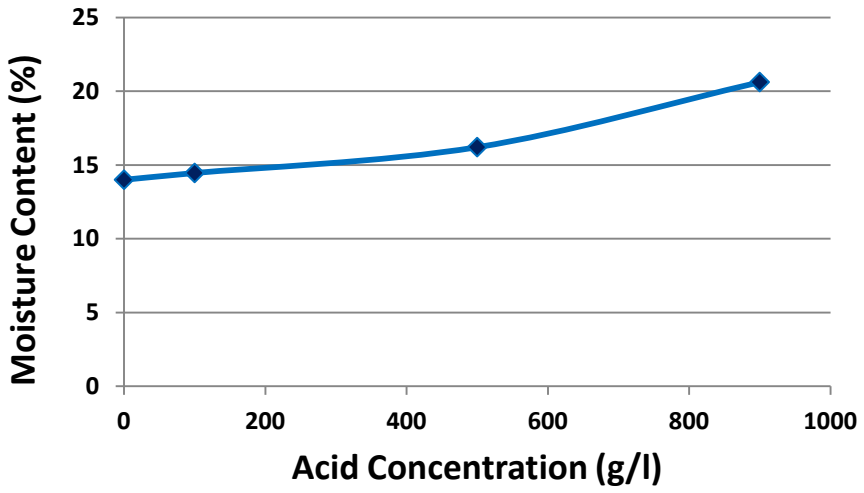

Figure 4.1 Acid solution (moisture by fraction of glass beads weight) retention capacity using glass bead particle beds (3, 1, 0.5, and 0.1 mm mixed in equal weight proportions) as a function of acid concentration.

Table 4.2 Measured liquid weight retained and calculated liquid volume retained in glass beads (3, 1, 0.5, and 0.1 mm diameter particles mixed in equal weight proportions for each size class) from acid solution retention capacity experiments together with other related data.

Liquid	Weight% retained	Weight retained (compared with water)	Density (g/cm^3)	Calculated liquid volume retained (cm^3)
water	14.00%	0.00%	1.0	140.0
100 g/l H_2SO_4	14.46%	+3.34%	1.04	139.7
500 g/l H_2SO_4	16.21%	+15.78%	1.19	135.9
900 g/l H_2SO_4	20.62%	+47.28%	1.38	149.5

Consequently, water retention weight data can be converted to estimate the required agglomeration moisture using acid or solution density information. In other words, because the liquid volume is the key parameter in determining desired agglomeration moisture, the liquid retention capacity can be measured and multiplied by solution density to determine desired moisture. These results from glass bead tests were followed by testing with ore samples to verify their applicability to ore.

4.3 Agglomeration Result

Copper and nickel ores are often mixed with sulfuric acid solution, which reacts with the ore as a pretreatment and as a binder before leaching. The concentration of sulfuric acid solution has been varied in this study. The liquid retention capacities of copper and nickel ores are 9.2% and 24.4%, respectively. High acid concentrations result in high density of the feed solution. Copper ore was agglomerated with 6.5, 100 and 500 g/l acid concentrations. Size distribution information for copper ore as well as pictures of the agglomerates are shown in Figures 4.2-4.7.

The liquid retention capacity of copper ore is 9.2wt% moisture which is equal to 46 ml of liquid in 500 g ore sample. Mud will form if the liquid volume added is more than 46 ml (acid solution retention limit). Excess liquid addition will result in agglomerate breakage. A summary of volume of acid added to 500 grams of copper ore and agglomeration results is shown in Table 4.3.

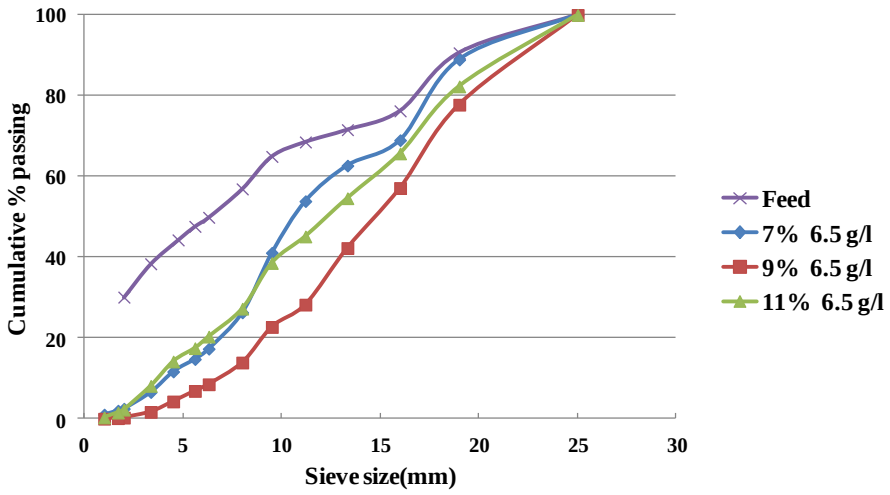

Figure 4.2 Particle size distribution of agglomerated copper ore at different moisture levels for 6.5 g/l acid concentration, 3 minutes of agglomeration time, and 30% critical speed

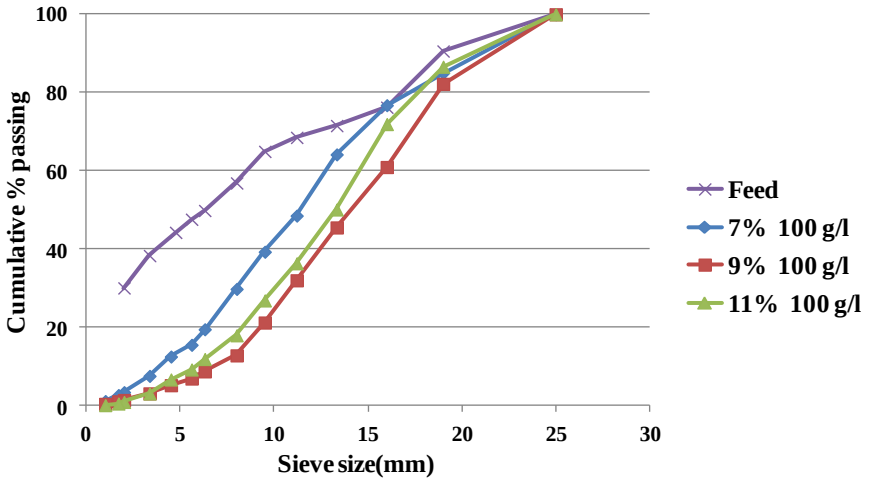

Figure 4.3 Particle size distribution of agglomerated copper ore at different moisture levels for 100 g/l acid concentration, 3 minutes of agglomeration time, and 30% critical speed

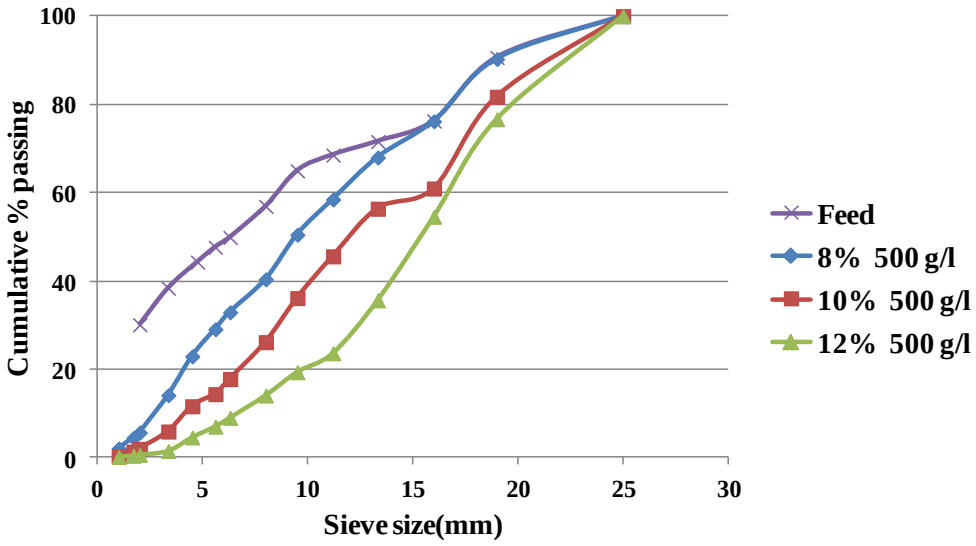

Figure 4.4 Particle size distribution of agglomerated copper ore at different moisture levels for 500 g/l acid concentration, 3 minutes of agglomeration time, and 30% critical speed

(a)

(b)

(c)

Figure 4.5 Agglomerated ore images agglomerated copper ore with 6.5 g/l acid at 7% agglomerate moisture content (below acid solution retention limit) (a), agglomerated copper ore at 9% agglomerate moisture content (at acid solution retention limit) (b), and agglomerated copper ore at 11% agglomerate moisture content (above acid solution retention limit) (c)

(a)

(b)

(c)

Figure 4.6 Agglomerated ore images agglomerated copper ore with 100 g/l acid at 7% agglomerate moisture content (below acid solution retention limit) (a), agglomerated copper ore at 9% agglomerate moisture content (at acid solution retention limit) (b), and agglomerated copper ore at 11% agglomerate moisture content (above acid solution retention limit) (c)

(a)

(b)

(c)

Figure 4.7 Agglomerated ore images agglomerated copper ore with 500 g/l acid at 8% agglomerate moisture content (below acid solution retention limit) (a), agglomerated copper ore at 10% agglomerate moisture content (at acid solution retention limit) (b), and agglomerated copper ore at 12% agglomerate moisture content (above acid solution retention limit) (c)

Table 4.3 Volume of acid solution added to 500 grams of copper ore sample during agglomeration and associated agglomeration results.

Acid concentration	Moisture content (dry weight basis)	Liquid Volume (ml) added to 500 g sample	Agglomeration results
6.5 g/l	7%	35	Good agglomeration
6.5 g/l	9%	45	Best agglomeration
6.5 g/l	11%	55	Bad agglomeration
100 g/l	7%	35	Good agglomeration
100 g/l	9%	45	Best agglomeration
100 g/l	11%	55	Bad agglomeration
500 g/l	8%	33	Good agglomeration
500 g/l	10%	42	Good agglomeration
500 g/l	12%	50	Best agglomeration

Nickel ore agglomeration was also evaluated and compared to estimated acid solution retention capacity data. Figure 4.8 shows the D_{50} data from nickel ore agglomeration experiments. The data trends show that size increases with increasing moisture.

Pictures of agglomerated ore, which correspond to the data in Figure 4.8, are shown in Figures 4.9-4.11. Figure 4.9a shows that the 20 % agglomerate moisture content is insufficient for good agglomeration. Figure 4.9b shows good agglomerates can be obtained with 25 % agglomerate moisture content for the 100 g/l concentration of acid. Similarly, Figure 4.10 shows agglomerates are best achieved at 28 % agglomerate moisture content for 500 grams of acid per liter solution. Figures 4.11a-c indicate 35 % is appropriate for 900 grams of acid per liter solution.

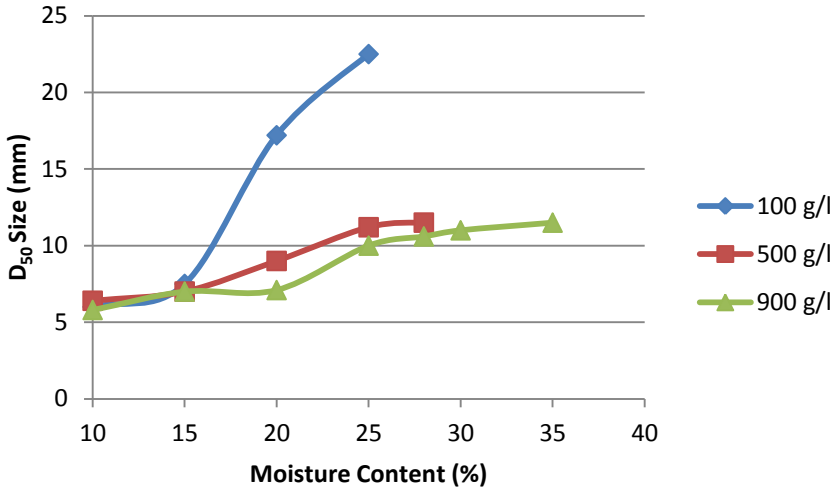

Figure 4.8 D_{50} size of the agglomerated nickel ore for 100, 500 and 900 g/l acid as indicated for which the optimum moisture contents are 25, 28, and 35 %, respectively.

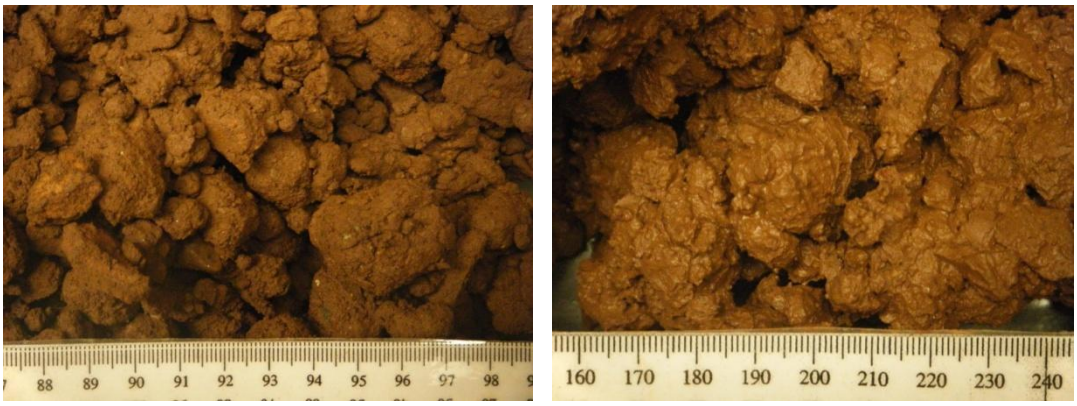

(a) (b)

Figure 4.9 Agglomerated nickel ore with 100 g/l acid at 20% agglomerate moisture content (below acid solution retention limit) (a), and agglomerated nickel ore at 25% agglomerate moisture content (at acid solution retention limit) (b)

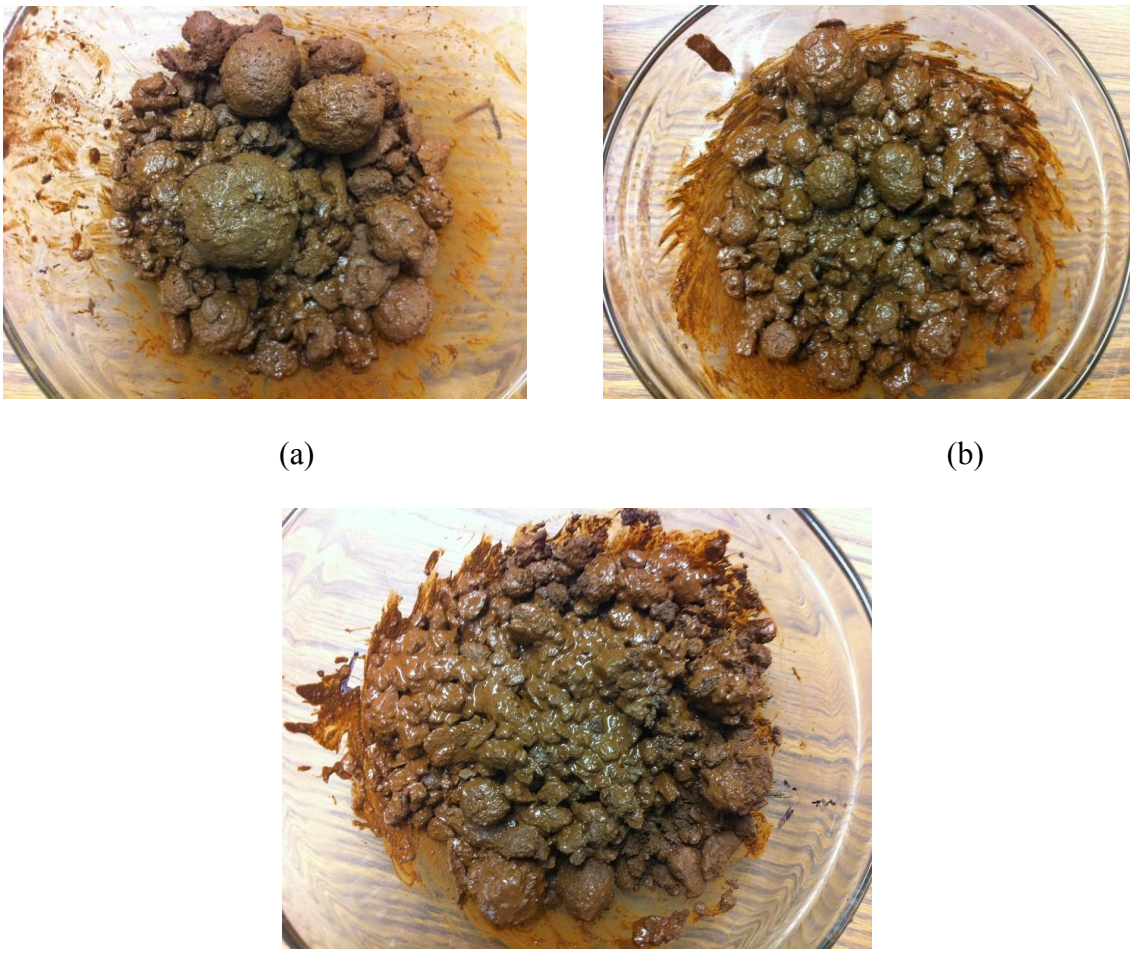

(a) (b)

(c)

Figure 4.10 Agglomerated ore images agglomerated nickel ore with 500 g/l acid at 25% agglomerate moisture content (below acid solution retention limit) (a), agglomerated nickel ore at 28% agglomerate moisture content (at acid solution retention limit) (b), and agglomerated nickel ore at 30% agglomerate moisture content (above acid solution retention limit) (c)

(a)

(b)

(c)

Figure 4.11 Agglomerated nickel ore with 900 g/l acid at 30% agglomerate moisture content (below acid solution retention limit) (a), agglomerated nickel ore at 35% agglomerate moisture content (at acid solution retention limit) (b), and agglomerated nickel ore at 40% agglomerate moisture content (above acid solution retention limit) (c)

Based on the information in Figures 4.9-4.11, Table 4.4 was constructed to compare the volume of liquid and moisture used for agglomeration at different acid concentration levels. The optimum moisture contents are presented in the middle of each section of data for the three acid levels shown (100, 500, and 900 grams of acid per liter). The optimum moisture contents for the three acid levels are presented along with the calculated volume of liquid. Note that the volumes of liquid needed for appropriate agglomerates, which tend to form a thin mud layer, are similar for each acid level (within 5 % of 123 ml for a 500 gram sample). In contrast, the moisture content needed increases significantly (40 % for the range shown) in accordance with the increase in solution density.

The findings presented in Tables 4.3 and 4.4 are consistent with the glass bead tests which showed that liquid retention is related to volume rather than weight. Consequently, these results from nickel ore agglomeration show that optimum estimated agglomeration moisture can be estimated by liquid retention capacity volume. The liquid retention capacity can be converted to an estimated optimum agglomeration moisture content by multiplying liquid retention capacity by the solution density as shown in Table 4.5.

Liquid retention capacity in term of liquid volume per 100g of sample was compared with liquid volume added per 100 gram of samples in optimum agglomeration conditions as shown in Figure 4.12. These results show the correlation is very good.

Table 4.4 Volume of acid solution added to 500 grams of nickel ore sample during agglomeration and associated agglomeration results

Acid concentration	Moisture content (dry weight basis)	Liquid Volume (ml) added to 500 g sample	Agglomeration results
100 g/l	20%	97	Good agglomeration
100g/l	25%	121	Best agglomeration
100 g/l	30%	145	Bad agglomeration
500 g/l	25%	105	Good agglomeration
500 g/l	28%	118	Best agglomeration
500 g/l	30%	126	Bad agglomeration
900 g/l	30%	109	Good agglomeration
900 g/l	35%	127	Best agglomeration
900 g/l	40%	145	Bad agglomeration

Table 4.5 Comparison of liquid retention, agglomeration moisture and experimentally measured optimal agglomerate moisture

Ore type	acid concentration (g/l)	Solution density (g/cm^3)	Liquid retention capacity (%)	Estimated agglomerate moisture(%) based on liquid retention capacity	Experimental optimum agglomerate moisture(%)
Copper	6.5	1.00	9.2	9.2	9
	100	1.04		9.2	9
	500	1.19		10.9	12
Nickel	100	1.04	24.4	25.4	25
	500	1.19		29.0	28
	900	1.38		33.7	35

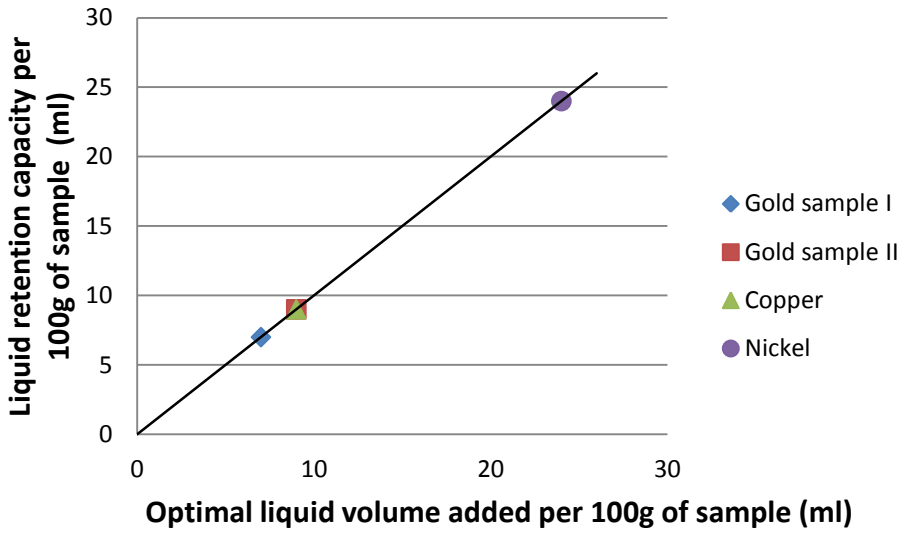

Figure 4.12 Liquid retention capacity in terms of liquid volume per 100g of sample was compared with liquid volume added per 100 gram of samples in optimum agglomeration conditions

CHAPTER 5

GOLD ORE COLUMN LEACHING

5.1 Agglomeration Procedures

Twenty-five kg of gold ore (sample II) was agglomerated in a 30-gallon plastic drum in batch mode. The drum has four 0.5-cm plastic lifters installed inside to assist the tumbling motion. The samples were dry mixed for 15 minutes with the needed amount of Portland cement (Type II) as binder prior to the agglomeration to insure that the solids were well-mixed prior to agglomeration. Moisture was added using a 1000 ppm NaCN solution, which was introduced into the agglomeration drum through a tube with small spray holes facing downward. The pH of the mixture was greater than 11 due to the alkalinity of the cement. The solution flow rate and amount was controlled using a peristaltic pump. Liquid was introduced for the first 1/3rd of the retention time. The drum operated at 30% of the critical speed. The remainder of the agglomeration time was used to allow the agglomerates to grow without additional moisture. Three batches (75 kg) were prepared for each column leaching test. All 3 batches were placed on a tarp. After 1 hour of curing time, the agglomerates were sampled by the cone and quartering method until a representative sample was obtained (1-1.2 kg) for the purpose of performing the quality control tests. The remaining portion of the 75 kg was loaded into a column for leaching.

5.2 Agglomerated Gold Ore Size Distribution

The particle size distribution of agglomerates, which was determined from the sample split from the 75 kg agglomerated ore, is shown in Figure 5.1 for several samples. From the size distribution plot and visual inspection, which is shown in Figure 5.2, 9% agglomeration moisture is the optimal moisture content. Moisture content beyond 9% results in forming mud-like agglomerates, which break up after drying and lead to more fines as indicated in Figure 5.2.

(a) (b)

(c)

Figure 5.1 Pictures of agglomerated gold ore (sample II) 7% agglomerate moisture content (a), 9% agglomerate moisture content (b), 11% agglomerate moisture content (c), 3 minutes of agglomeration time, and 30% critical speed

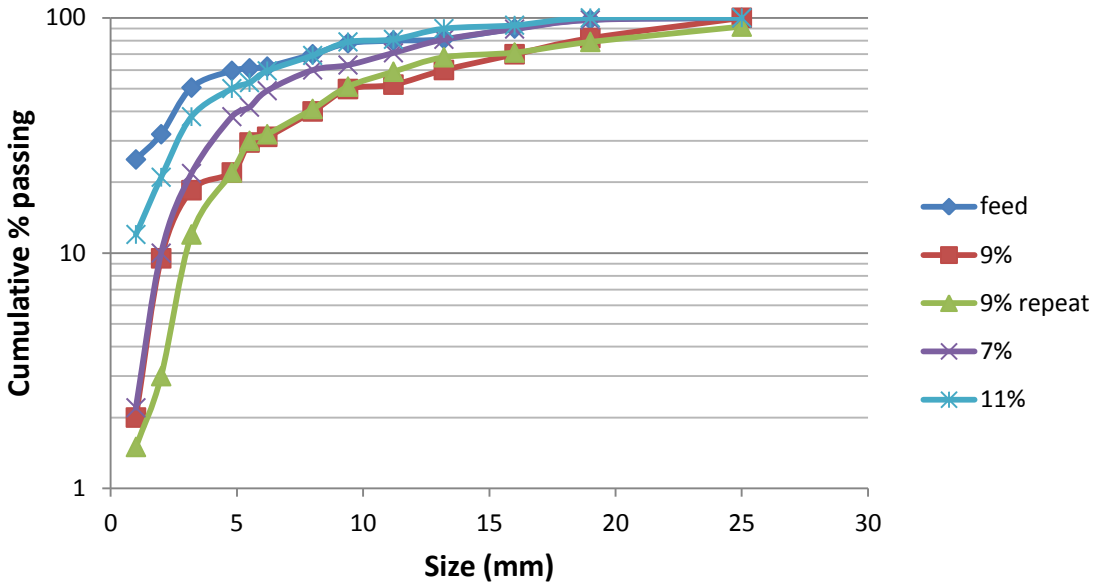

Figure 5.2 Particle size distribution of the agglomerates at different moisture levels after 24 hours of curing and air drying.

5.3 Column Leaching Setup

The columns consisted of three 50.8 cm (20-inch) sections for a total vertical height of 152.4 cm. A schematic diagram of a column set up for leaching is shown in Figure 5.3. Two hundred ppm cyanide solution was applied at the rate of 5.4 mL/min. Pregnant leaching solution (PLS) was collected for ICP analysis. A 2^2 factorial experimental design with a midpoint performed in triplicate was used to evaluate the effects of agglomeration moisture and binder addition on column leaching performance.

Agglomerated gold ore (sample II) was cured for a day inside each column. Recirculated pregnant leaching solution (PLS) was applied through a tube at the top of the column and the (PLS) is collected at the bottom of the column.

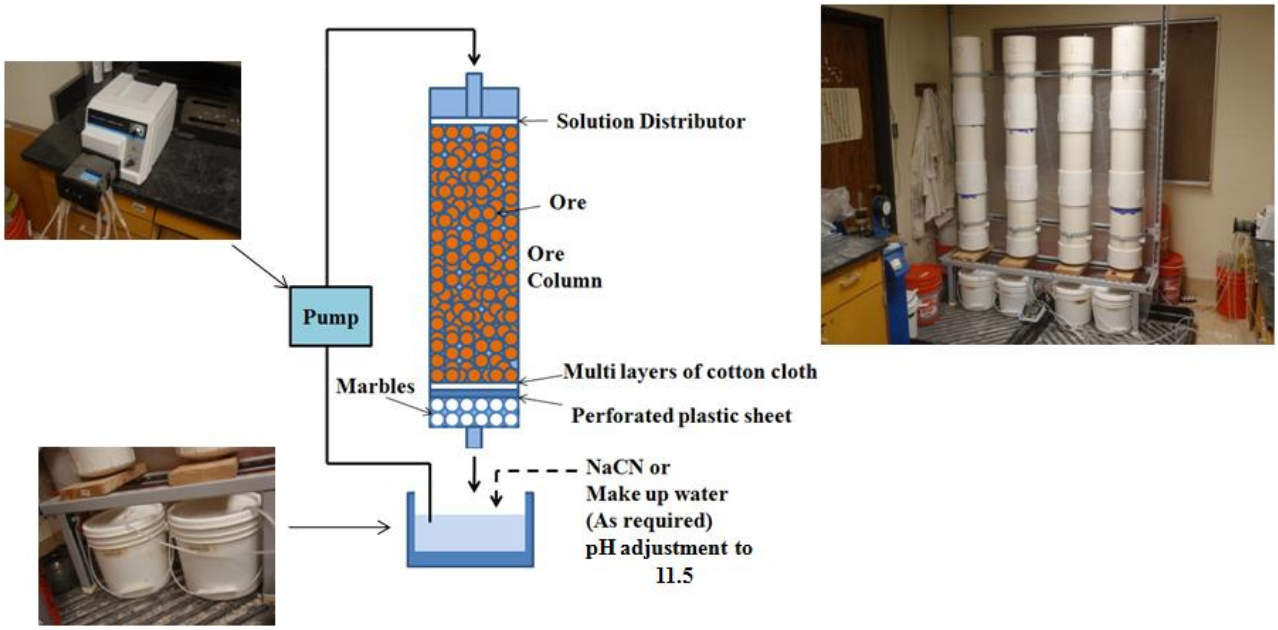

Figure 5.3 Cyanide leaching column design

The PLS is collected every day within the first 2 weeks, then once in 3 days for the following month, and finally once a week for the rest of the experiments. The columns were leached for 90 days. Cyanide and pH were controlled at pH 11.5-11.8 and 200 ppm of free cyanide by cyanide titration using silver nitrate and pH meter measurements. Pregnant leaching solution was collected regularly and titrated with 5 g/l silver nitrate solution and 2 drops of potassium iodide were used as the titration indicator during initial leaching solution evaluations.

5.4 Evaluation of Effect of Agglomerate Moisture Content on Column Leaching Test Results

The first set of column leaching tests evaluate the difference in agglomerate moisture content. Results are shown in Figure 5.4. The results in Figure 5.4 demonstrate that agglomerate moisture contents have an effect on gold recovery. Nine percent agglomerate moisture content gives the highest recovery rate, followed by 7% and 11%, respectively. Nine percent agglomerate moisture content tests had the largest D_{50} size, which improves permeability. The D_{50} decreases above 9% agglomerate moisture content. The agglomerates with 11% agglomerate moisture content formed a mud-like agglomerate material. The particle size distributions at different column positions after leaching (top = 100-150 cm above outlet, mid = 50-100 cm above outlet, bot = outlet - 50 cm) are shown in Figures 5.5-5.7.

From Figures 5.5-5.7, it is apparent that some fines migration can be found in all columns. Seven percent agglomeration moisture showed a little more fines migration than the 9% agglomeration moisture test column. The measurement of particle size distribution of the 11% agglomeration moisture was not performed due to solidification of the mud-like material inside the column as shown in Figure 5.8. Figure 5.9 shows cyanide consumption which is similar for 9% and 7% agglomerate moisture content. For 9%, 7% and 11% agglomerate moisture contents, cyanide consumption was 0.13, 0.12 and 0.11 kg/ton, respectively.

The breakthrough time, which is the time between the beginning of leaching and the observation of first drop of PLS, and drain down liquid volume data is shown in Table 5.1 and Figure 5.10.

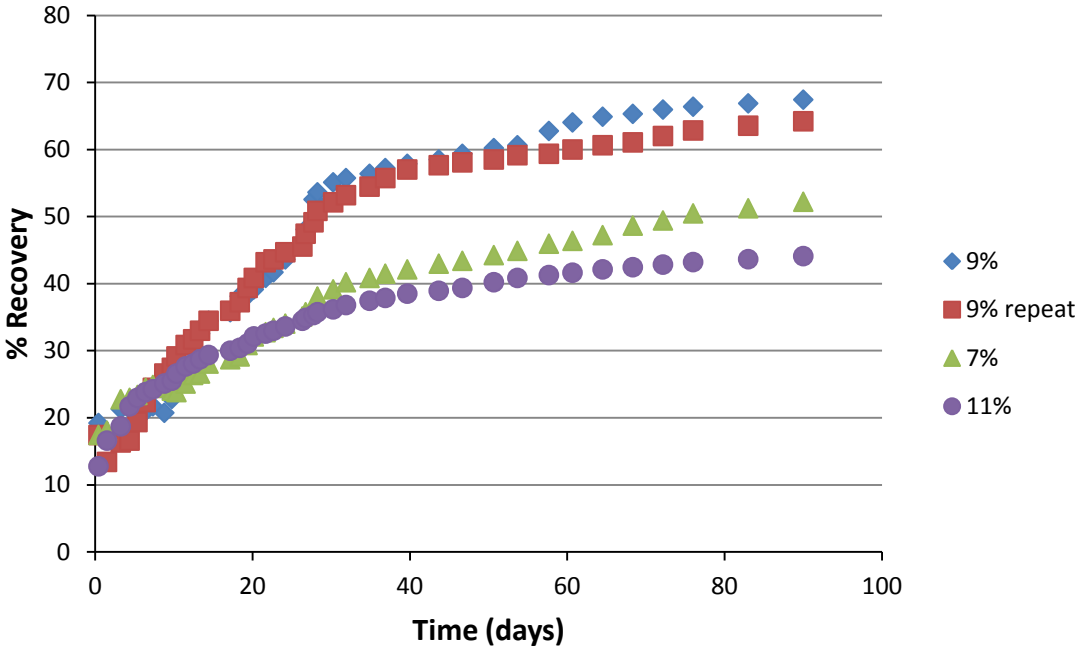

Figure 5.4 Gold recovery results for 90 days leaching time agglomerates with different moisture levels.

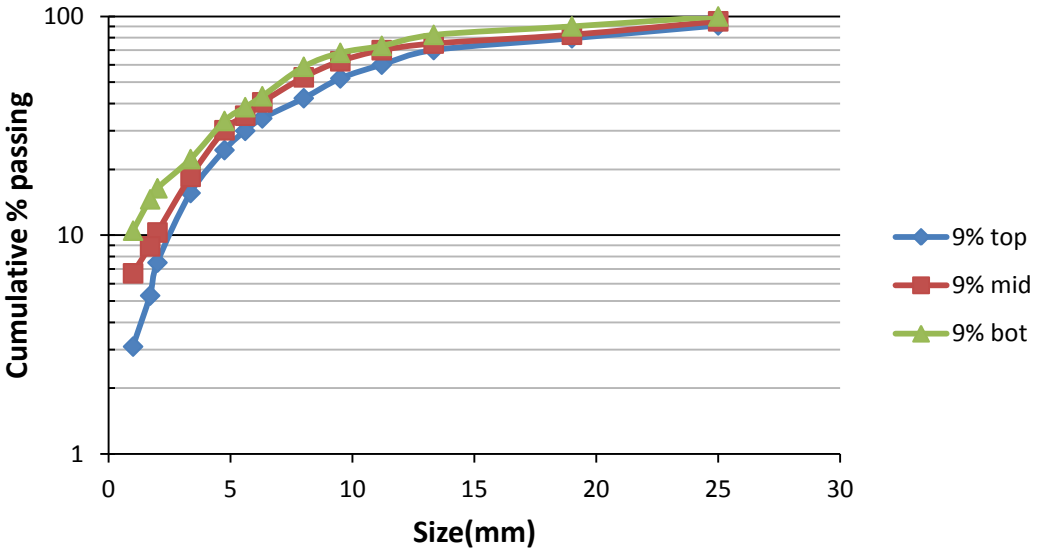

Figure 5.5 Particle size distribution at different column positions after column leaching with 9% agglomeration moisture.

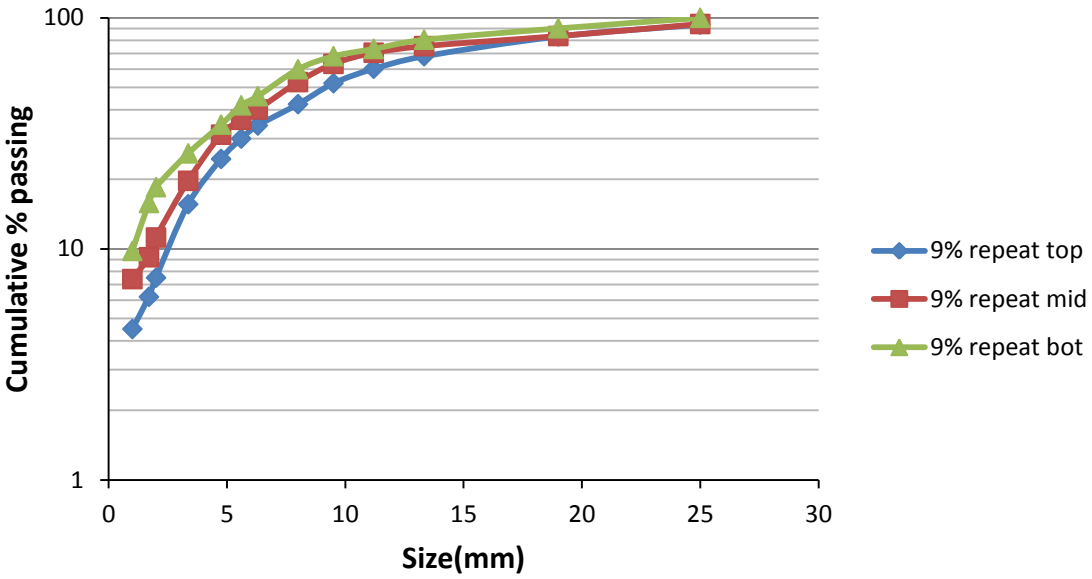

Figure 5.6 Particle size distribution at different column positions after column leaching with 9% agglomeration moisture (repeat).

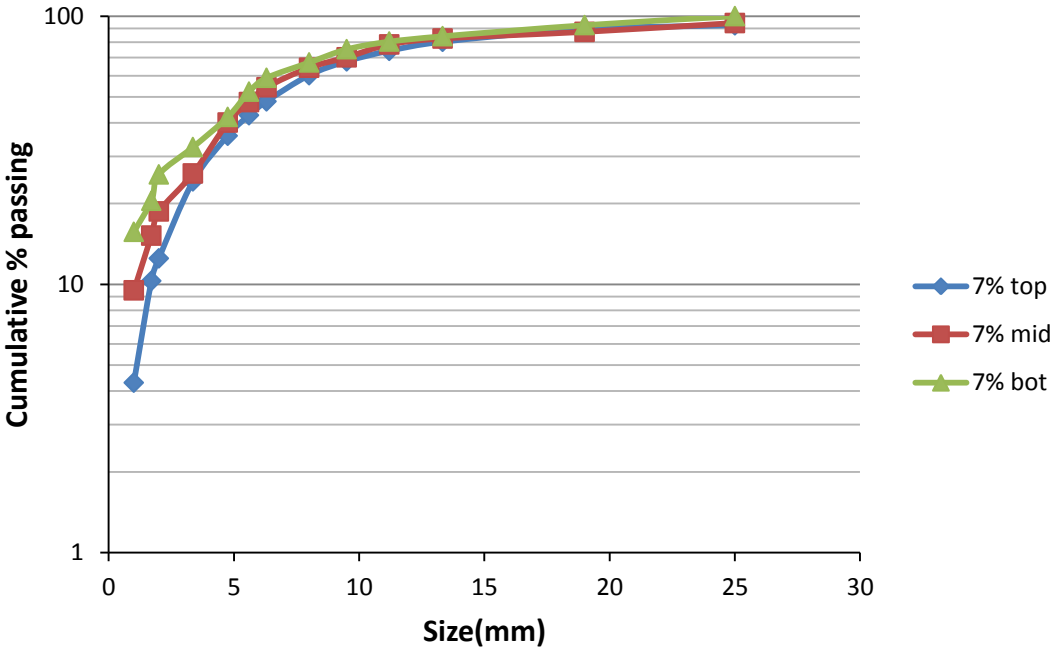

Figure 5.7 Particle size distribution at different column positions after column leaching with 7% agglomeration moisture.

Figure 5.8 Solidified mud-like materials inside 11% agglomeration moisture column.

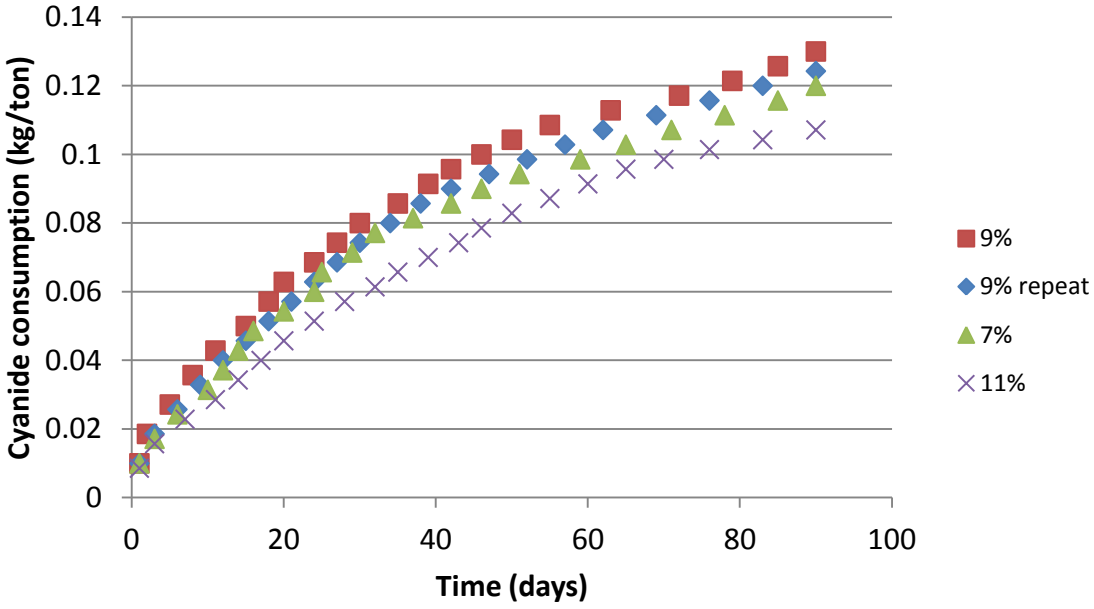

Figure 5.9 Cyanide consumption for 7%, 9% and 11% agglomerate moisture contents

Table 5.1 The breakthrough times and drain down liquid volume data.

Moisture content	Breakthrough time (hours)	Drain down volume collected over 24 hours
9%	3.5	630 cm^3
9% repeat	3.5	642 cm^3
7%	3.7	819 cm^3
11%	1.5	300 cm^3

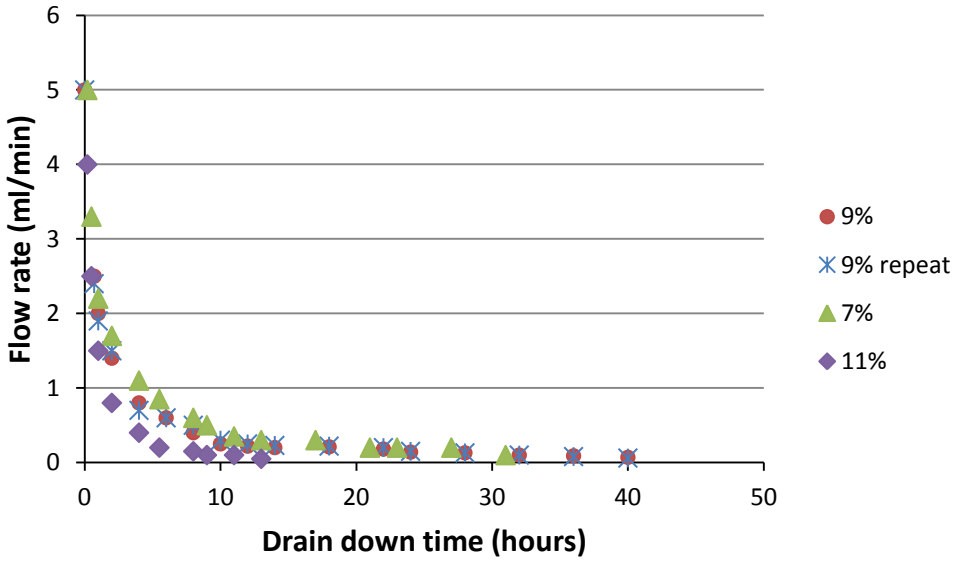

Figure 5.10 Drain down rate after column leaching test completion.

From the drain down data, the breakthrough times for 7% and 9% agglomerate moisture content levels were similar. At 11% agglomerate moisture content, the breakthrough time was faster. The faster time may have been due to channeling and reduced bed porosity. The drain down rate and volume were quite similar for all 3 columns except the 11% agglomerate moisture content.

5.5 Evaluation of Effect of Cement Binder Addition on Column Leaching Test Results

The second set of column leaching tests evaluates the effect of cement binder addition on leaching. Results are shown in Figure 5.11. The results in Figure 5.11 do not show a significant effect of binder on recovery. Low cement binder addition (6kg/ton) and high cement addition (10kg/ton) give similar recovery rates. A comparison of the second set of column leaching test results with the 9% agglomerate moisture content and 8kg/ton cement binder from the first set are also shown in Figure 5.11. Particle size distributions at different column positions (top = 100-150 cm above outlet, mid = 50-100 cm above outlet, bot = outlet - 50 cm) after leaching are presented in Figures 5.12-5.14. Figures 5.12-5.14 show that the fraction of fines is greater near the bottom of the column, indicating some migration of fines occurs during leaching. The test with 6 kg/ton cement addition showed slightly more fines migration than the 8 kg/ton cement addition test. The test with 10 kg/ton cement addition shows fines migration similar to that in the 8 kg/ton test.

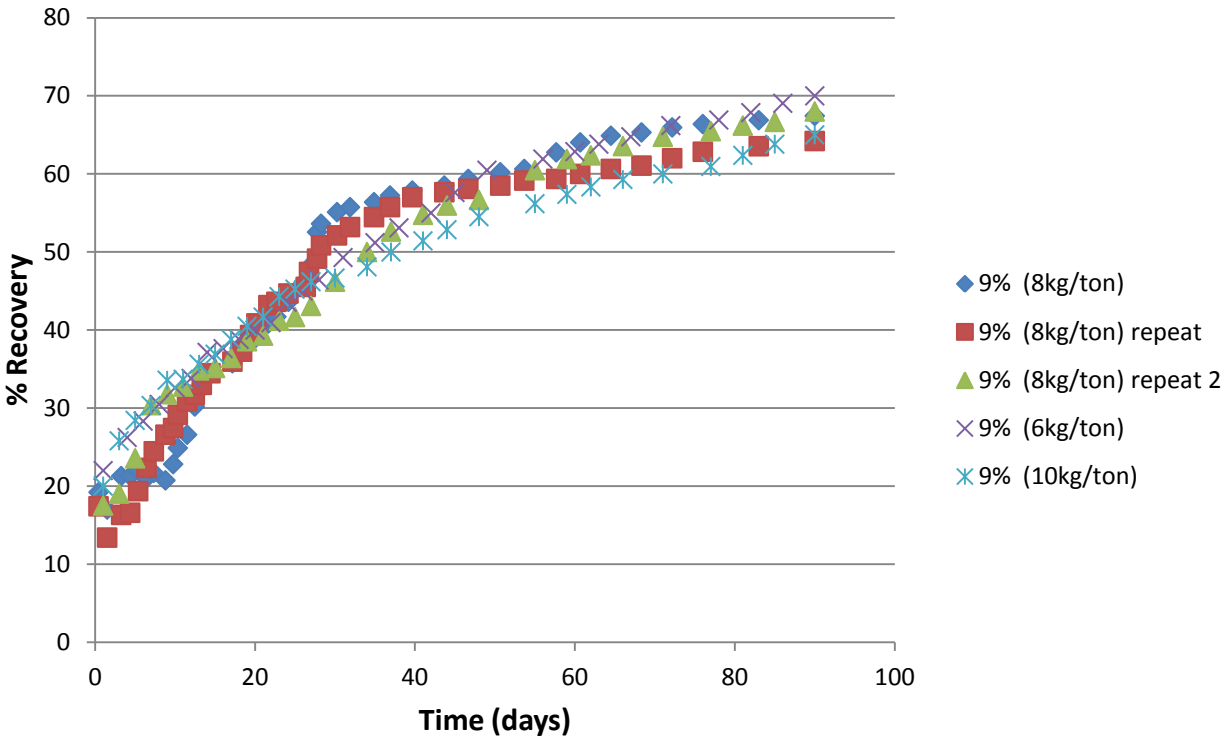

Figure 5.11 Gold recovery results for 90 days leaching time using agglomerates with different cement binder additions as noted in the figure legend.

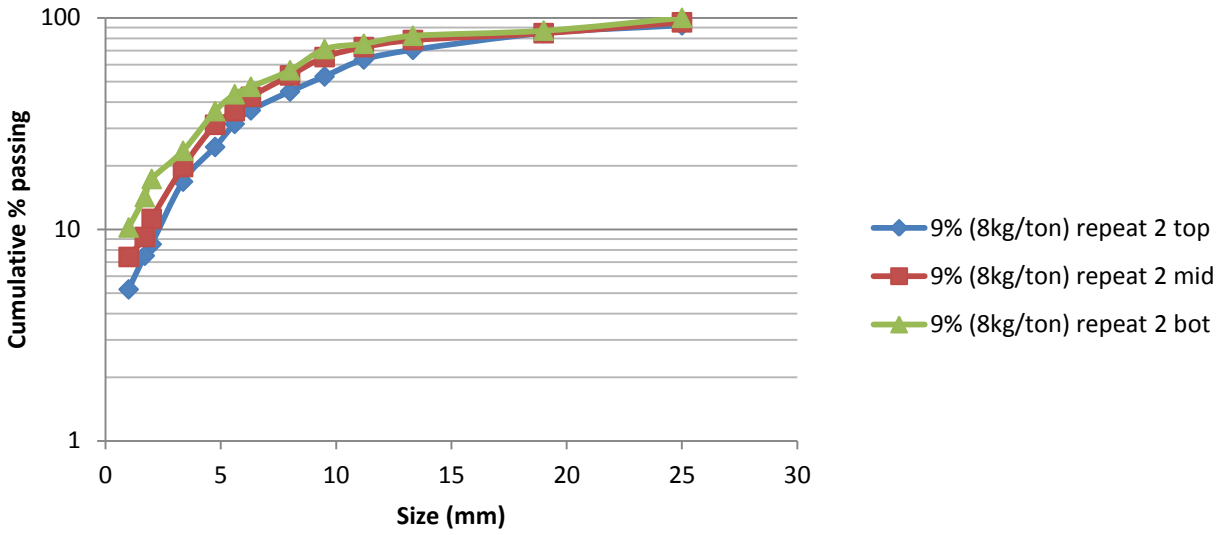

Figure 5.12 Particle size distribution at different column positions after column leaching with 9% agglomeration moisture (repeat 2) and 8 kg/ton cement binder addition.

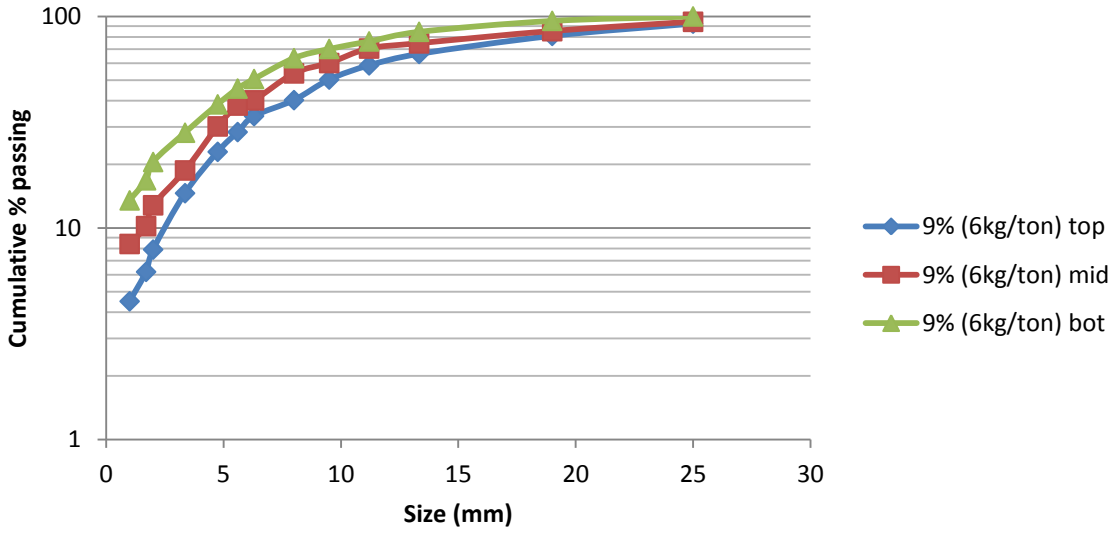

Figure 5.13 Particle size distribution at different column positions after column leaching with 9% agglomeration moisture and 6 kg/ton cement binder addition.

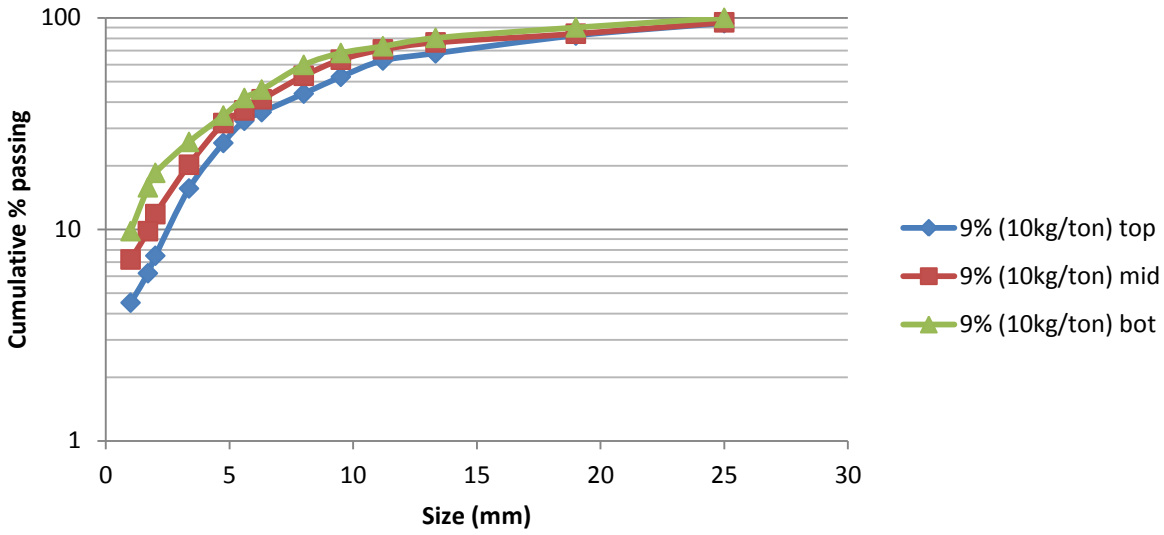

Figure 5.14 Particle size distribution at different column positions after column leaching with 9% agglomeration moisture and 10 kg/ton cement binder addition.

Cyanide consumption in the second set of column leaching tests is shown in Figure 5.15. Figure 5.15 shows cyanide consumption of 0.19 kg/ton. Cyanide consumption was not significantly influenced by binder addition. Break through times and drain down liquid volumes are shown in Table 5.2 and Figure 5.16. Drain down times and volumes are similar for all tests due to similar size distributions and limited fines migration, although the test with 6 kg/ton of cement binder had a slightly longer time and slightly lower volume than the other tests. This slight increase in drain down time for the 6 kg/ton test is consistent with the observation of slightly more fines migration to the bottom of the column.

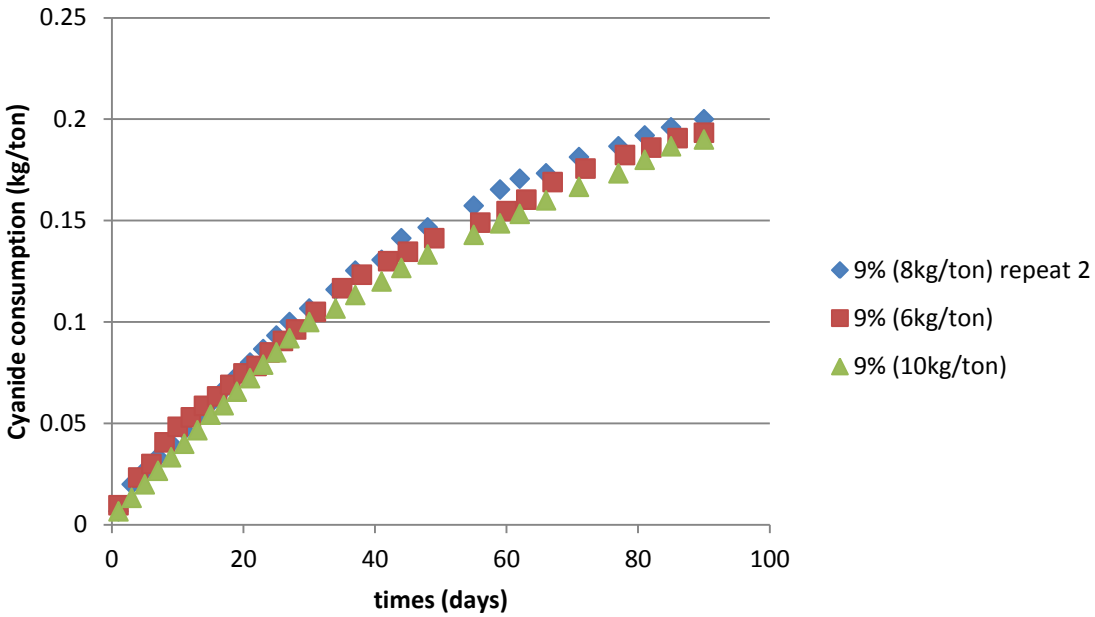

Figure 5.15 Cyanide consumption for column leaching tests with 6 kg/ton, 8 kg/ton and 10 kg/ton of cement binder addition and 9% agglomeration moisture.

Table 5.2 The breakthrough times and drain down liquid volume data for the second set of column leaching tests.

Moisture content	Breakthrough time (hours)	Drain down volume collected over 24 hours
9% (8 kg/ton)	3.5	630 cm^3
9% (8 kg/ton) repeat	3.5	642 cm^3
9% (8 kg/ton) repeat 2	3.7	615 cm^3
9% (6 kg/ton)	3.8	598 cm^3
9% (10 kg/ton)	3.3	622 cm^3

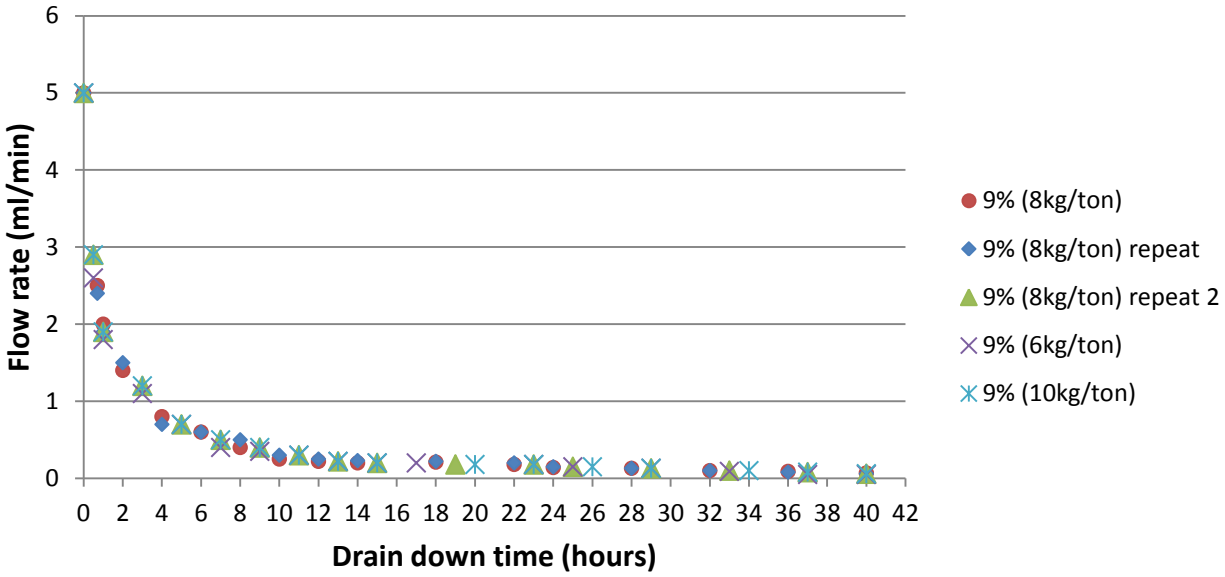

Figure 5.16 Drain down data for column leaching test completion for the second set of the column leaching tests.

5.6 Comparison of Column Leaching Results With Computational Software Model for Gold Column Leaching (HeapNET)

Column leach model simulations were performed using HeapNET, a Visual.NET application program assisting the user in the setup and running of column leaching simulations. This software was provided through Process Engineering Resources Incorporated (PERI). The computational procedure model accounts for variably saturated flow through porous media and implements a three-dimensional porous flow algorithm within a computational modeling software framework (PHYSICA). A shrinking core model is used to describe the chemical dissolution reactions between solid particles and liquid. The model predicts gold recovery by evaluating critical parameters such as particle size, column dimensions, leaching solution application rate, diffusion rate, and

cyanide concentration. The principal reactions cyanide with gold, silver, copper, and gangue minerals were calculated without thermal effects due to low oxygen levels. There are more detailed discussions of the model formulation and solution strategies described in (Bennet, McBride, Cross, Gebhardt, & Taylor, 2006). Figure 5.17 shows generic computational procedure of HeapNET software.

The gold column leaching in these evaluations was simulated using materials and particles data that have been created using the materials and particles editor for each size class of the ore. The average particle size was calculated as the geometric mean of the adjacent sieve openings sizes. Percent weight and average particle size of the gold ore are shown in Table 5.3.

Initial ore moisture (the fraction of moisture before leaching) which is equal to the natural moisture of the ore and residual ore moisture (the fraction of moisture after leaching) was used this simulation. Diffusion rate and diffusivity of the ore were calculated based on particle size by the software. Cyanide concentration was set to 200 ppm and application rate was set to 5.4 mL per minute. Column diameter was set to 20.32 cm and column height to 152.4 cm. Permeability was set to 4.1×10^{-6} cm^2 (based on experimental data). The results of the software simulation compared with experimental leaching data are shown in Figure 5.18.

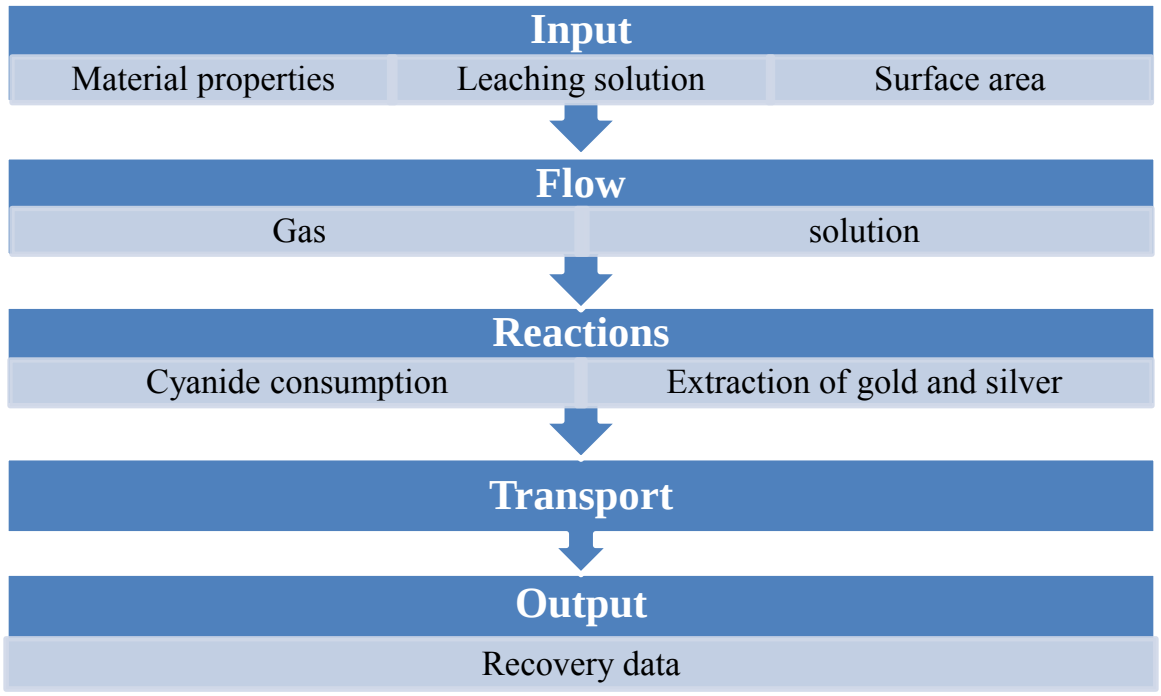

Figure 5.17 HeapNET leach model generic computational procedure (Bennet, McBride, Cross, Gebhardt, & Taylor, 2006)

Table 5.3 Percent weight and average particle size of the gold ore based on geometric mean size of upper and lower sieves for the size class.

Size	Weight (%)	Average particle size
-19 mm to +12.5 mm	19.40	15.41 mm
-12.5 mm to +6.3 mm	19.40	8.87 mm
-6.3 mm to +3.35 mm	19.40	4.59 mm
-3.35 mm to +1 mm	20.90	1.83 mm
-1 mm	20.90	0.5 mm

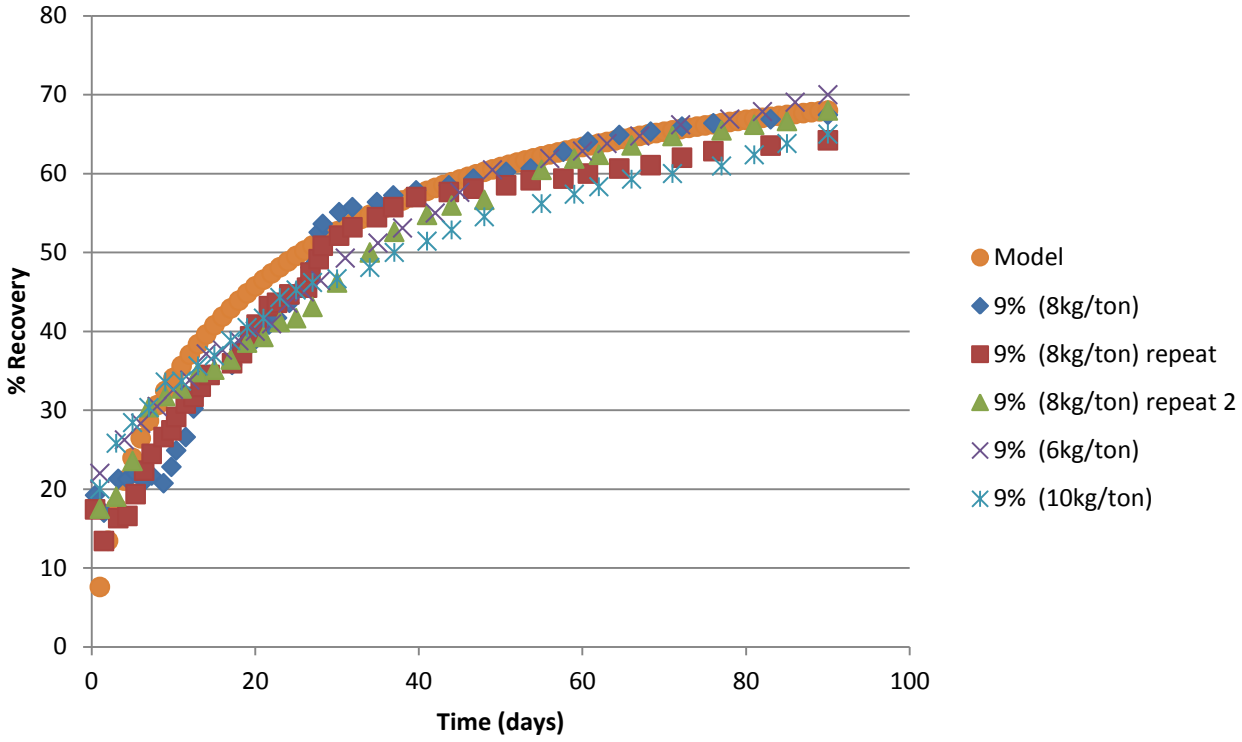

Figure 5.18 Comparison of the HeapNET model simulation to the experimental results.

The HeapNET simulation shows good agreement between the experimental and the calculated data. The experimental data show better recovery than the model during the first 5 days of leaching because there is no cure time parameter used in the model to account for the actual cure time in the column leaching simulations. For experimental data the ore was cured with 1000 ppm cyanide in the agglomerate solution and for 1 day.

CHAPTER 6

CONCLUSIONS

6.1 Evaluation and Development of Quality Control Tools

6.1.1 Liquid Retention Capacity

Results show liquid retention capacity data can be used to estimate optimum agglomeration moisture for basic and acidic solution applications. Tests suggest that an ore sample height of 10 centimeters provides liquid retention capacity values that are similar to optimum agglomerate moisture content values for typical ores.

The effect of sample height on liquid retention capacity was also evaluated. As the height of the sample increases, the ability of the liquid to fill all of the pores decreases. Thus, the height of the ore sample has a strong influence on liquid retention capacity as expected.

The effects of particle size distribution and fine particles were evaluated. Particle size distribution and the amount of fines in an ore sample are significantly related to the amount of liquid that an ore can retain. More fine particles in the ore require more moisture to form stable agglomerates.

Pressure reduced void space and correspondingly reduced liquid retention slightly.

The liquid uptake time in the liquid retention capacity measurements depends on particles size distribution. Fine particles require more time to reach steady state uptake levels during liquid retention capacity measurements. Most ore samples evaluated in this study took 20-60 minutes to reach steady state liquid retention capacity values.

Liquid retention capacity measurement data show that the total liquid volume that a feed ore retains using a 10 cm high column in a short term test is very similar to the optimum agglomeration moisture content determined in batch agglomeration. The similarity of the moisture levels is related to the liquid bridging states and the need for sufficient moisture to bind particles by capillary forces during the agglomeration process. A simple liquid uptake test lasting approximately 1 hour is generally sufficient to evaluate the agglomeration moisture need for an ore sample 10 cm in height.

Measurements indicate that the volume of liquid needed for optimum agglomeration remains relatively constant at different acid solution levels (0, 100, 500, and 900 g/l). Thus, the volume-based liquid retention capacity is reasonably constant. Consequently, simple multiplication of the liquid retention capacity of an ore by the solution density provides a good estimate of the optimum agglomerate moisture content.

6.1.2 Other Tools

Results from the experiments demonstrate the usefulness of the other quality control tool set in evaluating agglomeration performance. Electrical conductivity is a good tool to evaluate the moisture content of the agglomerated gold ore. Electrical conductivity measurements showed a consistent increase in conductivity with increasing moisture. Agglomerate moisture and ionic strength of the solution affect conductivity

(Figure 2.70). Compaction of the agglomerates increases contact point and results in increased conductivity.

Hydraulic permeability and turbidity testing can be used to evaluate agglomerate quality. Permeability has some difficulty differentiating agglomerates with similar sizes. Turbidity evaluates agglomerate strength to resist hydraulic flow and associated release of fines during the permeability test (Figure 2.72).

The soak test is a good tool to characterize agglomerate strength. Soak test results determine fines release in a stagnant solution environment (Figure 2.71).

6.2 Gold Ore Agglomeration

Scoping test results for gold ore (sample I) indicated that the highest permeability values are obtained when the largest agglomerate size (D_{50}) is reached (Figures 2.13-2.14) at 7% agglomerate moisture, which also corresponded to the least turbidity produced during permeability measurements. Scoping test results for gold ore (sample II) showed that the best agglomerates, based on largest D_{50} size, were formed at 9 % agglomerate moisture content. Agglomerate moisture above the optimum moisture level created mud and bad agglomerates.

Effect of agglomeration time and drum speed were evaluated. An agglomeration time of 2-5 minutes and agglomeration drum speed of 20%-30% of the critical speed are adequate to produce good permeability and generate minimal fine particle migration and turbidity (Figures 2.71-2.72). At 45%-60% of critical speed, small agglomerates and fine particles inside the drum stick to the drum wall due to the centrifugal force.

Gold ore (sample I) has been evaluated by HRXMT, QEMSCAN and SEM/EDS imaging and analysis. The resulting data show important features in agglomerates such as agglomerates structures, associated minerals and chemical compositions. The data can be used to evaluate agglomerate porosity as well as the potential for evaluating some binder information.

6.3 Gold Ore Column Leaching Results

Column leaching tests with 9% agglomeration moisture resulted in the best recovery (7%, 9% and 11% agglomerate moisture in these tests were agglomerated with 8 kg/ton of Portland cement type II binder). Eleven percent agglomerate moisture results in mud formation inside the column, which prevented sieve analysis following leaching. For the other columns some fine particles migration can be observed. The 7% agglomerate moisture content showed more fine particles migration than 9% agglomerate moisture content. Cyanide consumption is slightly different for all of the columns. Cyanide consumption for 9% 7%, and 11% agglomerate moisture contents was 0.13, 0.12 and 0.11 kg/ton, respectively. Channeling and reduced bed porosity in 9% agglomerate moisture content column led to faster breakthrough time and less liquid volume drain down over 24 hours.

The amount of cement binder addition does not have a large effect on gold recovery . Fines migration data are relatively low, revealing some stability of the agglomerates. Increasing cement binder addition to 10 kg/ton improves the agglomerate stability somewhat but does not improve gold recovery. On the other hand, decreasing cement binder addition to 6 kg/ton reduces agglomerate stability but does not have a

substantial effect on gold recovery. Cyanide consumption is 0.19 kg/ton for each binder addition (10, 8, and 6 kg/ton of cement addition). Break through time and drain down data are similar for all of the column tests involving different binder additions. Computational software modeling of gold ore column leaching (HeapNET) showed a good fit of model and experimental data even though it is not designed to account for the initial agglomeration and curing.

REFERENCES

Abdul, A. S., & Gillham, R. W. (1984). Laboratory studies of the effects of the capillary fringe on steamflow generation. Wat. Resour. Res. , 691-698.

Bartlett, R. W. (1997). metal extraction from ores by heap leaching. The Iron and Steel Society of AIME , 529-545.

Bennet, C. R., McBride, D., Cross, M., Gebhardt, J. E., & Taylor, D. A. (2006). Simulation technology to support base metal ore heap leaching. Mineral Processing and Extractive Metallurgy , 41-48.

Bertin, E. P. (1978). Introduction to X-ray Spectrometric Analysis. Plenum Press, New York , 439-473.

Bouffard, S. C. (2005). Review of agglomeration practice and fundamentals in heap leaching. Mineral Processing & Extractive Metall , 233-294.

Bowles, J. E. (1992). Engineering Properties of Soils and Their Measurement. McGraw-Hill, New York.

Bowling, R. (1988). A Theoretical Review of Particle Adhesion. Particles on Surfaces Detection Adhesion and Removal , 129-155.

Buranelli, V. (1979). Gold-An Illustrated History. Hammond, New Jersey.

Butwell, J. W. (1990). Heap leaching of fine agglomerated tailings at Goosebery mine, Nevada. Advances in Gold and Silver Processing , 3-13.

Capes, C. E. (1980). Handbook of Powder Technology. Elsevier Scientific Pub Co.

Chamberlin, P. D. (1986). Agglomeration: Cheap insurance for good recovery when heap leaching gold and silver recovery. Mining Engineering , 1105-1109.

DeMull, T. J., & Womakc, R. A. (1984). Heap leaching practice at Alligator Ridge. SME, 9-21.

Dierks. (2005). Gold MSDS. Electronic Space Products International.

Ellenhorn, M., & Barceloux, D. (1988). Diagnosis and Treatment of Human Poisoning. New York: Elsevier Science Publishing Company.

Fernandez, G. V. (2003). The use of electrical conductivity in agglomeration and heap leaching. Hydrometallugy of Copper , 161-175.

Gellert, W., Kustner, H., Hellwich, M., & Kastner, H. (1977). The VNR Concise Encyclopedia of Mathematica. Van Nostrand Reinhold Company, New York.

Godt, J. W., & Mckenna, J. P. (2008). Numerical modeling of rainfall threshold for shallow land sliding in the Seattle, Washington, area. U.S. Geological Survey , 102-121.

Graton, L. C., & Fraser, H. J. (1935). Systematic packing of spheres with particular relation to porosity and permeability. Journal of Geology , 795-909.

Heinen, H. J., McClelland, G. E., & Lindstrom, R. E. (1979). Enhancing Percolation Rate in Heap Leaching of Gold-Silver Ores. U.S. Bureau of Mines , 20.

Holley, C. A. (1979). Disc Pelletizing Theory and Practice. Ferro-Tech Company.

Israelson, O. W., & West, F. L. (1922). Water Holding Capacity of Irrigated Soils. Utah State Agricultural Experiment Station , 1-24.

Kaliyan, N., & Morey, V. (2010). Natural binders and solid bridge type binding mechanisms in briquettes and pellets made from corn stover and switchgrass. Bioresource Technology , 1082-1090.

Kinard, D. T., & Schweizer, A. A. (1987). Engineering properties of agglomerated ore in a heap leach pile. Geotechnical Aspects of Heap Leach Design , 55-64.

Kristensen, G., & Schaefer, T. (1987). Granulation: A review on pharmaceutical wet-granulation. Drug Development and Industrial Pharmacy , 803-872.

Kudryk, V., & Kellogg, H. (1954). Mechanism and rate-controlling factors in the dissolution of gold in cyanide solution. Journal of Metals , 541-547.

Lane, K. S., & Washburn, S. E. (1947). Capillary tests by capillarimeter and by soil filled tubes. Highway Research Board Proceedings , 460-473.

Marsden, J., & House, I. (1992). The Chemistry of Gold Extraction. Ellis Horwood: West Sussex.

McClelland, G. E., & Eisele, J. A. (1981). Improvements in Heap Leaching to Recover Silver and Gold From Low-Grade Resources. U.S. Bureau of Mines , 1-20.

Miller, G. (2003). Ore geotechnical effects on copper heap leach kinetics. The Minerals, Metals & Materials Society , 329-342.

Miller, J. D., & Lin, C. L. (2003). Ultimate recovery in heap leaching operations as established from mineral exposure analysis by X-ray microtomography. Int. J. Miner. Process , 331-340.

Mular, A. L., Halbe, D. N., & Barratt, D. J. (2002). Mineral processing plant design, practice, and control. SME, Colorado.

Ohring, M. (1995). Engineering Materials Science, Volume 1. Academic Press, San Diego.

Phifer, S. E. (1988). Agglomerating gold ores at the haile gold mine. Mining Engineering, 447-450.

Pietsch, W. (1997). Size Enlargement by Agglomeration. Handbook of Powder Science and Technology 2nd Ed, Chapman & Hall, New York, 33-37.

Potter, G. (1983). Some factors in design of heap leaching operations. Nevada Bureau of Mine & Geology , 69-76.

Puri, A. N. (1939). Physical Characteristics of Soils: The Capillary Tube Hypothesis of Soil Moisture. Irrigation Research Institute , 73-78.

Rumpf, H. (1962). The strength of granules and agglomerates. Agglomeration , 379-418.

Schaefer, H. K. (1987). A review on wet granulation. Drug Dev. Ind , 803-872.

Schlitt, W. J. (1983). The Role of Solution Management in Heap and Dump Leaching. SME Fall Meeting , 72-74.

Simeonova, F. P. (2004). Hydrogen Cyanide and Cyanides: Human Health Aspects. Geneva: International Programme on Chemical Safety.

Suggitt, R. M., Aziz, P. M., & Wetmore, F. E. (1949). The Surface Tension of Aqueous Sulfuric Acid Solutions at 25°. J. Am. Chem. Soc. , 676-678.

Yang, W.-c. (2003). Handbook of Fluidization and Fluid-Particle Systems. Marcel Dekker, New York.